

Polymorphisms of heat shock protein receptors

Dissertation
Zur Erlangung des Doktorgrades
der Mathematisch-Naturwissenschaftlichen Fakultäten
der Georg-August-Universität zu Göttingen

vorgelegt von
Muppala Vijaya Kumar
aus Chennai, Indien

Göttingen, 2008

D7

Referent: Prof. Dr. Sigrid Hoyer-Fender

Korreferent: Prof. Dr. Friedrich-Wilhelm Schürmann

Tag der mündlichen Prüfung:

Table of Contents:

1. Abbreviations	8
2. Introduction	14
2.1 Heat shock proteins	14
2.2 HSP-mediated antigen cross-presentation	14
2.3 HSP-mediated signaling and release of pro-inflammatory cytokines	15
2.4 Extracellular source of HSP	16
2.5 HSP-based immunotherapy	16
2.6 Heat shock protein receptors	17
2.7 CD91 (Low density lipoprotein receptor-related protein 1)	18
2.8 Polymorphisms in the CD91 gene	20
2.9 Expression of CD91	20
2.10 Lectin-like oxidized low-density lipoprotein receptor-1 (LOX-1)	21
2.11 Expression of LOX-1 and its signaling functions	22
2.12 LOX-1 polymorphisms and disease association	22
2.13 The lectin-like domain of LOX-1 and its ligand binding	23
3. Aim	24
4. Materials	25
4.1 Chemicals/Reagents	25
4.2 Instruments	27
4.3 Antibodies	28
4.3.1 Primary	28
4.3.2 Secondary	28
4.3.3 Isotype control	28
4.4 Kits	28
4.5 Plastic ware	29
4.6 Miscellaneous	29
4.7 Primers	30
4.8 Enzymes	31
4.9 Antibiotics/Drugs	32
4.10 Cell lines	32
4.11 Vectors	32
4.12 Ladders/Markers	32
4.13 Bacterial strains	33
4.14 Solutions and buffers	33
4.14.1 Protein concentration determination	33
4.14.2 SDS-Page / Western blotting	33
4.14.3 Recombinant HSP70 preparation	34
4.14.4 Cell culture medium	35
4.14.5 Preparation of DNA	35
4.14.6 Analysis of DNA	35
4.14.7 Mini-prep of plasmid DNA	35

4.15	Study samples	36
4.15.1	HIV-infected human cohort	36
4.15.2	SIV-infected rhesus macaques and control animals	37
4.15.3	Human healthy volunteers	37
4.16	List of suppliers	37
5.	Methods	39
5.1	Biochemical methods	39
5.1.1	Protein quantitation by Bradford reagent	39
5.1.2	Lysis of cultured mammalian cells	39
5.1.3	Preparation of protein samples for SDS polyacrylamide gel electrophoresis (SDS-PAGE)	40
5.1.4	SDS-PAGE	40
5.1.5	Staining with coomassie blue	40
5.1.6	Western blot	41
5.1.7	Preparation of recombinant HSP70	41
5.1.7.1	Induction of HSP70	41
5.1.7.2	Preparation of inclusion bodies containing HSP70	42
5.1.7.3	Purification of HSP70	42
5.1.8	Fluorescein isothiocyanate (FITC) conjugation of HSP70	42
5.1.8.1	Conjugation reaction	42
5.1.8.2	Purification	43
5.2	Cell culture methods	43
5.2.1	Cell culture	43
5.2.2	Cell counting	43
5.2.3	Freezing cells	43
5.2.4	Thawing cells	43
5.2.5	Transient transfection	44
5.2.6	Stable transfection	44
5.2.7	Limiting dilution	44
5.2.8	Preparation of PBMCs by density gradient centrifugation	45
5.3	Molecular biology methods	45
5.3.1	Cultivation of <i>Escherichia coli</i> (<i>E. coli</i>)	45
5.3.1.1	On Luria Bertani (LB) agar plates	45
5.3.1.2	In Luria Bertani (LB) medium	45
5.3.2	Preparation of competent <i>E. coli</i> cells (DH5 α)	45
5.3.3	Transformation of competent <i>E. coli</i> cells	46
5.3.4	Preparation of glycerol stocks of bacterial strains	46
5.3.5	Mini-preparation of plasmid DNA	46
5.3.6	Restriction digestion of plasmid DNA	46
5.3.7	Preparation of DNA from whole blood	47
5.3.8	Preparation of DNA from serum	47
5.3.8.1	Microwave irradiation	47
5.3.8.2	Alkaline lysis method	47
5.3.8.3	Proteinase K/Sodium dodecyl sulfate (SDS) lysis method	47
5.3.9	Agarose gel electrophoresis of DNA	48

5.3.10	Determining the concentration of DNA	48
5.3.11	Purification of DNA	49
5.3.12	Genotyping of SNP by allele-specific polymerase chain reaction (AS-PCR)	49
5.3.13	Restriction fragment length polymorphism (RFLP)	50
5.3.14	Preparation of RNA	50
	5.3.14.1 Trizol method	50
	5.3.14.2 SV total RNA isolation system kit (Promega)	51
5.3.15	Reverse transcription (RT)	51
5.3.16	Real-time PCR	52
5.3.17	Cloning of full-length LOX-1 cDNA	53
5.3.18	PCR-based site-directed mutagenesis (SDM)	54
5.3.19	Sequencing	56
	5.3.19.1 PCR	56
	5.3.19.2 Purification of PCR products and sequencing	56
5.4	Flow cytometry	56
	5.4.1 Processing of blood samples from normal healthy volunteers for HSP70 receptors expression analysis	56
	5.4.2 Processing of PBMCs from HIV-infected individuals for CD14/CD91 FACS analysis	57
	5.4.3 Processing of blood samples from SIV-infected rhesus macaques for CD14/CD91 FACS analysis	58
	5.3.4 Analysis of HSP70 binding to monocytes by FACS	58
5.5	Computational methods	58
	5.5.1 Statistical tests and models for MFI	58
	5.5.2 Levels of significance	59
	5.5.3 Statistical tools	59
	5.5.4 Haplotypes prediction and data analysis	59
6.	Results	60
	6.1 Binding of HSP70 to monocytes in PBMCs	60
	6.2 Expression of HSP70 receptors on monocytes	61
	6.3 Expression of CD91 in HIV-infected individuals	63
	6.4 Genotyping of CD91 promoter and exon 3 polymorphisms in HIV-infected individuals	64
	6.5 Effect of CD91 promoter and exon 3 polymorphism on CD91 cell surface expression on monocytes in HIV cohort	66
	6.6 Expression of CD91 mRNA in HIV cohort	67
	6.7 Genotyping of CD91 promoter and exon 3 polymorphisms in healthy volunteers	68
	6.8 Analysis of the effects of the CD91 promoter and exon 3 polymorphism on the CD91 cell surface expression on monocytes in healthy volunteers	69
	6.9 Analysis of the influence of the CD91 promoter and exon 3 polymorphism on CD91 mRNA expression in healthy volunteers	70
	6.10 Analysis of HapMap data for LRP1 (CD91) gene	71
	6.11 Genotyping of the tag SNPs in the first block of the CD91 gene	74
	6.12 Analysis of the effect of independent tag SNPs on CD91 protein expression in the HIV cohort	76

6.13	Analysis of the effect of independent tag SNPs on CD91 protein expression in the healthy volunteers	77
6.14	Generation of haplotypes	78
6.15	Effect of CD91 haplotypes on CD91 expression in HIV cohort and healthy volunteers	79
6.16	Genotyping of the tag SNP in second block of the CD91 gene	81
6.17	Analysis of the effect of tag 67 SNP on CD91 protein expression in the HIV cohort and healthy volunteers	81
6.18	Genotyping of CD91 exon 3 polymorphism from serum DNA of LTNPs	82
6.19	Study of CD91 expression in rhesus macaques	83
6.20	CD91 expression on CD14 positive cells in rhesus macaques before SIV infection	83
6.21	Expression of CD91 and proportion of CD14/CD91 positive cells in the course of SIV infection	85
6.22	Expression of CD91 and proportion of CD14/CD91 positive cells in non-infected rhesus macaques	87
6.23	Expression of CD91 and proportion of CD14/CD91 positive cells in different groups of rhesus macaques	87
6.24	Screening for polymorphisms in CD91 promoter region of rhesus macaque	88
6.25	Genomic organization and selected SNPs of the OLRI (LOX-1) gene	90
6.26	LD plot and HapMap haplotypes of the OLR1 gene	90
6.27	Genotype distribution and allele frequencies of LOX-1 SNPs	92
6.28	Effect of LOX-1 SNPs on LOX-1 expression	94
6.29	Generation of LOX-1 haplotypes	94
6.30	Effect of LOX-1 haplotypes on LOX-1 expression	95
6.31	Generation of a full-length cDNA for LOX-1	96
6.32	Generation of exon 4 SNP mutant by SDM	97
6.33	Generating constructs of LOX-1 Wt and LOX-1 Mut	98
6.34	Analysis of LOX-1 expression and HSP70 binding in Chinese hamster ovary (CHO) cells	100
6.35	Transient transfection of pAcGFP1-N1 / LOX-1 Wt and Mut constructs in CHO cells	100
6.36	Evaluation of HSP70 binding to LOX-1 Wt and LOX-1 Mut transfected CHO cells	101
6.37	Comparison of LOX-1 expression and HSP70 binding on LOX-1 Wt and LOX-1 Mut transfected CHO cells	102
6.38	Screening for LOX-1 Wt and LOX-1 Mut stable CHO cells	104
6.39	Analysis of LOX-1 expression and HSP70 binding in HT1080 cells	105
6.40	Expression of LOX-1 Wt and LOX-1 Mut after induction by doxycycline	105
6.41	Control of LOX-1 Wt and LOX-1 Mut protein expression levels by different induction conditions	107
6.42	Differences in induction of protein but not mRNA of LOX-1 in LOX-1 Wt and LOX-1 Mut clones	109
7.	Discussion	111
7.1	Analysis of HSP70 binding to its receptors on monocytes	111
7.2	Expression of CD91 on cell surface of monocytes in HIV cohort	112

7.3	Genotype distribution of CD91 exon 3 polymorphism and its influence on CD91 expression	113
7.4	Genotype distribution of CD91 promoter polymorphism and its effect on CD91 expression	114
7.5	Evaluation of additional SNPs of CD91 gene determined from the HapMap database	115
7.6	CD91 expression on monocytes of SIV-infected rhesus macaques	116
7.7	Genotype distribution of LOX-1 SNPs and their effect on LOX-1 expression	117
7.8	Functional effect of LOX-1 exon 4 SNP	118
7.9	Possible regulation of LOX-1 expression by exon 4 SNP	118
7.10	Implications of HSP70 receptor polymorphisms for immunotherapy	119
7.11	Conclusion and future perspectives	121
8.	Summary	122
9.	References	124
10.	Acknowledgements	134

1. ABBREVIATIONS

ABC	ATP-binding cassette
AD	Alzheimer disease
AP-1	Activator protein 1
APC	Antigen presenting cell
APO	Apolipoprotein
APP	Amyloid precursor protein
APS	Ammonium persulfate
AS-PCR	Allele-specific PCR
ATCC	American type culture collection
α_2 M	Alpha-2-macroglobulin
BC	Breast cancer
BIP	Immunoglobulin heavy chain-binding protein
BSA	Bovine serum albumin
bp	Base pair
$^{\circ}$ C	Degree Celsius
CCR5	Chemokine (C-C motif) receptor 5
CD	Cluster of differentiation
cDNA	Complementary DNA
CHO	Chinese hamster ovary
CMV	Cytomegalovirus
CO ₂	Carbon dioxide
DAB	Diaminobenzoic acid
DMEM	Dulbecco's Modified Eagle's Medium
DMSO	Dimethyl sulfoxide
DEPC	Diethylpyrocarbonate
DNA	Deoxyribonucleic acid
DNase	Deoxyribonuclease
DTT	Dithiothreitol
dATP	Desoxyriboadenosintriphosphate
dCTP	Desoxyribocytosintriphosphate

dGTP	Desoxyriboguanosintriphosphate
dTTP	Desoxyribothymosintriphosphate
dNTP	Deoxynucleotidetriphosphate
dH ₂ O	Distilled water
EDTA	Ethylene diamine tetraacetic acid
EMSA	Electrophoretic mobility shift assay
ER	Endoplasmic reticulum
Ex	Exon
<i>E. Coli</i>	<i>Escherichia coli</i>
FACS	Fluorescence-activated cell sorter
FCS	Fetal calf serum
FITC	Fluorescein isothiocyanate
FL	Full-length
FSC	Forward scatter
GAPDH	Glyceraldehyde-3-phosphate dehydrogenase
GFP	Green fluorescent protein
GRP	Glucose-regulated protein
GVHD	Graft-versus-host disease
g	Gram
gp	Glycoprotein
x g	Acceleration of gravity
H ₂ O ₂	Hydrogen peroxide
HCl	Hydrochloric acid
HAART	Highly active anti-retroviral therapy
HAP	Haplotype analysis tool
HEPES	N-(-hydroxymethyl) piperazin, N'-3-propansulfoneacid
HIV	Human immunodeficiency virus
HLA	Human leukocyte antigen
HRP	Horse radish peroxidise
HSC	Heat shock cognate protein
HSP	Heat shock protein
HWE	Hardy-Weinberg equilibrium
htSNP	Haplotype tagging SNP

IFN γ	Interferon gamma
IL-1 β	Interleukin-1 β
IPTG	Isopropyl- β -thiogalactopyranoside
Ig	Immunoglobulin
kb	Kilobase pairs
LB	Luria Bertani
LD	Linkage disequilibrium
LOX-1	Lectin-like oxidized low-density lipoprotein receptor-1
LPS	Lipopolysaccharide
LTNP	Long-term nonprogressors
M	Molar
MAPK	Mitogen-activated protein kinase
MCP-1	Monocyte chemotactic protein 1
MCS	Multiple cloning site
MFI	Mean fluorescence intensity
MI	Myocardial infarction
MHC	Major histocompatibility complex
MIP	Macrophage inflammatory protein
MMLV	Moloney murine leukemia virus
Mut	Mutant
MW	Molecular weight
mg	Milligram
min	Minute
ml	Milliliter
mM	Millimolar
mRNA	Messenger ribonucleic acid
μ l	Microliter
μ m	Micrometer
NaCl	Sodium chloride
NaOAc	Sodium acetate
NaOH	Sodium hydroxide
NF- κ B	Nuclear factor kappa B

NFAT	Nuclear factor of activated T cells
nm	Nanometer
OD	Optical density
Ox-LDL	Oxidized low density lipoprotein
PAGE	Polyacrylamide gel electrophoresis
PBMC	Peripheral blood mononuclear cell
PBS	Phosphatebuffersaline
PBST	Phosphatebuffersaline with tween 20
PCR	Polymerase chain reaction
PDGFRA	Platelet-derived growth factor α -receptor
PE	Phycoerythrin
PFA	Paraformaldehyde
PI	Propidium iodide
PMSF	Phenylmethylsulfonyl fluoride
PmB	Polymyxin B
<i>Pfu</i>	<i>Pyrococcus furiosus</i>
pH	Preponderance of hydrogen ions
RANTES	Regulated on activation, normal T cell expressed and secreted
RFLP	Restriction fragment length polymorphism
RNA	Ribonucleic acid
RNase	Ribonuclease
RNasin	Ribonuclease inhibitor
rpm	Revolution per minute
RT	Room temperature
RT-PCR	Reverse transcriptase-PCR
SD	Standard deviation
SDS	Sodium dodecylsulfate
SDM	Site-directed mutagenesis
SEM	Standard error of means
SIV	Simian immunodeficiency virus
SNP	Single nucleotide polymorphism
SP1	Specificity protein 1

SR	Scavenger receptor
SSC	Side scatter
TAP	Transporters associated with antigen processing
<i>Taq</i>	<i>Thermus aquaticus</i>
TBE	Tris-borate-EDTA-electrophoresis buffer
TC	Tri-Color
TE	Tris-EDTA buffer
TEMED	Tetramethylethylene diamine
TGF- β	Transforming growth factor beta
TLR	Toll-like receptor
TNF- α	Tumor necrosis factor alpha
Tris	Trihydroxymethylaminomethane
U	Unit
UTR	Untranslated region
UV	Ultra violet
V	Voltage
v/v	Volume/Volume
Wt	Wild type
w/v	Weight/Volume

Symbols of nucleic acids

A	Adenine
C	Cytosine
G	Guanine
T	Thymine

Symbol of amino acids

A	Ala	Alanine
B	Asx	Asparagine or Aspartic acid
C	Cys	Cysteine
D	Asp	Aspartic acid

E	Glu	Glutamic acid
F	Phe	Phenylalanine
G	Gly	Glycine
H	His	Histidine
I	Ile	Isoleucine
K	Lys	Lysine
L	Leu	Leucine
M	Met	Methionine
N	Asn	Asparagine
P	Pro	Proline
Q	Gln	Glutamine
R	Arg	Arginine
S	Ser	Serine
T	Thr	Threonine
V	Val	Valine
W	Trp	Tryptophan
Y	Tyr	Tyrosine
Z	Glx	Glutamine or Glutamic acid

2. Introduction

2.1 Heat shock proteins

Heat shock proteins (HSPs) are a group of proteins induced under stress conditions such as exposure to high temperatures, toxins, infections and other stresses. HSPs normally constitute up to 5% of the total intracellular proteins, but under stress conditions their levels can rise to 15% or more (Srivastava, 2002). They are induced to such high levels through powerful transcriptional activation, mRNA stabilization and preferential translation (Lindquist and Craig, 1988). HSPs are present in various compartments of the cell, such as cytosol, endoplasmic reticulum (ER) and mitochondria. Many functions have been attributed to HSPs, such as thermotolerance (Lindquist, 1986), folding and unfolding of proteins (Gething and Sambrook, 1992), degradation of proteins (Parsell and Lindquist, 1993), assembly of multisubunit complexes (Haas, 1991), and buffering the expression of mutations (Rutherford and Lindquist, 1998).

The best described HSP family is the 70 kDa HSP70. Some of the better known mammalian members are HSC70 (or HSP73), the constitutive cytosolic member; HSP70 (or HSP72), the stress-induced cytosolic form; GRP78 (or BiP), the ER form; and GRP75 (or mito-HSP70), the mitochondrial form. In yeast the homologs of HSC70 and BiP are known as Ssa1–4 and Kar2. In *E. coli*, the major form of HSP70 is DnaK. All the HSP70 proteins have three major domains. The N-terminal ATPase domain binds ATP (adenosine triphosphate) and hydrolyzes it to ADP (adenosine diphosphate). The exchange of ATP drives conformational changes in the other two domains. The substrate binding domain contains a groove with an affinity for neutral, hydrophobic amino acid residues. The C-terminal domain rich in alpha helical structure acts as a 'lid' for the substrate binding domain. When an HSP70 protein binds ATP, the lid is open and peptides bind and release relatively rapidly. When HSP70 proteins bind ADP, the lid is closed, and peptides are tightly bound to the substrate binding domain (Bukau and Horwich, 1998).

HSPs are now understood to be molecules that are relevant for immune surveillance, not only against infections, but also other abnormal situations such as the presence of cancer cells. Indeed, HSP are thought to function as “danger signals” within the body alerting the immune system to the presence of stressed, infected or diseased tissue (Gallucci and Matzinger, 2001). Their ability to interact with wide range of proteins and peptides, the latter property that is also shared by major histocompatibility complex (MHC) molecules, and the presence of certain HSP receptors on immune cells has made them uniquely suited to participate in innate and adaptive immune responses.

2.2 HSP-mediated antigen cross-presentation

Exogenous antigens endocytosed by antigen presenting cells (APC) are mainly loaded into the MHC class II molecules for recognition by CD4⁺ T-cells, whereas, in contrast, endogenous antigens (self and viral proteins) are loaded on the MHC class I molecules for recognition by CD8⁺ T-cells. However, in some conditions, APC can present

exogenous antigens on MHC I molecules, a process known as cross-presentation (Heath and Carbone, 2001; Yewdell and Bennink, 1999).

For the molecular chaperone function, HSP70 is equipped with two major functional domains, a C-terminal region that binds peptides and denatured proteins and an N-terminal ATPase domain that controls the opening and closing of the peptide binding domain (Bukau and Horwich, 1998). These two domains play important roles in the function of HSP70 in tumor immunity, mediating the acquisition of cellular antigens and their delivery to immune effector cells (Noessner et al., 2002; Srivastava and Amato, 2001). In most mammalian cells, damaged, denatured or superfluous proteins are degraded through the ubiquitin proteasome pathway to small peptides and after release from the proteasome the peptides are broken down into amino acids (Goldberg et al., 2002; Rock et al., 2002). A fraction of the peptides released from the proteasome are, however, not degraded further and are instead used for immune surveillance purposes (Gromme and Neefjes, 2002). Cytosolic heat shock proteins, such as HSP70 and HSP90 appear to bind those peptides before further degradation (Srivastava et al., 1994). Such peptides are taken up into the ER through an ATP-binding cassette (ABC) family transport system that involves the transporters associated with antigen processing (TAP) 1 and TAP2. TAP1 and TAP2 form a complex that transports peptides across the ER membrane and delivers them to MHC class I protein complexes (Schumacher et al., 1994; Shepherd et al., 1993). Peptides of suitable size and sequence are then bound by MHC class I molecules, transported via the vesicular system, and displayed on the cell surface where they are subject to surveillance by cytotoxic, CD8⁺ T lymphocytes (Neefjes et al., 1993). The cell surface display of antigens via the MHC class I pathway permits identification of non-self foreign antigens in microorganism-infected cells, which are then targeted for lysis by cytotoxic T lymphocytes (CTL).

2.3 HSP-mediated signaling and release of pro-inflammatory cytokines

One immunoregulatory function described for HSPs is activation of the innate immune system (Srivastava et al., 1998). Originally it was reported that the mycobacterial recombinant HSP60 induces the release of pro-inflammatory cytokines from monocyte-derived cells and macrophages (Friedland et al., 1993); (Peetermans et al., 1995). In recent studies human recombinant HSP60 as well as recombinant HSP70 were also recognized as being able to induce cytokine release from human peripheral blood mononuclear cells

(PBMCs), monocytes, and macrophages (Chen et al., 1999); (Asea et al., 2000). Furthermore, the cytokine-like function of HSPs was shown to be mediated via the CD14 and Toll-like receptor (TLR2 and TLR4) complex signaling pathways (Asea et al., 2002). The induction and secretion of cytokines, chemokines and other pro-inflammatory molecules as a result of HSP activation of macrophages and DCs is brought about by the translocation of NF κ B into the nuclei of these cells and activation of genes encoding these cytokines (Basu et al., 2000).

2.4 Extracellular source of HSP

The extracellular source of HSP is suggested to be derived mainly from two sources a) cells dying under a number of pathological conditions, such as necrosis (Mambula and Calderwood, 2006a) and b) active release from intact cells. Many cell types have been shown to secrete stress proteins, including neuronal cells, monocytes, macrophages, B cells and tumor cells of epithelial origin (Clayton et al., 2005; Davies et al., 2006; Robinson et al., 2005). This suggests that stress protein release is a widespread phenomenon and may be implicated in a number of physiological or pathological events. Little is known about how HSP70, a protein with no signal sequence for secretion, exits the cell by mechanisms other than escape from cells undergoing necrotic lysis. However, a number of non-canonical pathways for release of “leaderless” proteins are known. Macrophages upon stimulation with LPS and ATP are shown to secrete interleukin-1 β (IL-1 β) through secretory vesicles (MacKenzie et al., 2001). This pathway involves the entry of the leaderless protein into secretory lysosomal endosomes, migration of these organelles to the cell surface and release of the contents of the endolysosome into the extracellular space. Indeed HSP70 has been shown to be secreted from tumor cells and macrophages by this pathway (Mambula and Calderwood, 2006b). Furthermore, heat shock proteins such as HSP27, HSP70, HSC70 and HSP90 can be released within the lumen of “exosomes”, e.g., when B cells are exposed to heat shock (Clayton et al., 2005). Recently, our group showed that, from a HSP70 over expressing melanoma cell line, HSP70 was released in exosomes which were able to activate natural killer cells (Elsner et al., 2007). A lipid raft-based mechanism has also been suggested for membrane delivery and release of HSP70 (Broquet et al., 2003). Study of these processes is still in its infancy and further studies are required to determine the favoured pathways for HSP release by immune and non-immune cells.

2.5 HSP-based immunotherapy

The immunogenic potential of HSP-peptide complexes was first demonstrated in animal studies (Udono and Srivastava, 1993). Mice immunized with HSPs purified from a tumor were protected from a tumor challenge if the tumor cells used for the challenge were the same as those from which the HSP was purified. Hence, the immunogenicity of HSP was specific to the tumor from which it was purified and identical to the nature of immunity elicited by whole cells. However, HSPs derived from a different tumor or from normal tissue did not confer immunity (Udono and Srivastava, 1994). The requirement for peptide binding has been validated by the finding that HSPs deprived of peptides do not induce immunity (Udono and Srivastava, 1993) and that loading of ‘empty’ HSPs with peptides results in reconstitution of the HSP immunogenicity (Blachere et al., 1997). In a major study, mice bearing several different tumor types were treated with the respective-purified HSP preparation (Tamura et al., 1997). HSP preparations significantly reduced the size of the primary tumors, increased the survival of tumor-bearing mice, and cured mice of established metastases. These studies provided the basis for the development of HSP-based vaccines against cancer and infectious diseases in humans. Here the HSP vaccine is defined as the HSP molecule itself chaperoning peptides that reflect the entire antigenicity of the cell from which the HSP was purified. Several clinical trials with HSP70-based vaccines are ongoing at the moment. The most intensive clinical trials have been conducted on metastatic melanoma. A phase II clinical trial was carried out in stage IV melanoma patients who received heat shock protein glucose-regulated protein (gp) 96-

peptide complexes (5 or 50 µg) intradermally or subcutaneously at weekly intervals commencing 5 to 8 weeks after surgical resection of tumor metastases (Belli et al., 2002). Of 28 patients with measurable disease, two complete responses and three long-term stable diseases were observed. In 11 of 23 patients, enzyme-linked immunospot assays showed that this vaccination significantly increased the ability of PBMCs to release IFN γ when exposed to autologous or human leukocyte antigen (HLA)-A-matched melanoma cells. The results of randomized phase III clinical trial of heat shock protein gp96-peptide complexes were reported in 2006 (Srivastava, 2006). The trial randomized 322 patients with stage IV melanoma to the HSP vaccine (215 patients) and physician's choice therapy (107 patients), which included IL-2 and/or dacarbazine-/temozolomide-based therapy and/or complete tumor resection. Overall, there was no difference in survival benefit between patients with HSP vaccine and with the physician's choice treatment. However, patients who received at least 10 doses of vaccine experienced an extension in median survival of 29% compared with those who received the physician's choice treatment.

2.6 Heat shock protein receptors

The unique ability of HSP to activate both innate and adaptive immunity, and the powerful synergies that can result, can be explained by the recent identification of HSP receptors on DCs and macrophages. Some of the receptors described for binding HSP are CD91 (Basu et al., 2001), LOX-1 (Delneste et al., 2002), TLR2 and TLR4 (Asea et al., 2002), CD40 (Becker et al., 2002), CD36 (Nakamura et al., 2002), SR-A (Berwin et al., 2003) and CCR5 (Whittall et al., 2006). It is becoming increasingly clear that the two types of consequences due to engagement of APC by HSP, i.e., signaling and re-presentation of chaperoned peptides might be mediated by different sets of receptors. This idea derives support from the fact that certain receptors of HSP are endocytic receptors (e.g., CD91 and LOX-1), whereas certain others are specifically signaling receptors (e.g., CD40, TLR2 and TLR4). The HSP-peptide complexes are taken up by the APC through endocytic receptors and the peptides are re-presented on the MHC class I molecules. In the other mechanism, HSPs induce the secretion of pro-inflammatory cytokines, such as tumour necrosis factor- α (TNF- α), IL-1 β , IL-12, IL-6 and GM-CSF by macrophages and DCs (Asea et al., 2000; Basu et al., 2000; Chen et al., 1999), chemokines such as MCP-1, MIP-1 α and RANTES by macrophages (Lehner et al., 2000); (Panjwani et al., 2002) and nitric oxide by macrophages and DCs (Panjwani et al., 2002).

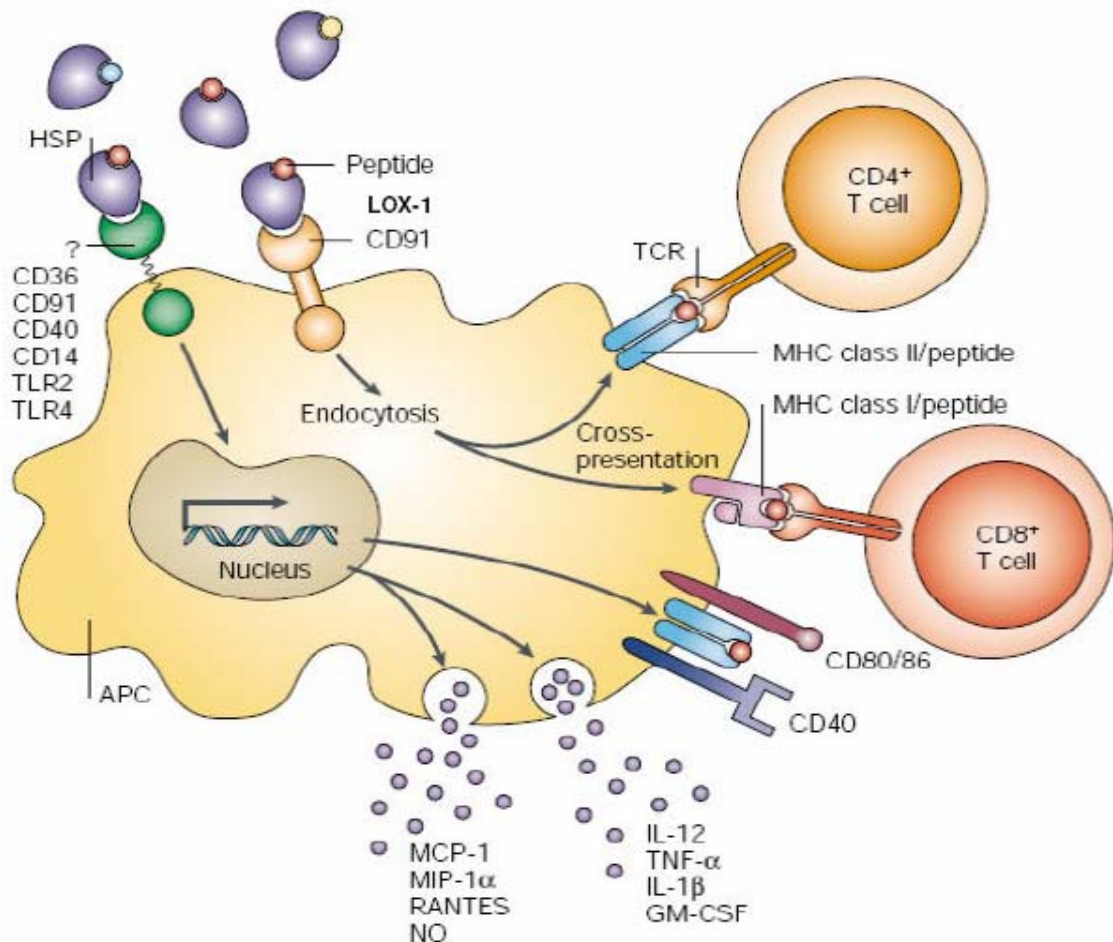


Fig 1. Heat shock proteins bind to receptors on antigen presenting cells and elicit innate and adaptive immune responses. The cross-presentation of heat shock protein-chaperoned peptides on MHC class I molecules is believed to be mediated by CD91 and LOX-1. Heat shock proteins can also elicit non-antigen specific innate immune responses including cytokine secretion via cell surface receptors such as CD36, CD91, CD40, CD14, TLR2, and TLR4. The figure is adapted from (Srivastava, 2002).

2.7 CD91 (Low density lipoprotein receptor-related protein 1)

CD91 is a multifunctional endocytotic receptor that belongs to the low density lipoprotein receptor gene family (Herz et al., 1988). It is one of the largest human receptors known. Its cDNA is composed of 14896 bp spanning 89 exons (Herz et al., 1990). CD91 is large multidomain 600 kDa protein consisting of amino terminal external domains (4400 amino acids), followed by a transmembrane domain (25 amino acids) and a cytoplasmic tail (100 amino acids) (Binder et al., 2000). It is a rather widely expressed protein that has a dual role in endocytosis and signal transduction (Herz and Strickland, 2001). It recognizes more than 30 different ligands that represent several families of proteins (Fig. 2). CD91 has also been shown to be a receptor for several heat shock proteins, including gp96 (Binder et al., 2000), HSP70, HSP90, and calreticulin (Basu et al., 2001). The interaction of CD91 with gp96 has been confirmed by several independent studies. It has been reported that α_2 -macroglobulin (α_2 M), a previously known CD91 ligand, competes with gp96 for binding to macrophages, as does gp96 itself (Habich et al., 2002). T-helper

cells express CD91 on the cell surface and gp96 binds to CD91 on the T-helper cell surface (Banerjee et al., 2002). α_2M inhibited strongly the binding of HSP70 to human macrophages and displayed a weaker but detectable inhibition of the same reaction on human myeloid DCs (Delneste et al., 2002). It has also reported that α_2M inhibits the binding of HSP70 to PBMCs (Martin et al., 2003). Interaction of HSP-peptide complexes with CD91 leads to internalization of the complexes and presentation of peptides by MHC class I molecules (Binder et al., 2000).

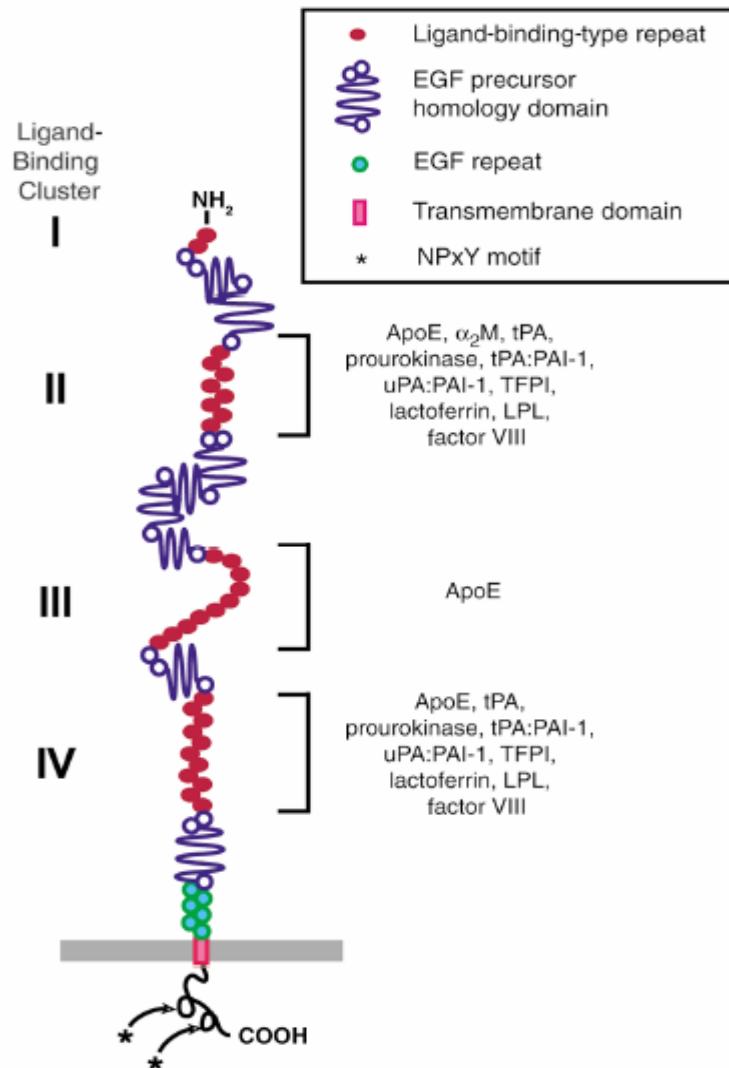


Fig 2. Binding of CD91 ligands to different ligand binding clusters. Four cysteine-rich ligand binding clusters (red ovals) in the CD91 receptor are shown. Each ligand binding cluster is followed by 1-4 epidermal growth factor precursor homology domains (blue). Binding of various ligands to different clusters is indicated. The NPxY motifs in the cytoplasmic tails are indicated by asterisks. The figure is taken from (Herz and Strickland, 2001).

Increased expression of CD91 was recently shown on long-term nonprogressors (LTNPs) with HIV infection (Stebbing et al., 2003). The authors argued that enhanced representation of HSP-chaperoned peptides in the LTNPs may be responsible for enhanced

presentation of HIV epitopes and enhanced cellular immunity and consequent viral resistance.

2.8 Polymorphisms in the CD91 gene

A polymorphism in the promoter region of CD91 at -25 position (-25 C>G) has been described (Schulz et al., 2002). The authors evaluated the effect of this polymorphism in patients with coronary artery disease. They observed an increased frequency of CG genotype carriers correlating with the severity of the coronary artery disease. This polymorphism (-25 C>G) leads to the creation of a new GC-box that is recognized by the constitutively expressed SP1 transcription factor (Schulz et al., 2002). The individual CD91 gene expression depending on polymorphic variants was then evaluated in patients with severe coronary artery disease and healthy controls. In monocytes an increase in the CD91 mRNA level for the heterozygous CG-carriers was found compared to the wildtype (CC-carriers).

A polymorphism in exon 3 (766 C>T) of the CD91 gene has been shown to be associated with Alzheimer's disease (AD), breast cancer (BC) and myocardial infarction (MI). Among 157 patients with late-onset AD (85 with a family history and 72 without a family history of AD), an increased frequency of the C allele of exon 3 polymorphism compared to controls has been found (Kang et al., 1997). The authors suggested that the polymorphism, predicted to be silent, may be in linkage disequilibrium (LD) with a putative nearby AD susceptibility locus. Further studies (Baum et al., 1998; Hollenbach et al., 1998) also provided evidence of increased frequency of the 766 C allele in patients with AD. No association with the exon 3 polymorphism and development of AD has been found in a Northern Ireland population (McIlroy et al., 2001). Furthermore, an association of T allele of the 766 C>T exon 3 polymorphism with an increased risk of breast cancer development in women of Caucasian origin has been shown (Benes et al., 2003).

2.9 Expression of CD91

Increased expression of CD91 was observed on monocytes of HIV-1 infected LTNPs compared to HIV-1 infected patients on HAART therapy (Stebbing et al., 2003). In the same study the authors observed that the CD91 expression was decreased on monocytes after incubation with HIV-1. The assumption was that the binding of HSPs which have been found within virion coats (Gurer et al., 2002) to CD91 decreases anti-CD91 antibody binding by competition for the binding site. Alternatively, the interaction of virion HSP70 with CD91 may lead to endocytosis of the complex, reducing the availability of surface CD91 for binding the anti-CD91 antibody. Furthermore, high levels of CD91 on monocytes may lead to the enhanced cross-presentation of HIV antigens by these cells and to the consequent enhanced stimulation of anti-HIV CTLs. This observation may explain the preservation of CD8⁺ cytotoxic T-lymphocyte responses that have been consistently observed in LTNPs (Stebbing et al., 2003). Increased expression of CD91 on CD14⁺ monocytes was also observed in HIV-1-exposed yet seronegative subjects (Kebba et al., 2005) and interestingly also on advanced melanoma slow progressors (Stebbing et al., 2004).

2.10 Lectin-like oxidized low-density lipoprotein receptor-1 (LOX-1)

LOX-1 is a member of the scavenger receptor family, a structurally diverse group of cell surface receptors of the innate immune system that recognize modified lipoproteins. It has four domains, a short 34-residue cytoplasmic domain, a single 17-residue transmembrane domain, and an extracellular region consisting of an 82-residue neck domain followed by a 130-residue C-terminal C-type lectin-like domain.

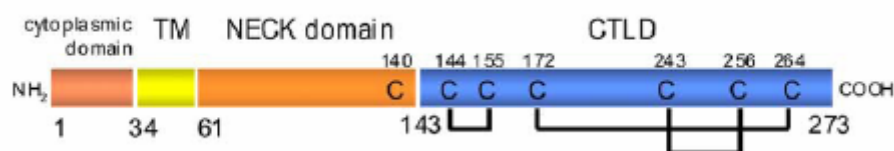


Fig 3. Different domains of human LOX-1. A schematic representation of four domains of LOX-1 is shown. The start point and the end of each domain are indicated by the number of the respective amino acid in the primary structure of LOX-1. The position of cysteine residues and the intrachain disulphide bridges are indicated. The cysteine residue at position 140 in the neck domain is responsible for homodimer formation. The figure is taken from Okhi et al. (2005).

LOX-1 was originally identified from cultured aortic endothelial cells as a receptor for oxidized LDL (Ox-LDL); however, recent investigations revealed that LOX-1 has diverse roles in the host-defense system and inflammatory responses, and it is involved in the pathogenesis of various diseases such as atherosclerosis-based cardiovascular diseases and septic shock. Beside Ox-LDL, LOX-1 recognizes multiple ligands including apoptotic cells, platelets, advanced glycation end products and bacteria. Upon recognition of Ox-LDL, LOX-1 is observed to initiate Ox-LDL internalization and degradation as well as the induction of a variety of pro-atherogenic cellular responses. In addition to binding Ox-LDL, LOX-1 is reported to be a receptor for HSP70 on DCs and to be involved in antigen cross-presentation to naive T cells (Delneste et al., 2002). The interaction between HSP70-peptide complexes and LOX-1 promotes antigen cross-presentation on DCs and the activation of an *in vitro* and *in vivo* tumor antigen-specific T cell immune response (Delneste et al., 2002).

Members of the scavenger receptor family differ in their organization at the membrane. Class A macrophage scavenger receptors (SR-A) are trimeric transmembrane glycoproteins with three extracellular C-terminal domains connected by a long triple-helical stalk. The trimeric form is necessary for effective ligand binding (Kodama et al., 1990). In contrast to class A scavenger receptors, class B scavenger receptors (SR-B) exist as monomers on the cell surface. LOX-1, the class E scavenger receptor has been traditionally thought to exist and to function as a monomer. However, it has been demonstrated that that human LOX-1 exists as a covalent homodimer with the two 40-kDa monomers linked by an interchain disulfide bond through their Cys140 residues (Xie et al., 2004). These authors also demonstrated that the dimers might interact further to form non-covalently associated oligomers. Recently, it has been shown that the oligomer is the functional unit of LOX-1 and that the oligomerization is dependent on the LOX-1 density on the cell surface (Matsunaga et al., 2007).

2.11 Expression of LOX-1 and its signaling functions

In vivo, the basal expression of LOX-1 is very low on many cell types. However, the LOX-1 expression can become enhanced by several pathological conditions, including hypertension (Nagase et al., 1997), diabetes mellitus (Chen et al., 2001a), and hyperlipidemia (Chen et al., 2000). These pathological states elevate LOX-1 levels via intracellular signaling and transcription factor activation causing increased LOX-1 mRNA synthesis. LOX-1 mRNA and protein levels are also elevated by pro-inflammatory, pro-oxidant, and mechanical stimuli such as Ox-LDL (Li and Mehta, 2000), TNF- α (Kume et al., 1998), phorbol ester (Li et al., 2002), angiotensin II (Li et al., 1999), and fluid shear stress (Murase et al., 1998). LOX-1 induction has been suggested to induce several intracellular signaling pathways, including protein kinases and transcription factors, regulating the expression of genes related to atherosclerosis. These signaling pathways include p38 MAPK, protein kinase C, transcription factor NF- κ B, and AP-1. In a recent study, it was shown that in endothelial cells another LOX-1 dependent signaling pathway is apoptosis (Chen et al., 2004). In this study, the authors demonstrated that Ox-LDL induces a caspase-9 dependent apoptotic pathway, and that this process is LOX-1 dependent, since LOX-1 mRNA antisense significantly blocked Ox-LDL-induced apoptosis.

2.12 LOX-1 polymorphisms and disease association

Luedecking-Zimmer and colleagues first reported evidence of association of a 3' untranslated region (UTR) 188 C>T polymorphism of LOX-1 (rs1050283) with AD in a white North American case-control sample of more than 1500 subjects (Luedecking-Zimmer et al., 2002). Individuals who carried the apolipoprotein (APO) E*4 allele (*APOE**4 allele on chromosome 19 confers an increased risk of late-onset AD) and were homozygous for TT genotype of 3'UTR polymorphism were at increased risk for AD. Also others presented evidence that genetic variation in the LOX-1 gene might modify the risk of AD (Lambert et al., 2003). These authors described an association of the 3'UTR polymorphism of LOX-1 with AD in French sporadic and American familial cases. The age- and sex-adjusted odds ratio between the CC/CT genotypes versus the TT genotypes was 1.56 in the French sample and 1.92 in the American sample. In studies of LOX-1 expression in lymphocytes from AD cases compared with controls, they found the LOX-1 expression significantly lower in AD cases bearing the CC and CT genotypes. Contrary to these findings (Lambert et al., 2003); (Luedecking-Zimmer et al., 2002), another study found no evidence favouring a genetic involvement of the 3'UTR (188 C>T) polymorphism of the LOX-1 gene in AD (Bertram et al., 2004). This study involved a large sample of 437 AD families from the American population.

In 2 independent studies, an association between polymorphisms in the LOX-1 gene and myocardial infarction has been reported (Tatsuguchi et al., 2003); (Mango et al., 2003). Tatsuguchi and colleagues identified a single nucleotide polymorphism (SNP) in the LOX-1 gene, a 501G>C transversion, resulting in a lysine to asparagine (K167N) substitution (Tatsuguchi et al., 2003). In 102 patients with a history of MI, the authors found a significantly higher frequency (38.2%) of the 501G>C polymorphism compared to 102 controls (17.6%). Another study showed that the polymorphism in the 3'UTR of the LOX-1 gene, 188C>T, was significantly associated with MI in a group of 150

patients (Mango et al., 2003). Genotypes with the T allele were found in 91.3% of patients compared to 73.8% of controls, yielding an odds ratio of 3.74. In a study of 589 white and 122 black women who underwent angiography for suspected ischemia, it has been found that the frequency of the 3'UTR T allele was significantly higher in whites than in blacks (Chen et al., 2003). Among white women, the frequency of the T allele was 67.9%, 75.0%, and 79.2% in individuals with less than 20%, 20 to 49%, and greater than 49% stenosis, respectively. The T allele carriers had significantly higher anti-Ox-LDL IgG levels than those with the CC genotype and electrophoretic mobility shift assay (EMSA) data indicated that the 3'UTR binds so far uncharacterized regulatory proteins and that the C allele has a higher affinity for binding of these proteins than the T allele.

2.13 The lectin-like domain of LOX-1 and its ligand binding

In 2001, a serial-deletion analysis of the lectin-like domain of LOX-1 has been performed and defined that this domain is essential for binding of Ox-LDL (Chen et al., 2001b). The authors showed that deletion of last 10 amino acids of LOX-1 completely abrogated the Ox-LDL binding activity. Furthermore, substitutions of Lys-262 or Lys-263 to alanine (K262A or K263A) moderately reduced the binding and internalization of Ox-LDL. When both lysine residues were replaced simultaneously (K262A and K263A), the ligand binding was decreased further. This indicates that positive charge of the pair of basic amino acid residues constitutes an important part of the ligand binding activity. The 501G>C polymorphism in the exon 4 of LOX-1 causes an amino acid substitution at codon 167 (Lys>Asn) which is located within the C-type lectin domain of the protein. This could have an influence on the binding of Ox-LDL to the LOX-1 receptor. HSP70 has recently been shown to bind to LOX-1. Hence, the effect of this polymorphism on binding of LOX-1 to HSP70 and its internalization could be of clinical significance, since LOX-1 is also responsible for HSP70-mediated antigen cross-presentation.

3. AIM

The aim of the project was to determine whether polymorphisms of the heat shock protein receptor genes affect functions of HSP70 in the immune system. Such polymorphisms could affect heat shock protein receptor expression levels, receptor affinity, receptor internalization, receptor signaling, and receptor distribution on immune cells. Such effects could in turn influence the immunological functions of HSP70 which might be important for HSP70-based immunotherapies of infectious and malignant diseases. Increased expression of CD91 has been linked to improved immune response against HIV and malignant melanoma. Our first focus was to analyze the polymorphisms of CD91 gene that might influence its expression. For this purpose, we chose two SNPs, a promoter SNP which has been reported to increase the expression of CD91 mRNA in monocytes and an exon 3 SNP shown to be associated with several diseases such as Alzheimer's disease, myocardial infarction and breast cancer. Furthermore, we analyzed SNPs in the LOX-1 gene to study if they influence its expression and ligand binding function. We chose to look at two SNPs, one of which occurs in the exon 4 of LOX-1 gene and other in the 3'UTR region of the gene. The exon 4 SNP was particularly interesting because it causes an amino acid substitution in the ligand binding domain of the protein, and hence could alter the binding affinity of its ligand. The SNP in the 3'UTR region was shown to be associated with several diseases like myocardial infarction, Alzheimer's disease and stroke and was also shown to alter the binding of uncharacterized regulatory proteins.

4. Materials

4.1 Chemicals/Reagents

Name	Supplier
Acetic acid	Merck
Acrylamide solution (40%)	Carl Roth
Agarose	Invitrogen
Ammonium persulphate (APS)	Sigma
Biocoll	Biochrom
Bisacrylamide	AppliChem
Boric acid	Merck
Bovine Serum Albumin (BSA), Fraction V	Merck
Bromophenol blue	Merck
Calcium chloride (CaCl ₂)	Merck
Chloroform	Merck
Chymostatin	AppliChem
Coomassie brilliant blue	Sigma
Diaminobenzoic acid (DAB)	Sigma
Dimethylsulfoxide (DMSO)	Merck
Dithiothreitol (DTT)	Sigma
Disodium hydrogen phosphate	Merck
dNTP (dATP, dGTP, dCTP and dTTP)	Genecraft
Dulbecco's Modified Eagle's Medium (DMEM)	Biochrom
Ethanol	Merck
Ethidium bromide	Merck
Ethylendiamine tetraacetic acid (EDTA)	Carl Roth
FACS lysing solution	Becton Dickinson
Fetal calf serum (FCS)	Biochrom
Formaldehyde	Biochrom
Formamide	Fluka
Glycerol	Carl Roth
Glycine	Carl Roth
Heparin	Rotexmedica GmbH
N-2-Hydroxyethylpiperazine-N'-2-ethanesulfonic acid (HEPES)	Sigma
Hi-Di™ Formamide	Applied Biosystems
Hydrochloric acid (HCl)	Merck
Hydrogen peroxide	Merck
Isopropyl β-D-thiogalactopyranoside (IPTG)	Carl Roth
Isoamyl alcohol	Merck
Isopropanol	Merck

Leupeptin	AppliChem
β-Mercaptoethanol	Sigma
Methanol	Merck
Metafectene	Biontix
Nonidet P40 (NP-40)	AppliChem
Oligo-dT	Promega
Paraformaldehyde (PFA)	Merck
Pepstatin	AppliChem
Phenylmethylsulphonyl fluoride (PMSF)	Carl Roth
Phenol (Tris-saturated)	Biomol
Phosphate buffered saline (PBS)	Biochrom
Phosphoric acid	Merck
Ponceau S	Sigma
Potassium acetate	Merck
Propidium iodide	Sigma
Pyruvic acid	Sigma
Random hexamers	Promega
RNasin	Promega
Saponin	Carl Roth
Saccharose	Carl Roth
Select agar	Gibco BRL
Select peptone	Gibco BRL
Select yeast extract	Gibco BRL
Sodium acetate	Carl Roth
Sodium azide	Sigma
Sodium bicarbonate	Merck
Sodium chloride	Carl Roth
Sodium dihydrogen phosphate	Merck
Sodium deoxycholate	Sigma
Sodium dodecyl sulfate (SDS)	Carl Roth
Sodium hydroxide	Merck
Sodium pyruvate	Biochrom
N,N,N',N'-Tetramethylethylenediamine (TEMED)	AppliChem
Tris	Carl Roth
Triton X-100	Sigma
Trizol	Invitrogen
Trypan blue	Sigma
Tween 20	AppliChem
Urea	Carl Roth
Xylene cyanol	Merck

4.2 Instruments

Name	Type	Manufacturer
Autoclave	A40145	Webeco
Balances	Vicon	Acculab
	BP 61	Sartorius
Centrifuges	Multifuge 1 L	Heraeus
	Multifuge 3 S-R	Heraeus
	3K30	Sigma
	Labofuge GL	Heraeus
	Minifuge GL	Heraeus
	Sorvall RC-5B	Dupont Instruments
Flow cytometer	FACScan	Becton Dickinson
Gel dryer	No. 85031407	Zabona AG, Basel
Heat block	SBH 130	Stuart
Horizontal shaker	Celloshaker Variospeed	Biotec-Fischer
Incubators	Hera cell 150	Heraeus
Laminar flow	HLB 2448	Haraeus
	HLB 2472	Haraeus
Magnetic stirrer	VIC 1501	IKA
Microscopes	No. 471202-9901	Carl Zeiss
	No. 491220	Ernst Leitz GmbH
Microwave oven	MWS 2822	Bauknecht
PCR thermocycler	Gene Amp PCR System	Applied Biosystems
	2700	
	T personal	Biometra
pH meter	RH basic 2	Schott
Polaroid camera	CU-5	Bachofer
Power supplies	Power Pack P25	Biometra
	Boskamp PheroStat 273	Schütt Labortechnik GmbH
Real-time PCR cycler	ABI 7500	Applied Biosystems
Shaking incubator	IKC-1-U	Kühner AG
Spectrophotometer	Ultrospec II	Biochrom
SpeedVac	SC 110	Schütt Labortechnik GmbH
Sequencer	3130XL	Applied Biosystems
Vortex	MS1 minishaker	IKA

4.3 Antibodies

4.3.1 Primary

Name	Species	Isotype	Conjugation	Clone	Supplier
anti-CD91	mouse	IgG ₁	FITC	A2MR- α 2	BD Pharmingen
anti-CD14	mouse	IgG _{2a}	PE	Tuk4	Caltag
anti-TLR2	mouse	IgG _{2a}	PE	TL2.1	Stressgen
anti-TLR4	mouse	IgG _{2a}	FITC	HTA125	Stressgen
anti-CD36	mouse	IgM	FITC	CB38(NLO7)	BD Pharmingen
anti-LOX-1	mouse	IgG ₁	-	23C11	Hycult Biotechnology
anti-HSP70	mouse	IgG ₁	-	C-92F3A5	Stressgen
anti-HSC70	mouse	IgG _{2a}	-	1B5	Stressgen
anti-Ox-LDL	goat	IgG	-	Polyclonal	Santa Cruz
anti- β -actin	mouse	IgG ₁	-	AC-15	Sigma

4.3.2 Secondary

Name	Species	Conjugation	Supplier
anti-mouse IgG (H+L)	Goat	FITC	Caltag
anti-mouse IgG (H+L)	Goat	TC	Jackson ImmunoResearch
anti-mouse IgG	Goat	HRP	Dianova
anti-goat IgG	Rabbit	HRP	Jackson ImmunoResearch

4.3.3 Isotype control

Name	Species	Conjugation	Supplier
IgG ₁	mouse	FITC	Caltag
IgG _{2a}	mouse	PE	Caltag
IgM	mouse	FITC	Caltag

4.4 Kits

Name	Supplier
BigDye Cycle Sequencing Kit	Applied Biosystems
DNA Clean and Concentrator	Zymo Research
FluoReporter FITC Protein Labeling Kit	Molecular Probes
Plasmid Midi Kit	Qiagen

QuantiTect Primer Assay (GAPDH)	Qiagen
Reverse Transcription System	Promega
SV Total RNA Isolation System	Promega
SYBR green qPCR kit	Applied Biosystems
TaqMan Gene Expression Assay	Applied Biosystems
TaqMan Universal PCR Master Mix	Applied Biosystems
Transcriptor High Fidelity cDNA Synthesis Kit	Roche
Zymoclean Gel DNA Recovery Kit	Zymo Research

4.5 Plastic ware

Type	Supplier
0.5 ml tubes	Sarstedt
1.5 ml tubes	Sarstedt
2.0 ml tubes	Sarstedt
13 ml tubes	Sarstedt
15 ml tubes	Sarstedt
50 ml tubes	Sarstedt
0.2 ml PCR tubes	Sarstedt
96-well PCR plate	Sarstedt
96-well optical PCR plate	Applied Biosystems
Cell culture 96-and 24-well plates	Sarstedt
Cell culture flasks (250 ml)	Sarstedt
Cell culture plates (10 cm)	Sarstedt
Cryotubes	Nunc A/S
	Becton Dickinson
FACS tubes	GmbH
Petri dish	Sarstedt
Pipette tips (10 µl, 200 µl & 1000 µl)	Sarstedt
Pipettes (10 ml)	Sarstedt
Sterile filters (2.2 µm and 4.5 µm)	Sarstedt
Syringes (5 ml)	Dispomed Witt oHG
Syringes (10 ml)	Dispomed Witt oHG
Syringes (20 ml)	Dispomed Witt oHG

4.6 Miscellaneous

Name	Supplier
Amicon filters	Millipore
Cell scraper	Sarstedt
Electrophoresis chambers	Peqlab Biotechnologies
Glassware	Schott
Homogenizer	B. Braun
Microsyringe	Hamilton
Motorized pipette controller	Desaga
Nitrocellulose membrane	Whatman GmbH

Pasteur pipette
 Pipettes (2 µl, 20 µl, 200 µl, 100 µl)
 Whatmann paper
 96-well PCR plate optical adhesive film

WU
 Eppendorf
 Schleicher & Schuell
 Applied Biosystems

4.7 Primers

Primer	Forward Sequence (5'to 3')	Reverse Sequence (5'to 3')
CD91 Promoter	CGGGCAGCGCGTCAAATC	ACCGGGTAGGGGAGCCTT
CD91 Promoter AS (C)	TCTCCCCCATCAGCCCCC	
CD91 Promoter AS (G)	TCTCCCCCATCAGCCCCG	
CD91 Ex3p	ACAGAGTAAGGCCAGCGAT	TGTCTGACCAAGCTCCAGG
CD91 Ex3p AS (C)	CAGGACTGCATGGAC	
CD91 Ex3p AS (T)	CAGGACTGCATGGAT	
CD91 Tag 10	CAGGCTGTCAGAGGCTTACTGTG	GCCCAGCAAGAGAAAGACAGGA A
CD91 Tag 10 AS (C)		CTGAATATGAATAATTTTCCCAA GATG
CD91 Tag 10 AS (G)		CTGAATATGAATAATTTTCCCAA GATC
CD91 Tag 23	TGGTGATAGAGGTTGGGAGGAGT	ACCCGGCTGACAACCTAACTCT
CD91 Tag 23 AS (T)		GCAGTTTTTTTCCATGTATCATCA
CD91 Tag 23 AS (C)		GCAGTTTTTTTCCATGTATCATCG
CD91 Tag 27	AGTAAGTGGTGTAATCGGAGGCA	TAGTGGCTCCCTTTCCAGC
CD91 Tag 27 AS (T)		AAGCAGGGGAGAGGCTAAAA
CD91 Tag 27 AS (C)		AAGCAGGGGAGAGGCTAAAG
CD91 Tag 34	TTGTCCACTGACCTACTCAACAG	ACAGAAGCTGGGATGAGAGAA
CD91 Tag 34 AS (C)	CCCCAGGAGAAGCTGGTAC	
CD91 Tag 34 AS (G)	CCCCAGGAGAAGCTGGTAG	
CD91 Tag 67	ACCAAGATCACATGGCCCAATGG	CACTGCAGTTCTCAATCGCAG
CD91 Tag 67 AS (C)		GTGTCCTCAGGCCATATCCTCCG
CD91 Tag 67 AS (T)		GTGTCCTCAGGCCATATCCTCCA

Rhe CD91 Promoter	TTCCCCTAGAAAATCGGGC	TTCACTCCTCGCTGCTCTTT
CD91 Ex3p Nested	ATGCCAGCCAAACGAGCATAA	AAGGTAAATCTAGGCAGGGGA
LOX-1 FL	TGACTGCTTCACTCTCTCATT	CCCAAGTGACAAAGAATAGC
LOX-1 Ex4p	TGAGAGA ACTAAGGGGATCA	CCAGATTAATTTCCCTATCA
LOX-1 Ex4p AS (C)	CAAGCACTTCTCTTGGCTC	
LOX-1 Ex4p AS (G)	CAAGCACTTCTCTTGGCTG	
LOX-1 3'UTR	ACTTGGGTGCCAAACATGAGA	AATTTTAGGAGTGTGAGGGGA
LOX-1 3'UTR AS (C)	TCAACATTTTTGATTCTAGCTAC	
LOX-1 3'UTR AS (T)	TCAACATTTTTGATTCTAGCTAT	
LOX-1 Ex5		AAGTGGGGCATCAAAGGAGAA
LOX-1 Tag 45	TGAAAAGTAATCACAAGATAACCAG	TTCTTGGAGACTCTTGTGACACAG
LOX-1 Tag 45 AS (C)	TGACTATTAGTAGGAAATGTCAT TAGC	
LOX-1 Tag 45 AS (T)	TGACTATTAGTAGGAAATGTCAT TAGT	
LOX-1 Ex4 SDM	CATTTAACTGGGAAAACAGCCAA GAGAAGT	
Lox-1 5'UTR cDNA	CCCGAATTCGAGCTCGGTA	TCATCAGGCTGGTCCTTCACA
Lox-1 3'UTR cDNA	CGGAAA ACTGCATTTTAGCTGCC	CAATCAAGGGTCCCCAAACTCAC

4.8 Enzymes

Name

Supplier

DNase

Promega

DNA ligase

New England Biolabs

Lysozyme

Sigma

MMLV reverse transcriptase

Promega

Pfu DNA polymerase

Promega

RNase A

Roche

Proteinase K

Merck

Taq DNA polymerase

Genecraft

Trypsin

Biochrom

Restriction enzymes

BccI	New England Biolabs
EcoRV	New England Biolabs
RsaI	New England Biolabs
NheI	MBI Fermentas

4.9 Antibiotics/Drugs

Name	Supplier
Ampicillin	Sigma
Doxycycline	Sigma
Geneticin (G418 sulphate)	AppliChem
Kanamycin	Sigma
Penicillin/Streptomycin sulphate	Sigma
Puromycin	AppliChem

4.10 Cell lines

Name	Supplier
CHO-K1	ATCC
HT-1080	ATCC (Prof. Thomas Dierks)

4.11 Vectors

Name	Supplier
pBI	Clontech
pcDNA3.1/CT-TOPO-GFP	Invitrogen
pcDNA3.1/NT-TOPO-GFP	Invitrogen
pAcGFP1-N1	Clontech
pPUR	Clontech

4.12 Ladders/Markers

Name	Supplier
50 bp DNA ladder	Genecraft
100 bp DNA ladder	Genecraft

1 kb DNA ladder
Protein marker (SDS-6H)

Genecraft
Sigma

4.13 Bacterial strains

Name	Supplier
<i>E.coli</i> DH5 α	Invitrogen
<i>E.coli</i> TOP10	Invitrogen

4.14 Solutions and buffers

4.14.1 Protein concentration determination

Bradford reagent	100 mg Coomassie brilliant blue 50 ml 95% Ethanol 100 ml 85% Phosphoric acid
------------------	--

4.14.2 SDS-Page / Western blotting

2 X Laemmli buffer	125 mM Tris-HCl (pH 6.8) 4% SDS 0.004% Bromophenol blue 20% (w/v) Glycerol 10% β -Mercaptoethanol
--------------------	---

RIPA buffer	25 mM Tris (pH 7.6) 150 mM NaCl 1% NP-40 1% Sodium deoxycholate 0.1% SDS
-------------	--

Protease inhibitor cocktail (300 X)	Leupeptin 2.5 mg/ml in dH ₂ O Sodium azide 0.2 mg/ml in dH ₂ O PMSF 34.8 mg/ml in Ethanol Pepstatin 5 mg/ml in Methanol Chymostatin 5 mg/ml in DMSO
-------------------------------------	---

Electrophoresis buffer	SDS (w/v) 10 g/10 litre Glycine (w/v) 144.27 g/10 litre Tris (w/v) 60.53 g/10 litre 10% APS in dH ₂ O
------------------------	---

Separating gel (10% acrylamide)	40% Acrylamide solution 5 ml Separating buffer (1.5 mM Tris, pH 8.8; 0.4% SDS) 5 ml dH ₂ O 9.8 ml 10% APS 200 µl TEMED 20 µl
Stacking gel (4% acrylamide)	40% Acrylamide solution 1 ml Stacking buffer (0.5 mM Tris, pH 6.8; 0.4% SDS) 2.5 ml dH ₂ O 6.4 ml 10% APS 100 µl TEMED 10 µl
Coomassie staining solution	0.2% Coomassie brilliant blue 30% Methanol 10% Acetic acid
Ponceau S staining solution	0.5% Ponceau S (w/v) 1% Acetic acid (v/v) Solution was diluted to 100 ml with dH ₂ O
PBST	PBS with 0.05% Tween 20
Transfer buffer	Electrophoresis buffer with 20% Methanol
DAB solution	50 ml PBS 25 mg DAB 50 µl 30% H ₂ O ₂

4.14.3 Recombinant HSP70 preparation

Lysis buffer (pH 8.0)	50 mM Tris 1 mM EDTA 25% Saccharose 0.5% Lysozyme
Detergent buffer (pH 7.5)	20 mM Tris 2 mM EDTA 200 nM NaCl 1% Sodium deoxycholate 1% Nonidet P40
Wash buffer (pH 7.5)	1 mM EDTA 0.5% Triton X-100
Mono-S buffer	8.5 M Urea 10 mM Phosphate buffer 1 mM β-Mercaptoethanol

Phosphate buffer (10 ml)	6.48 ml 1 M Sodium dihydrogen phosphate 3.52 ml 1 M Disodium hydrogen phosphate
--------------------------	--

4.14.4 Cell culture medium

DMEM medium (per litre)	8.26 g DMEM 3.7 g Sodium bicarbonate 0.11 g Sodium pyruvate 1, 00,000 U Penicillin 100 mg Streptomycin sulfate 10% FCS (v/v)
-------------------------	---

HEPES-buffered DMEM (per litre)	8.26 g DMEM 4.7 g HEPES pH 7.2
---------------------------------	--------------------------------------

4.14.5 Preparation of DNA

DNA lysis buffer	50 mM Tris (pH 8.0) 100 mM EDTA (pH 8.0) 0.5% SDS
------------------	---

Proteinase K	10 mg/ml of proteinase K were dissolved in dH ₂ O and stored at -20 °C.
--------------	--

4.14.6 Analysis of DNA

DNA loading dye	0.025 g Bromophenol blue 0.025 g Xylene cyanol 1.25 ml 10% SDS 12.5 ml Glycerol 6.25 ml dH ₂ O
-----------------	---

10 X TBE buffer (pH 8.3)	121.1 g Tris 51.35 g Boric acid 3.72 g EDTA The components were dissolved in 800 ml of dH ₂ O and the pH was adjusted to 8.3 and the solution was diluted to 1 litre.
--------------------------	---

4.14.7 Mini-prep of plasmid DNA

LB medium	10 g Select peptone 5 g Select yeast extract 10 g NaCl
-----------	--

The components were dissolved in dH₂O and the solution was diluted to 1 litre. LB medium was sterilized by autoclaving and stored at 4 °C.

Buffer P1	50 mM Tris (pH 8.0) 10 mM EDTA 100 µg/ml RNase A The buffer P1 was stored at 4 °C after addition of RNase A.
RNase A	RNase A was dissolved at a concentration of 10 mg/ml in 0.01 M sodium acetate (pH 5.2) and heated at 100 °C for 15 minutes. The solution was allowed to cool to room temperature and the pH was adjusted by adding 0.1 volume of 1M Tris-HCl (pH 7.4). RNase solution was dispensed into aliquots and stored at -20 °C.
Buffer P2	200 mM NaOH 1% SDS (w/v)
Buffer P3	3 M Potassium acetate (pH 5.5)

4.15 Study samples

4.15.1 HIV-infected human cohort

Frozen PBMCs were obtained for the samples in the HIV infected human cohort. The frozen PMBCs were thawed and approximately 1 million cells were taken for the flow cytometry analysis. Remaining cells were divided into two aliquots for the extraction of DNA and RNA. For the samples, where the cell number was low, cells were taken only for flow cytometry and DNA extraction. The subjects in the HIV-1 positive cohort were categorized into three groups.

LTNPs (N=8) LTNPs had been diagnosed as HIV-1 positive for a duration of more than 10 years, had never received anti-retroviral treatment, and consistently maintained a CD4 count of greater than 400 cells/mm³ and CD8 counts greater than 800 cells/mm³ (Stebbing et al., 2003).

TIMS (Trizivir induction maintenance study) (N=10) Patients enrolled in the Trizivir induction maintenance study (TIMS) were receiving first line combination (efavirenz and combivir) anti-retroviral therapy (Woolfson et al., 2005).

RESTART (A randomized trial to investigate the recycling of stavudine and didanosine with or without hydroxyurea in salvage therapy) (N=11) These were HIV-1-infected individuals with treatment failure requiring salvage therapy. Patients enrolled in the randomized trial to investigate the recycling of stavudine and didanosine (RESTART)

had received a median of 4 previous lines of anti-retroviral therapy with non-nucleoside reverse transcriptase or protease inhibitor–based regimens and at the time of blood draw and freezing, were receiving the nucleoside analogs stavudine and didanosine (Woolfson et al., 2005).

4.15.2 SIV-infected rhesus macaques and control animals

Blood was obtained from rhesus macaques before infection and at several time points after SIV infection. Blood was also obtained from uninfected rhesus macaques (controls).

4.15.3 Human healthy volunteers

Blood of normal healthy volunteers was obtained.

4.16 List of suppliers

Acculab	See Sartorius
AppliChem GmbH	Ottoweg 4, 64291 Darmstadt, Germany
Applied Biosystems	850, Lincoln Center Drive, Foster City, CA 94404, USA
Bauknecht Hausgeräte GmbH	Industriestrasse 48, 70565 Stuttgart, Germany
Bachofer GmbH	7410 Reutlingen, Germany
BD Pharmingen	See Beckton Dickinson
Becton Dickinson GmbH	Tullastrasse 8-12, 69126 Heidelberg, Germany
Biochrom AG	Leonorenstrasse 2-6, 12247 Berlin, Germany
Biometra Biomedizinische Analytik GmbH	Rudolf-Wissell-Strasse 30, 37079 Göttingen, Germany
Biomol GmbH	Waidmannstrasse 35, 22769 Hamburg, Germany
Biontex Laboratories GmbH	Am Klopferspitz 19, 82152 Martinsried/Planegg, Germany
Biotec-Fischer GmbH	Daimlerstrasse. 6, 35447 Reiskirchen, Germany
Caltag Laboratories	Brauhausstieg 15-17, 22041 Hamburg, Germany
Carl Roth GmbH + Co. KG	Schoemperlenstrasse 3-5, 76185 Karlsruhe, Germany
Carl Zeiss MicroImaging GmbH	Königsallee 9-21, 37081 Göttingen, Germany
Clontech/Takara Bio Europe	2 Avenue du President Kennedy, 78100 Saint-Germain-en-Laye, France
Desaga (Sarstedt-Group)	In den Ziegelwiesen 1-7, 69168 Wiesloch, Germany
Dianova	Warburgstrasse 45, 20354 Hamburg, Germany
Dispomed Witt oHG	Am Spielacker 10-12, 63571 Gelnhausen, Germany
DuPont Instruments	Wilmington, Delaware 19898, USA
Eppendorf AG	Barkhausenweg 1, 22339 Hamburg, Germany
Ernst Leitz Wetzlar GmbH	Now: Wild Leitz Holding AG
Fluka Chemie AG	Postfach 260, CH-9471 Buchs, Switzerland
GeneCraft GmbH	Raiffeisenstrasse 12, 59348 Lüdinghausen, Germany
Gibco BRL	See Invitrogen
Hamilton Bonaduz AG	Via Crusch 8, CH-7402 Bonaduz, GR, Switzerland
Heraeus Holding GmbH	Heraeusstrasse 12-14, 63450 Hanau, Germany

Hycult Biotechnology	Vilshofener Strasse 35, 94501 Beutelsbach, Germany
IKA Werke GmbH & Co. KG	Janke & Kunkel-Strasse 10, 79219 Staufen, Germany
Invitrogen GmbH	Emmy-Noether Strasse 10, 76131 Karlsruhe, Germany
Jackson ImmunoResearch	Unit 7, Acorn Business Center, Oaks Drive,
Europe, Ltd	Newmarket, Suffolk, UK CB8 7SY
MBI Fermentas GmbH	Opelstrasse 9, 68789 St. Leon-Rot, Germany
Merck Biosciences GmbH	Ober der Roeth 4, 65824 Schwalbach/Ts, Germany
Molecular Probes	See Invitrogen
New England Biolabs GmbH	Brüningstrasse 50, Geb.G810, 65926 Frankfurt am Main, Germany
Nunc A/S	Kamstrupvej 90, 4000 Roskilde, Denmark
Millipore GmbH	Am Kronberger Hang 5, 65824 Schwalbach/Ts., Germany
Peqlab Biotechnologie GmbH	Carl-Thiersch-Strasse 2b, 91052 Erlangen, Germany
Promega GmbH	Schildkrötstrasse 15, 68199 Mannheim, Germany
Qiagen GmbH	QIAGEN Strasse 1, 40724 Hilden, Germany
Roche Diagnostics GmbH	Sandhofer Strasse 116, 68305 Mannheim, Germany
Rotex Medica GmbH	Bunsenstrasse 4, 22946 Trittau, Germany
Santa Cruz Biotechnology, Inc	Berheimer Strasse 89-2, 69115 Heidelberg, Germany
Sarstedt AG & Co.	Postfach 1220, 51582 Nümbrecht, Germany
Sartorius AG	Weender Landstrasse 94-108, 37075 Göttingen, Germany
Schleicher & Schuell GmbH	Postfach 4, 37582 Dassel, Germany
Schott AG	Hattenbergstrasse 10, 55122 Mainz, Germany
Schütt Labortechnik GmbH	Rudolf-Wissell-Strasse 11, 37079 Göttingen
Sigma-Aldrich Chemie GmbH	Grünwalder Weg 30, 82041 Deisenhofen, Germany
Sigma Laborzentrifugen GmbH	Postfach 1713, 37507 Osterode am Harz, Germany
Stressgen	See Biomol GmbH
Stuart (VWR International GmbH)	John-Deere-Strasse 5, 76646 Bruchsal, Germany
Webeco GmbH & Co. KG	An der Trave 14, 23923 Selmsdorf, Germany
Whatman GmbH	Hahnestrasse 3, 37586 Dassel, Germany
WU	Zum Eichelberg 10, 96050 Bamberg, Germany
Zymo Research	Colombistrasse 27, 79098 Freiburg, Germany

5. Methods

For the methods where the references are not quoted, they were adapted from textbooks of Molecular Cloning: A Laboratory Manual (Third edition) and Current Protocols in Molecular Biology (Volume 5)

5.1 Biochemical methods

5.1.1 Protein quantitation by Bradford reagent

A standard curve was made using BSA in the range of 0 - 2000 µg/ml by plotting the absorbance values. The stock solution of BSA used was 5 mg/ml and it was diluted as given in Table 1. The protocol for the colorimetric assay is given below.

Table 1. Dilutions of BSA for preparation of standard curve

Amount of BSA (mg)	Volume of BSA stock solution (µl)	Water (µl)	Bradford reagent (µl)
0	0	800	200
0.05	10	790	200
0.1	20	780	200
0.2	40	760	200
0.5	100	700	200
1.0	200	600	200
2.0	400	400	200

10 to 40 µl of a sample were used for the estimation of the protein concentration. The sample volume was diluted to 800 µl with water and then 200 µl of the Bradford reagent was added. The sample was vortexed and incubated for 10 to 15 minutes at room temperature. The sample was then transferred to a 1 ml plastic cuvette and the absorbance was measured by a spectrophotometer at 595 nm. The protein concentration was determined by comparing the absorbance of the unknown sample with the absorbance of samples with known protein concentrations on the standard curve.

5.1.2 Lysis of cultured mammalian cells

The culture medium was carefully removed from adherent cells and washed twice with cold PBS. Cold RIPA buffer (containing a protease inhibitor cocktail) at a volume of 1 ml per 10 cm culture dish containing 5 million cells was added to the cells and kept on ice for 5 minutes. The plate was swirled occasionally for uniform spreading of RIPA buffer. The cell lysate was gathered using a cell scraper and transferred to a 1.5 ml tube. Samples were centrifuged at 14000 g for 15 minutes at 4 °C to pellet the cell debris. The supernatant containing the protein lysate was transferred to a new tube for further analysis.

5.1.3 Preparation of protein samples for SDS polyacrylamide gel electrophoresis (SDS-PAGE)

Equal volume of protein sample obtained from the cell lysate and 2 X Laemmli buffer were taken and mixed, boiled at 98 °C for 5 minutes and allowed then to cool down to room temperature. The samples were centrifuged at 19000 g for 1 minute and the supernatants were resolved by SDS-PAGE.

5.1.4 SDS-PAGE

The electrophoretic separation of proteins was performed by SDS-PAGE. A system with vertically oriented glass plates (16 X 16 cm; 1 mm spacer) was used. The gel was prepared as follows: first the separating gel was casted between glass plates and covered with a layer of isopropanol. After polymerization of the gel the isopropanol was removed and the space between glass plates was rinsed with water and later drained with a whatmann paper. Then the stacking gel was casted on top of the polymerized separating gel and the sample comb was inserted immediately. After approximately 15 minutes polymerization was complete and the sample comb and lower spacer were removed. The glass plates with the gel were fixed inside the electrophoresis chamber and covered with electrophoresis buffer. The protein samples were then introduced into the wells in the stacking gel with a micro-syringe. Electrophoresis was performed with the constant current of 40 mA till the dye front reached the bottom of the gel.

5.1.5 Staining with coomassie blue

After electrophoresis the SDS-PAGE gel was removed from the electrophoresis chamber and fixed in 30% methanol, 10% acetic acid for 1 hour. The gel was then placed in the staining solution for 1 hour on a horizontal shaker. Afterwards, the gel was removed from the staining solution and de-stained with 30% methanol, 10% acetic acid till the protein bands were clearly visible against a clear background.

5.1.6 Western blot

For western blotting SDS-PAGE gels were removed from the electrophoresis chamber and soaked in protein transfer buffer for 20 minutes. Two pieces of whatmann paper and 1 piece of nitrocellulose membrane were cut to the size of SDS gel and equilibrated in transfer buffer. The blot was assembled without air bubbles in the following order:

Cathode (-)
Plexiglass holder
Cloth mesh
Whatmann paper
Gel
Nitrocellulose membrane
Whatmann paper
Cloth mesh
Plexiglass holder
Anode (+)

The protein transfer was done at constant voltage of 15 volts overnight at 4 °C in a transfer chamber containing transfer buffer. On the next day, the membrane was removed and stained with Ponceau S for 30 seconds. The lanes and the marker proteins were marked on the membrane. The membrane was then rinsed with water to remove the Ponceau S stain. For Western blotting the membrane was washed with PBST buffer three times for 5 minutes each. The primary antibody was then added to the membrane (anti-HSP70: 0.5 µg/ml, anti-HSC70: 0.5 µg/ml, anti-LOX-1: 0.5 µg/ml, and anti-β-actin: 1/5000 dilution) and incubated at room temperature for 1 hour. The membrane was then again washed three times with PBST buffer with each wash for 5 minutes. A Horse radish peroxidase (HRP)-coupled secondary antibody was then added to the membrane and incubated for 45 minutes, washed five times with PBST buffer and developed in DAB solution for 1 minute.

5.1.7 Preparation of recombinant HSP70

5.1.7.1 Induction of HSP70

The bacteria clone expressing the HSP70 protein (Dressel et al. 2000) was grown overnight in 50 ml of LB medium containing 50 µg/ml ampicillin and 25 µg/ml kanamycin in a 37 °C shaking incubator. After overnight culture, the 50 ml of LB medium was split equally into two flasks and diluted ten-fold with fresh LB medium containing the same antibiotic concentrations as mentioned above. The culture was grown again for 2 to 3 hours at 37 °C till the optical density measured by a spectrophotometer at 600 nm reached 0.7. One ml of the bacteria culture was removed from each flask and the cells were spun down at 4000 g for 10 minutes. These bacterial cells served as uninduced control. To the remaining culture IPTG was added to a final concentration of 1 mM and incubated again at 37 °C in a shaking incubator for 3 hours. One ml of culture was removed and the bacterial cells obtained were tested for HSP70 induction on a SDS-PAGE gel. Briefly, 200 µl of 2 X Laemmli buffer was added to the bacterial cell pellet obtained from 1 ml of bacterial culture and placed in a water bath at 98 °C for 5 minutes. The sample was removed from the water bath and centrifuged at 19000 g for 5 minutes before 40 µl of the supernatant were then loaded on the SDS-PAGE gel. The protein induction was confirmed by coomassie blue staining of the gel. The remaining culture was divided into 50 ml aliquots and was spun down at 4000 g for 10 minutes at 4 °C. The supernatant was removed and the bacterial cell pellets were stored at -70 °C.

5.1.7.2 Preparation of inclusion bodies containing HSP70

All the steps during inclusion body preparation were performed on ice. The buffers used were supplemented with freshly prepared PMSF to a final concentration of 1 mM. The bacterial cell pellet obtained from 50 ml of IPTG-induced bacterial cell culture was re-suspended with 3.2 ml of lysis buffer. The cell suspension was then transferred to a glass homogenizer and the sample was homogenized by stroking the pestle up and down several times. After homogenization, the sample was incubated on ice for 15 minutes. Then, 6.25 ml of detergent buffer were added and the suspension was homogenized again until the solution became less viscous. The homogenate was transferred to a clean glass tube and spun down at 12000 g for 25 minutes at 4 °C. After the spin, the supernatant was discarded and the pellet was re-suspended in 4 ml of wash buffer and homogenized again.

This step was repeated twice. For the final wash step, the pellet was re-suspended in 2 ml of wash buffer and centrifuged at 27000 g for 25 minutes at 4 °C. The supernatant was discarded and the protein pellet was dissolved in 1 ml of mono-S buffer and stored at -70 °C.

5.1.7.3 Purification of HSP70

The HSP70 obtained from the inclusion bodies had to be exchanged from mono-s buffer to PBS buffer for further applications. 15 ml of PBS containing 1 mM PMSF was added to an Amicon Ultra-15 Centrifugal Filter Unit with a molecular weight cut-off of 30 KD. A 350 µl aliquot of HSP70 protein in mono-s buffer was then applied to the PBS buffer in the filter unit and centrifuged at 4000 g and 4 °C till the applied volume was reduced to 500 µl. 15 ml of PBS with 1mM PMSF was then applied again to the filter unit and centrifuged at the same conditions as mentioned above till the applied volume was reduced to 500 l. The above step was repeated again but this time the applied volume was reduced to 350 µl and HSP70 was collected in 350 µl of PBS and stored in aliquots at -70 °C.

5.1.8 Fluorescein isothiocyanate (FITC) conjugation of HSP70

HSP70 was conjugated with FITC using the FluoReporter® FITC Protein Labeling Kit (Molecular Probes). The amount of dye required for the conjugation reaction was calculated as follows

$$\mu\text{l dye stock solution} = \frac{\text{mg/ml protein} \times 0.2 \text{ ml}}{\text{MW}_{\text{protein}}} \times 389 \times 100 \times \text{MR}$$

0.2 ml is the volume of protein solution

389 is the molecular weight of the reactive dye

100 is a unit conversion factor

$\text{MW}_{\text{protein}}$ is the molecular weight of protein to be labeled

MR is the molar ratio of dye to protein in the reaction mixture. The recommended MR is 40 if the protein is at 1–3 mg/ml or MR = 30 if the protein is at 4–10 mg/ml.

5.1.8.1 Conjugation reaction

200 µl of protein solution were transferred to the reaction tube (2-ml-tube with a stir bar, provided in the kit) and 20 µl of freshly prepared 1 M sodium bicarbonate buffer (0.84 g in 9 ml water, pH adjusted to 9 and volume adjusted to 10 ml) was added. The volume of reactive dye calculated by the equation given above was then added from a 10 mg/ml reactive dye stock solution to the stirring protein solution. The reaction was carried out for 1 hour at room temperature and protected from light during this time. After the labeling reaction the sample was centrifuged at 16200 g for 5 minutes and supernatant was transferred to a fresh tube.

5.1.8.2 Purification

A spin column provided in the kit was prepared by pinching of the bottom closure and draining the buffer present in the column by gravity before centrifuging the spin column for 3 minutes at 1100 g. The sample was added to the center of spin column and allowed to get absorbed into the gel bed. The spin column was then placed into an empty collection tube and centrifuged at 1100 g for 5 minutes. After centrifugation the sample was obtained in approximately 200 to 250 μ l of PBS with 2 mM sodium azide. The labeled protein was divided into aliquots and stored at -30 °C.

5.2 Cell culture methods

5.2.1 Cell culture

All the cell culture work was carried out in sterile conditions under the laminar flow. Cells were cultured in cell culture dishes with DMEM culture medium in a humidified atmosphere containing 10% CO₂ at 37 °C. The cells were passaged every 2 to 3 days depending on the growth rate. After the cells reached 95% confluence, the medium was aspirated and 1.5 ml of trypsin working solution was added per 10 cm culture dish and incubated at 37 °C for 5 minutes. Trypsin was then neutralized by culture medium containing 10% FCS and the cells were resuspended by pipetting. The cells were then spun down at 280 g for 5 minutes and 1/10th of cells replated again for maintenance.

5.2.2 Cell counting

A cell suspension (~10 μ l) was injected into the grid under a cover slip placed on a Neubauer chamber. The main divisions separate the grid into 4 large squares. Each square has a surface area of one square mm, and the depth of 0.1 mm. Cells were then counted under the microscope in the four corner squares of the grid. Cell number was then determined by the following calculation:

Cells / ml = average cell count (total cell count / 4) x dilution factor x 10⁴.

5.2.3 Freezing cells

Generally, the cells confluent in a 10-cm-culture dish were divided into 10 cryotubes (1 X 10⁶ cells / tube). After trypsinisation, cells were pelleted and resuspended in 10 ml of DMEM medium containing 20% DMSO. Cells were then divided as 1-ml-aliquots and allowed to freeze gradually in a thermocol box for 72 h at -80 °C. For long term storage the cells were transferred to liquid nitrogen after 72 hours.

5.2.4 Thawing cells

A frozen cell vial was placed under running water till there was a slight melting of the cell suspension. Immediately, 1 ml of culture medium was added in sterile conditions to the vial and pipetted gently until the whole suspension was thawed. The cells were then

added to a tube with 10 ml of culture medium and spun down at 280 g for 5 minutes. The supernatant containing the DMSO was discarded and the cells were plated in 10 ml of culture medium in a 10-cm-culture dish.

5.2.5 Transient transfection

Transfection was done by metafectene reagent (Biontex) according to the manufacture's instruction. In a 12-well plate, 2×10^5 cells per well were seeded and cultured for 18 to 24 hours. Typically, 0.5 μg of DNA was used for a single well of a 12-well plate for transfection. 4 μl of metafectene reagent were added to 50 μl of culture medium free of serum and antibiotics and mixed gently by pipetting one time. Similarly, to 50 μl of medium free of serum and antibiotics, 0.5 μg of DNA was added and mixed. Both the metafectene and DNA solutions were then mixed together and incubated at room temperature for 20 minutes. After incubation, the DNA metafectene complexes were added dropwise to the cells while swirling the flask gently. Depending on the cell type and promoter activity, cells were cultured for 24 to 72 hours after transfection before further analysis.

5.2.6 Stable transfection

HT1080-N1 cells were co-transfected with full-length LOX-1 and puromycin resistance vector constructs by metafectene reagent as explained for transient transfection. 48 hours after transfection, the cells were transferred to a 10-cm-culture dish and cultured for 3 weeks in normal culture medium containing genitcin (G418 sulphate) in a concentration of 800 $\mu\text{g}/\text{ml}$ and puromycin in a concentration of 0.3 $\mu\text{g}/\text{ml}$. The drug resistant clones were then picked and expanded in 24-well plates. The clones were then analyzed for LOX-1 expression. The positive cells were further subjected to limiting dilution to obtain monoclonal cell lines.

5.2.7 Limiting dilution

Cell density was adjusted to obtain 1×10^4 cells /ml. In order to get a total of 100 cells, 10 μl of cell suspension was taken, for total of 300 cells, 30 μl of cell suspension was taken and for total of 1000 cells, 100 μl of cell suspension was taken and added to 10 ml of culture medium. Three 96-well-plates were labeled 100, 300 and 1000. Aliquots of 100 μl from each 10 ml cell suspension (100, 300, and 1000 cells) were pipetted into each well of 96-well-plates labeled 50, 300 and 1000 respectively. This would give approximately a total of 1, 3 and 10 cells in each well of a 96-well-plate respectively. Cells were cultured overnight and examined next day for the wells containing the cells. Clones in the plate with approximately one third of positive wells were used and grown and transferred in sequence from a 96-well-plate to a 48-well, 24-well, 12-well plate until it was possible to cultivate the cells in flasks.

5.2.8 Preparation of PBMCs by density gradient centrifugation

20 ml of blood were transferred into a 50-ml-tube containing 20 µl of heparin. An equal volume of HEPES-buffered DMEM was then added and mixed well. In five 13-ml-tubes, 4 ml of Biocoll was overlaid carefully with 8 ml of the diluted blood. The tubes were centrifuged at 560 g for 20 minutes at room temperature. PBMCs form the interphase between Biocoll and the DMEM; and red blood cells go into the Biocoll phase. PBMCs were carefully aspirated with a Pasteur pipette and transferred into 50-ml-tubes and washed once with 10 ml of HEPES-buffered DMEM. The cells were centrifuged at 280 g for 5 minutes at room temperature. Then the supernatant was discarded and cells were resuspended in 5 ml of culture medium.

5.3 Molecular biology methods

5.3.1 Cultivation of *Escherichia coli* (*E. coli*)

5.3.1.1 On Luria Bertani (LB) agar plates

For preparation of agar plates, 1.5% of select agar was added to the LB medium and autoclaved. After autoclaving, the LB-agar medium was allowed to cool down to 55 °C and an antibiotic (ampicillin, 50 µg/ml or kanamycin, 30 µg/ml) was added and mixed well. 25 ml of LB-agar medium was then added to each Petri dish under sterile conditions and was allowed to solidify. LB-Agar plates were stored at 4 °C.

250 µl of bacterial culture was added on the surface of solid LB-Agar medium and spread consistently over the plate with the help of a sterile glass rod. The plate was then placed in a 37 °C incubator and the colonies were grown overnight.

5.3.1.2 In Luria Bertani (LB) medium

For mini-prep culture, 3 ml of LB medium were taken in a 13 ml tube with a ventilation cap and a single colony of bacteria grown on a LB-Agar plate was added to the medium with the help of a pipette tip. The bacteria (*E. coli*) were then grown overnight at 37 °C in a shaking incubator at 150 rpm.

5.3.2 Preparation of competent *E. coli* cells (DH5α)

DH5α cells were cultured in 3 ml of LB medium overnight at 37 °C in a shaking incubator at 150 rpm. One ml of the overnight culture was inoculated in 100 ml LB medium and grown at 37 °C in a shaking incubator till the optical density measured by a spectrophotometer at 600 nm reached 0.6. Cells were chilled on ice for 5 minutes and were spun down at 2900 g for 10 minutes at 4 °C. The supernatant was discarded and the cell pellet was resuspended in 10 ml of ice cold 0.1 M CaCl₂ and kept on ice for 20 minutes. Cells were spun down again at 2900 g for 10 minutes at 4 °C. The cell pellet was then resuspended in 5 ml of 0.1 M CaCl₂ containing 15% glycerol and kept on ice for 1 hour. 50 µl aliquots of these competent cells (for transformation) were then snap frozen in liquid nitrogen and stored at -70 °C.

5.3.3 Transformation of competent *E. coli* cells

A 50 µl aliquot of competent *E. coli* cells was taken from -70 °C freezer and thawed on ice. 20 to 50 ng of DNA was added to the competent cells which were then left on ice for 30 minutes. Afterwards, the competent cells were heat shocked for 30 seconds at 42 °C and immediately placed on ice for 5 minutes. One ml of LB medium was then added to the competent cells and incubated at 37 °C in a shaking incubator at 150 rpm for 1 hour. The *E. coli* cells were then spun down at 4000 g for 5 minutes and the cell pellet was resuspended in 0.2 ml LB medium. The *E. coli* cells were spread on a LB-Agar plate and incubated overnight at 37 °C to obtain colonies.

5.3.4 Preparation of glycerol stocks of bacterial strains

700 µl from an overnight 3 ml bacterial culture was transferred to a freezing vial. 300 µl of sterile glycerol was then added to the freezing vial and mixed gently. The vials were then frozen in liquid nitrogen and stored at -70 °C.

5.3.5 Mini-preparation of plasmid DNA

One ml of mini-prep culture was spun down at 4000 g for 10 minutes and the bacterial cell pellet obtained was resuspended completely in 200 µl of buffer P1 by vortexing. 200 µl of buffer P2 were then added and mixed gently by inverting 5-6 times and incubated at room temperature for 5 minutes. 200 µl of cold buffer P3 were added and gently mixed by inverting and then incubated on ice for 20 minutes. Afterwards samples were centrifuged at 19000 g for 15 minutes at room temperature. The supernatant was carefully transferred to a fresh tube and 500 µl of isopropanol were added and incubated at -20 °C for 30 minutes. The DNA was then pelleted down by centrifuging at 19000 g for 30 minutes at 4 °C. The DNA pellet was washed once with 1 ml of 70% ethanol, briefly air-dried, and dissolved in dH₂O.

5.3.6 Restriction digestion of plasmid DNA

One to 2 µg of plasmid DNA or 0.5 to 1 µg of PCR product were used for the digestion with restriction enzymes. The BSA was added when required for the activity of certain restriction enzymes. These reactions were setup as given below:

Reaction Mix

DNA	Plasmid : 1 to 3 µl ; PCR product : 5 to 10 µl
Buffer 10X	2 µl
BSA (100X)	0.2 µl (added when required)
Enzyme	1 to 2 units
Distilled H ₂ O	up to 20 µl

One unit of enzyme is defined as the amount of enzyme that is required to digest 1 µg of bacteriophage λ DNA in 1 hour at 37 °C in a total reaction volume of 50 µl.

The reaction mix was incubated at optimal temperature of the enzyme (mostly 37 °C) for 2 hours and then the digested products were run on agarose gels (1 to 2%, depending on the expected size of fragments) to check the digestion.

5.3.7 Preparation of DNA from whole blood

PBMCs from whole blood were prepared by the Biocoll density gradient method. 700 µl of DNA lysis buffer containing 35 µl of proteinase K (10 mg/ml) were added to 5 million PBMCs. The cells were lysed by pipetting the solution up and down. The lysate was then incubated overnight at 55 °C. At the next day, the samples were removed from the incubator and 700 µl of Tris-saturated phenol were added and mixed by inverting the tubes several times. Samples were then centrifuged at 11500 g for 3 minutes at room temperature. The supernatant was transferred to a fresh tube and 700 µl of chloroform/isoamylalcohol (24:1) mix were added and mixed well. Samples were again centrifuged for 3 minutes at room temperature. The supernatant containing the aqueous phase was transferred to a fresh tube and the DNA was precipitated by adding 10% (v/v) of 3 M sodium acetate (pH 6) and 600 µl of absolute ethanol. Samples were centrifuged at 16500 g for 5 minutes at 4 °C, the supernatant was discarded, and the DNA pellet was washed with 1 ml of 70% ethanol. Samples were centrifuged again at 16500 g for 5 minutes at 4 °C. Supernatant was discarded and the DNA pellet was briefly air dried and then dissolved in 100 µl of nuclease free water. The DNA was then stored at 4 °C.

5.3.8 Preparation of DNA from serum

5.3.8.1 Microwave irradiation (Sandford and Pare, 1997)

20 µl of serum were added to a 0.2 ml polypropylene PCR tube and subjected to microwave irradiation for 5 minutes at maximum power in a microwave oven (850W). The irradiated sample was directly used as a template for PCR amplification.

5.3.8.2 Alkaline lysis method (Lin and Floros, 2000)

For alkaline lysis, 10 µl of serum were incubated with 1 µl of 0.2 M KOH at 45 °C for 20 minutes. During this treatment various macro-molecules in the serum may be denatured or hydrolyzed (i.e., RNA). To neutralize the serum lysate, 5 µl of neutralization buffer (9 parts 1 M Tris, pH 8.3: 1 part 2 M HCl) were added and vortexed briefly. The final DNA solution volume was 16 µl and 3 µl served as a PCR template.

5.3.8.3 Proteinase K/Sodium dodecyl sulfate (SDS) lysis method (Lin and Floros, 1998)

200 µl of serum were treated with proteinase K (1.7 mg/ml) and 5% SDS at 65 °C for 1 hour and then heated to 95 °C for 10 minutes to inactivate the proteinase K. The proteinase K treated serum was then phenol-extracted by mixing with 200 µl of Tris-saturated phenol and centrifuged at 16000 g for 3 minutes. The aqueous phase was

transferred to a new tube and 200 μ l of chloroform/isoamylalcohol (24:1) were added and mixed well before centrifuging at 16000 g for 3 minutes. After centrifugation, DNA from aqueous phase was precipitated by adding 10% (v/v) of 3 M sodium acetate (pH 6) and 600 μ l of absolute ethanol. Sample was spun down at 16000 g for 15 minutes at 4 °C. DNA pellet was washed once with 250 μ l of 70% ethanol and then dissolved in 20 μ l of nuclease free water.

5.3.9 Agarose gel electrophoresis of DNA

The size and purity of DNA was analyzed by agarose gel electrophoresis. The percentage of agarose used for DNA electrophoresis was 0.8 to 2 percent depending on the size of fragments to be analyzed.

<u>DNA</u>	<u>Agarose gel</u>
> 0.5 kb	2 %
0.5 to 1.5 kb	1.5 %
1.5 to 10 kb	1 %
> 10 kb	0.8 %

Agarose was weighed and dissolved in 1 X TBE buffer by boiling in a microwave oven. The agarose solution was cooled to 60 °C and ethidium bromide was added to a final concentration of 0.5 μ g/ml. This was poured into the agarose gel cassette and allowed to polymerize completely. The DNA sample was mixed with DNA loading dye and loaded onto the gel. The gel electrophoresis was carried out at 150 V. Ethidium bromide is a fluorescent dye which contains a planar group that intercalates between the stacked bases of the DNA. The fixed position of this group and its close proximity to the bases cause the dye to bind to DNA. It results in an increased fluorescent yield compared to that of the dye in solution. Ultraviolet radiation at 254 nm is absorbed by the DNA and transmitted to the dye; radiation at 302 nm and 366 nm is absorbed by the bound dye itself. In both cases, the energy is re-emitted at 590 nm in the red orange region of the visible spectrum. Hence, DNA can be visualized under a UV transilluminator. The gels were photographed using a polaroid camera.

5.3.10 Determining the concentration of DNA

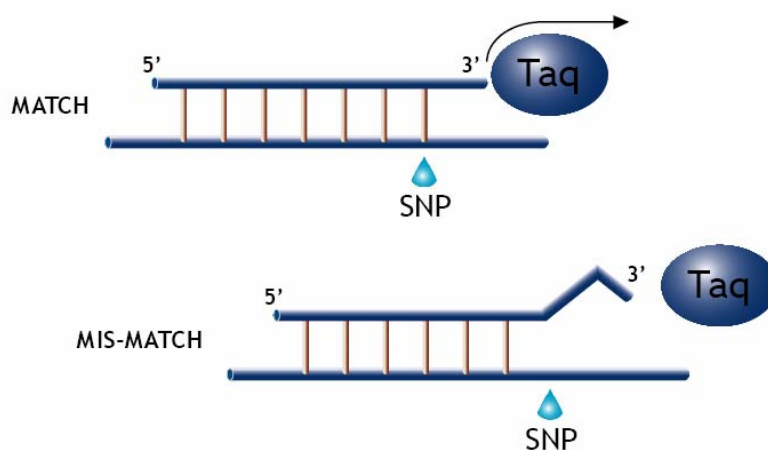
DNA concentration was determined using a spectrophotometer. DNA was diluted in water and the absorbance was measured at 260 nm. An absorbance or optical density (OD) of 1 at 260 nm corresponds to 50 μ g/ml of double stranded DNA, or 40 μ g/ml of single stranded DNA and RNA or 20 μ g/ml of oligonucleotides. The ratio between the readings at 260 nm and 280 nm (OD₂₆₀/OD₂₈₀) provides an estimate of the purity of the nucleic acid. Pure preparations of DNA and RNA have OD₂₆₀/OD₂₈₀ values of 1.8 and 2.0, respectively. Any contamination with proteins or phenol would yield values less than mentioned above.

5.3.11 Purification of DNA

PCR products and plasmid DNA were purified by Zymo DNA clean & concentrator columns. Two volumes of DNA binding buffer were added to 1 volume of PCR product and sample was added to a column and centrifuged at 19000 g for 20 seconds. Columns were washed two times with 200 μ l of wash buffer by centrifuging at 19000 g for 30 seconds. DNA was eluted with 10 to 30 μ l of nuclease free water.

5.3.12 Genotyping of SNP by allele-specific polymerase chain reaction (AS-PCR) (PCR: A practical approach by M. J. McPherson)

AS-PCR was employed to determine the genotype of the SNPs. Here the primers were designed in such a way that one of the primers (Forward or Reverse) carried a nucleotide base at their 3' end that represented each of the two alleles of SNP. If there is a match of 3' base with the allele, the PCR reaction would proceed and if there is a mismatch the PCR reaction would not occur as illustrated in Fig 4.



Proligo's AS-PCR manual (2002).

Fig 4. AS-PCR method for genotyping. The match of 3' base with the SNP allele allows the *taq* polymerase to amplify the PCR product and the mismatch leads to termination of the PCR reaction.

The reaction components used for the PCR reactions were as given below:

<u>Component</u>	<u>Amount</u>
DNA	50-100 ng
Forward primer (10 μ M)	1 μ l
Reverse primer (10 μ M)	1 μ l
dNTP Mix (2.5 mM)	2 μ l
Buffer (10 X)	2.5 μ l
<i>Taq</i> polymerase (5 units/ μ l)	0.5 μ l
Water	Made up to 25 μ l

After the mix of all reaction components in 0.2 ml thin walled PCR tubes, the PCR was done in a thermal cycler (Perkin Elmer or Biometra) with the indicated conditions.

Cycling Conditions

94 °C	5 min	} 35 cycles
94 °C	20 sec	
55-60 °C	30 sec	
72 °C	60 sec	
72 °C	5 min	

After the PCR was complete, the samples were stored at 4 °C until they were run on an agarose gel.

5.3.13 Restriction fragment length polymorphism (RFLP)

The RFLP method was used for the CD91 exon 3 and tag 34 SNP analysis. In this method the genomic region flanking the SNP was amplified by PCR. The PCR product was then digested by a restriction enzyme (exon 3 SNP: BccI ; tag 34 SNP : RsaI) which specifically recognizes one of the two alleles. When the PCR product is homozygous for the allele recognized by the enzyme, the PCR fragment is completely digested and the bands run lower than the original fragment size. When the PCR product is heterozygous for the allele recognized by the enzyme, the PCR fragment is half digested and the bands correspond to the original fragment size as well as digested fragment size. When the PCR product is homozygous for the allele not recognized by the enzyme, the PCR fragment is not digested and the band corresponds to the original fragment size.

5.3.14 Preparation of RNA

5.3.14.1 Trizol method (Chomczynski and Sacchi, 1987)

One ml of Trizol reagent (Invitrogen) was used for cells in a range from 5×10^6 to 10×10^6 . Cells were lysed in Trizol reagent by pipetting the solution up and down. After homogenization, the homogenate was centrifuged at 12000 g for 10 min at 4 °C and the clear supernatant was transferred to a fresh tube. 200 µl of chloroform were added for every 1 ml of Trizol reagent used and the tubes were shaken vigorously by hand for 15 seconds, followed by incubation at room temperature for 2 minutes. The mixture was then centrifuged at 12000 g for 15 minutes at 4 °C. Following centrifugation, the mixture separates into a lower red, phenol-chloroform phase, an interphase, and a colorless upper aqueous phase. RNA is exclusively present in the aqueous phase. The aqueous phase was transferred to a new tube and RNA was precipitated by adding 0.5 ml of isopropanol for every 1 ml of Trizol reagent. Samples were then incubated on ice for 10 minutes, followed by centrifugation at 12000 g for 10 minutes at 4 °C. The supernatant was removed and the RNA pellet was washed by adding 1 ml of 70% ethanol and centrifuging at 7500 g for 5 minutes at 4 °C. The RNA pellet was briefly air dried and dissolved in appropriate amount of nuclease free water.

5.3.14.2 SV total RNA isolation system kit (Promega)

All the reagents and spin columns used in this method were provided in the kit. To a cell pellet containing 2×10^5 to 2×10^6 cells, 175 μ l of RNA lysis buffer was added and cells were dispersed by vortexing. To the cell lysate, 350 μ l of RNA dilution buffer were added and mixed by inverting 3 to 4 times. The mixture was then placed on a heating block at 70 °C for 3 minutes. The sample was removed from heating block and centrifuged at 12000 g for 10 minutes at 25 °C. The clear lysate supernatant was transferred carefully to a fresh microcentrifuge tube by pipetting without disturbing the cell debris. 200 μ l of 95% ethanol were then added to the clear lysate and mixed 3 to 4 times by pipetting. The mixture was transferred to a spin column and centrifuged at 12000 g for 1 minute at 25 °C. 50 μ l of freshly prepared DNase solution were then added to the membrane of the spin column and incubated for 15 minutes at 25 °C. After the incubation, the DNase reaction was stopped by adding 200 μ l of DNase stop solution to the spin column and centrifuged at 12000 g for 1 minute. Spin columns were then washed twice with 650 μ l of RNA wash buffer. The RNA was then eluted from spin columns by adding 100 μ l of nuclease free water and centrifuging at 12000 g for 1 minute and stored at -70 °C.

5.3.15 Reverse transcription (RT)

This protocol was adopted to convert 1 to 5 μ g of total RNA into first strand cDNA. The following components were combined in a 0.2 ml tube:

<u>Component</u>	<u>Amount</u>
1 to 5 μ g total RNA	n μ l
Primer	1 μ l
50 μ M oligo dT or 50 ng/ μ l random hexamers	
10 mM dNTP mix	2 μ l
Nuclease free H ₂ O	to 12 μ l

The mix was incubated in a thermal cycler at 65 °C for 5 minutes and cooled down on ice for at least 1 minute. Then the cDNA synthesis mix was prepared with the following components:

<u>Component</u>	<u>Amount</u>
5 X Reverse transcriptase buffer	4 μ l
0.1 M DTT	1 μ l
Nuclease free H ₂ O	1 μ l
RNasin	1 μ l
M-MLV reverse transcriptase	1 μ l

The components were carefully mixed and 8 μ l of cDNA synthesis mix was added to RNA/primer mixture. The sample was then incubated as given below.

Oligo dT primer	60 minutes at 50 °C
Random hexamer primer	10 minutes at 25 °C, followed by 60 minutes at 50 °C

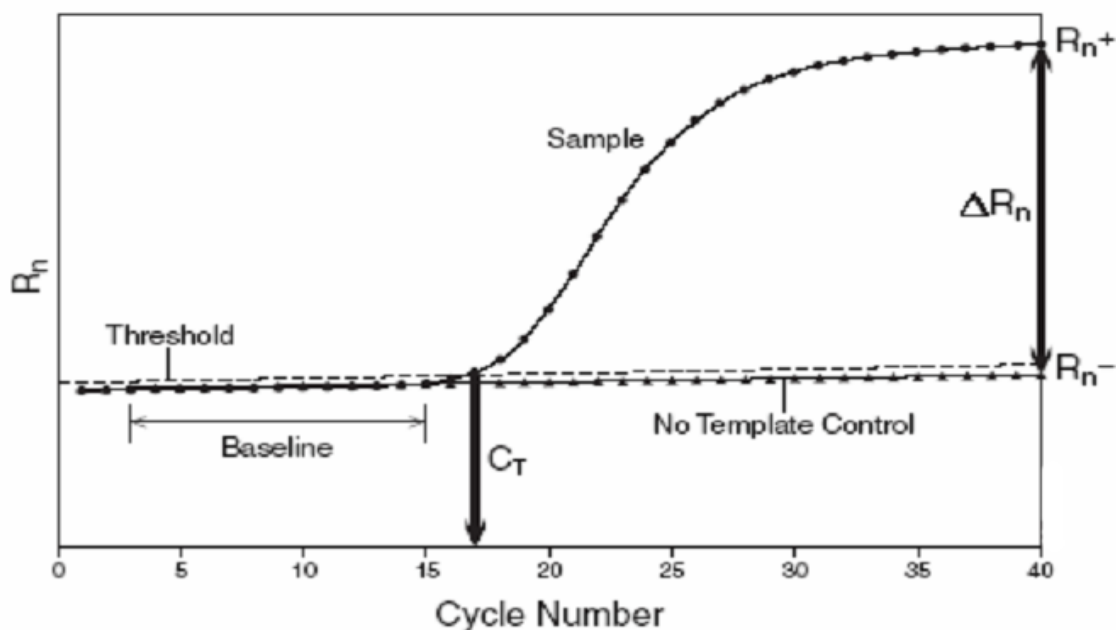
The reaction was then terminated by incubating at 85 °C for 5 minutes. The cDNA was then stored at -25 °C or was used for PCR immediately.

5.3.16 Real-time PCR

For real-time PCR, TaqMan gene expression assays (Applied Biosystems) were used. Each TaqMan gene expression assay consists of a FAMTM dye-labeled “TaqMan® MGB probe” and two PCR primers formulated into a single tube. Every assay is optimized to run under universal thermal cycling conditions with a final reaction concentration of 250 nM for the probe and 900 nM for each primer. The TaqMan gene expression assays for CD91 and CD14 expression analysis were obtained from the TaqMan gene expression assay inventory. The PCR reaction in the gene expression assay exploits the 5'-nuclease activity of the DNA polymerase system to cleave a TaqMan probe during PCR. The TaqMan probe contains a reporter dye at the 5'-end of the probe and a quencher dye at the 3'-end of the probe. During the reaction, cleavage of the probe separates the reporter dye and the quencher dye. This separation results in increased fluorescence of the reporter. Accumulation of PCR products is detected directly by monitoring the increase in fluorescence of the reporter dye as shown in Fig 5. The TaqMan gene expression assay for an endogenous control was also obtained from Applied Biosystems. Endogenous controls can normalize the expression levels of target genes by correcting differences in the amount of cDNA that is loaded into PCR reaction wells.

50 to 100 ng of cDNA were taken for each real-time PCR reaction. For each sample, a triplicate was used for the gene of interest and a triplicate for endogenous control. All the reactions were setup in a 96-well real-time optical PCR plate recommended for the assay. The PCR reaction components are as given below:

<u>Component</u>	<u>Amount</u>
TaqMan Gene Expression Assay (20 X)	1 μ l
cDNA template + H ₂ O	9 μ l
Taqman Universal PCR Master Mix (2 X)	10 μ l



Applied Biosystem's relative quantification manual (2004)

Fig 5. Real-time PCR amplification curve. This figure shows an amplification plot. At the end of each reaction, the recorded fluorescence intensity is used for the following calculations by the real-time 7500 system software. R_n is the ratio of the fluorescence emission intensity of the reporter dye to the fluorescence emission intensity of the passive reference dye. R_n^+ is the R_n value of a test sample (the sample of interest); R_n^- is the R_n value detected in no template control or background fluorescence (baseline value). ΔR_n is the difference between R_n^+ and R_n^- . It is an indicator of the magnitude of the signal generated by the PCR. The threshold is a level of ΔR_n , automatically determined by the SDS software or manually set, used for C_T determination in real-time assays. The level is set to be above the baseline and sufficiently low to be within the exponential growth region of the amplification curve. The threshold is the line whose intersection with the amplification plot defines the C_T .

The components were gently mixed by pipetting up and down. The plate was then covered with an optical adhesive film. Then the plate was briefly centrifuged to spin down the contents and to remove any air bubbles from the solutions. The reaction plate was then placed in 7500 Real-time PCR system (Applied Biosystems). The cycling conditions were setup as given below:

AmpliTaq Gold Enzyme activation	95 °C, 10 min	
Denature	95 °C, 15 Sec	} 35 cycles
Anneal/Extension	60 °C, 1 min	

5.3.17 Cloning of full-length LOX-1 cDNA

A cDNA from human brain tissue (kind gift from Dr. A. Mannan, Institute of Human Genetics, University of Göttingen) was used for amplification of the full-length LOX-1 gene with the primers LOX-1 F and LOX-1 R. The LOX-1 full-length gene reading frame was successfully amplified from brain cDNA by *Taq* polymerase (Genecraft). The PCR product with adenosine (A) overhangs was cloned into a plasmid vector (pcDNA3.1/CT-GFP-TOPO, Invitrogen) with single 3'-thymidine (T) overhangs for TA

cloning and Topoisomerase I covalently bound to the vector (referred to as "activated" vector). The cloning reaction was setup as given below:

PCR product	0.5 – 4 μ l
Salt solution (1.2 M NaCl; 0.06 M MgCl ₂)	1 μ l
TOPO Vector	1 μ l
Water	adjusted to 6 μ l
Final Volume	6 μ l

The reaction mix was mixed gently and incubated at room temperature for 5 minutes for the ligation to complete. The reaction mix was then placed on ice and transformed into TOP10 competent cells (Invitrogen) according to the instruction manual.

5.3.18 PCR-based site-directed mutagenesis (SDM) (Higuchi et al., 1988)

A SNP in the exon 4 of LOX-1 gene that leads to a change in amino acid (K>N) at position 167 was introduced into the full-length wild type cDNA of LOX-1 by PCR-based SDM. Two PCR reactions were setup with the following pairs of primers.

- 1) Forward : Exon 4 SDM F 5'CATTTAACTGGGAAAA**C**AGCCAAGAGAAGT 3'
Reverse : LOX-1 FL R 5'CCCAAGTGACAAAGAATAGC 3'
- 2) Forward : LOX-1 FL F 5' TGACTGCTTCACTCTCTCATT 3'
Reverse : Exon 5 R 5' AAGTGGGGCATCAAAGGAGAA 3'

The first pair of primers introduce the mutation at position 501 in cDNA, where G is replaced by C indicated by bold red font in Exon 4 SDM For primer. With this primer pair, a portion of exon 4 and exon 5, 6 was amplified. The second pair of primers amplify the complete regions of exon 1 to exon 5 (Fig 6). The reaction mixture and the cycling conditions used were as given below:

Reaction Mix		Cycling Conditions		
LOX-1 cDNA	2 μ l	94 °C	5 min	} 25 cycles
Primer (Forward)	1 μ l	94 °C	20 sec	
Primer (Reverse)	1 μ l	60 °C	30 sec	
dNTP (2.5 mM)	2 μ l	72 °C	60 sec	
Buffer (10X)	2 μ l	72 °C	5 min	
<i>Pfu</i> DNA Polymerase	0.2 μ l			
Water	made up to 20 μ l			

It was important to use the DNA polymerase with proof reading activity (*Pfu*, Promega) in the experiment, as the DNA polymerase without proof reading activity would introduce "A" overhang and this could lead to a frameshift in subsequent amplifications.

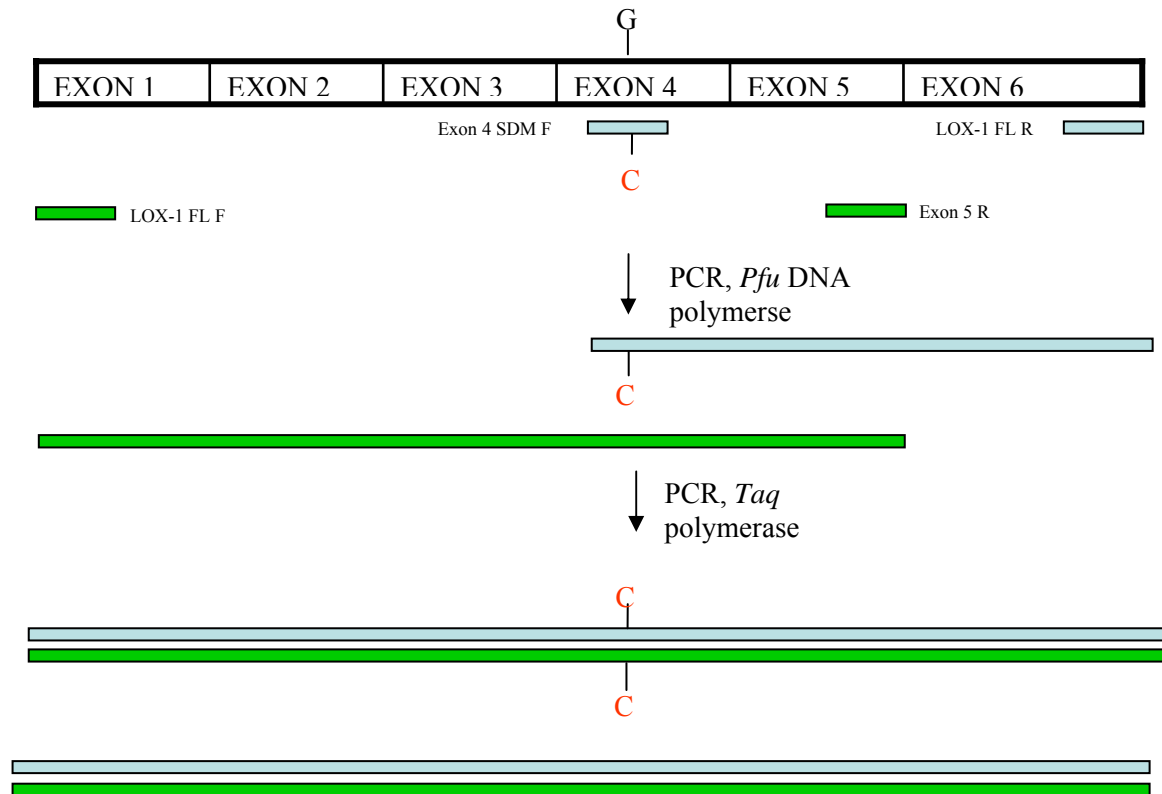


Fig 6. PCR-based SDM. A mutation in exon 4 (SNP location) of LOX-1 was introduced by a primer (LOX-1 Exon 4 SDM F) carrying the mutant base C. The PCR product containing part of exon 4 with the introduced mutation and upto the end of exon 6 was amplified as shown. The other PCR product contained the LOX-1 region from exon 1 to exon 5 as shown. These two PCR products with overlapping sequences served as template for each other and the mixture of full-length LOX-1 products carrying a mutation and the wild type product without mutation were obtained.

The cycling conditions used were the same as mentioned above. Here the two PCR products which overlap each other served as template for the synthesis of full-length cDNA of LOX-1. After the PCR, the products obtained were a mix of full-length wild type LOX-1 and full-length exon 4 mutant LOX-1.

The PCR products obtained were gel purified and used for the amplification of the full-length cDNA of LOX-1 with the exon 4 SNP mutation.

Reaction Mix

PCR product (1 st primer pair)	10 μ l
PCR product (2 nd primer pair)	10 μ l
dNTP (2.5 mM)	2 μ l
Buffer (10X)	2.5 μ l
<i>Taq</i> polymerase	0.5 μ l
Total volume	25 μ l

5.3.19 Sequencing (Applied Biosystems 3130 Genetic Analyzer handbook)

5.3.19.1 PCR

50 ng DNA for PCR products and 200 ng DNA for plasmid were used as a template for sequencing PCR reactions.

Reaction Mix

PCR product (or) plasmid DNA	1 to 6.5 μ l
Primer (3.3 pmol)	1 μ l
Sequencing buffer	1.5 μ l
Big Dye	1 μ l
Water	made up to 10 μ l

Cycling Conditions

96 °C	30 sec	} 25 cycles
50 °C	15 sec	
60 °C	4 min	

After the PCR samples were removed from the thermal cycler and stored at -20 °C until further processing.

5.3.19.2 Purification of PCR products and sequencing

90 μ l of dH₂O were added to 10 μ l sequence PCR product and the whole mix was transferred into a 1.5 ml tube. 250 μ l of absolute ethanol and 10 μ l of 3 M sodium acetate (pH 4.6) were then added, mixed well and centrifuged at 19000 g for 15 minutes at room temperature. The supernatant was carefully removed and the pellet was washed with 250 μ l of 70% ethanol and spun down at 19000 g for 5 minutes at room temperature. Once again the supernatant was carefully removed and pellet was vacuum dried. The pellet was dissolved in 10 μ l of Hi-Di™ Formamide (Applied Biosystems) and loaded onto the 96-well plate for sequence analysis.

5.4 Flow cytometry

5.4.1 Processing of blood samples from normal healthy volunteers for HSP70 receptors expression analysis

PBMCs from human blood were prepared by the Biocoll density gradient method. Cells were counted in a Neubauer chamber and 1 million cells were taken into each FACS tube for analysis. Cells were washed twice with PBS and spun down at 280 g for 5 minutes. Cells were resuspended in 100 μ l of PBS. Following antibodies and isotype controls were then added. Combinations of two antibodies with different fluorochromes were used in the same tube whenever possible.

Antibody	Isotype	Species	Fluorochrome	Dilution
1) anti-CD14	IgG _{2a}	mouse	PE	1 µl / 10 ⁶ cells
2) anti-CD91	IgG ₁	mouse	FITC	1 µl / 10 ⁶ cells
3) anti-CD36	IgM	mouse	FITC	1 µl / 10 ⁶ cells
4) anti-TLR2	IgG _{2a}	mouse	PE	1.25 µg/ml
5) anti-TLR4	IgG _{2a}	mouse	FITC	0.8 µg/ml
6) anti-LOX-1	IgG ₁	mouse	-	1 µg/ml

Since LOX-1 primary antibody was unlabelled, the cells were stained with a FITC-labelled secondary goat anti-mouse IgG antibody.

Isotype control monoclonal antibodies were used to estimate the non-specific binding of primary antibodies to cell surface antigens. Non-specific binding is due to Fc receptor binding or other protein-protein interactions.

Isotype Control	Species	Fluorochrome	Dilution
1) IgG ₁	mouse	FITC	1 µl / 10 ⁶ cells
2) IgG _{2a}	mouse	PE	1 µl / 10 ⁶ cells
3) IgM	mouse	FITC	1 µl / 10 ⁶ cells

After staining for 30 minutes the cells were washed twice with PBS and analyzed by flow cytometry.

5.4.2 Processing of PBMCs from HIV-infected individuals for CD14/CD91 FACS analysis

Frozen PBMCs from HIV-infected individuals were obtained from Dr. Justin Stebbing (Department of Immunology, Imperial College, Chelsea and Westminster Hospital, London). The blood samples were processed in the S3 laboratory of the Department of Virology and Immunology in the Primate Centre, Göttingen. The cells were thawed and approximately 5 X 10⁵ cells were taken in each of three FACS tubes and washed once with PBS. For each individual's cells, staining was done as indicated:

- 1) Control - Unstained
- 2) Isotype control - IgG₁-FITC / IgG_{2a}-PE
- 3) Antibodies – CD14-PE / CD91-FITC

After staining for 30 minutes, the cells were washed twice with PBS. 150 µl of 3.7% paraformaldehyde (PFA) was added to each sample tube and incubated for 10 minutes and they were then ready for measurement by flow cytometry.

5.4.3 Processing of blood samples from SIV-infected rhesus macaques for CD14/CD91 FACS analysis

All the blood samples obtained from SIV-infected rhesus macaques and from un-infected control animals were processed in the S3 laboratory of the Department of Virology and Immunology in the Primate Centre, Göttingen. For each experimental animal we received approximately 120-150 µl of blood anti-coagulated with EDTA. Three FACS tubes were prepared for the analysis of each experimental blood sample as explained for the HIV-infected human samples. 35 µl of blood was then added to each of the three FACS tubes from an experimental animal. The blood samples were stained with CD14/CD91 antibodies and their respective isotype controls for 30 minutes at room temperature. 500 µl of erythrocyte lysis buffer (FACS lysing solution, Becton Dickinson) was then added to each FACS tube and left at room temperature (~ 10 minutes) till the erythrocytes were lysed. The blood appears transparent once the erythrocytes are lysed. The samples were then washed twice with PBS by adding PBS to each FACS tube and spinning them down at 280 g for 5 minutes. The cells were then fixed by addition of 150 µl of 3.7% PFA to each sample tube for 10 minutes and they were then ready for flow cytometry analysis.

5.4.4 Analysis of HSP70 binding to monocytes by FACS

PBMCs were isolated from blood of healthy volunteers by the density gradient centrifugation. PBMCs were seeded in 10 cm culture dishes in 10 ml DMEM medium and incubated for 1 hour at 37 °C in 10% CO₂ humidified atmosphere. Floating cells from the culture dish were washed away by rinsing with 5 ml of PBS five times (monocytes attach to the cell surface early than others). Monocytes were then recovered by scraping the plate gently with cell scraper and were counted on a Neubauer chamber to calculate the number of recovered monocytes. One million cells were taken into each FACS tube and were washed once with PBS. Cells were then stained as given below:

- 1) Control (Unstained)
- 2) HSP70-FITC (4 µg/ml)
- 3) HSP70-FITC (4 µg/ml) / HSP70 unlabelled (10 X)
- 4) HSP70-FITC (4 µg/ml) / HSP70 unlabelled (20 X)
- 5) HSP70-FITC (4 µg/ml) / HSP70 unlabelled (30 X)

For the staining where the unlabelled HSP70 was used in 10, 20 and 30-fold excess, the unlabelled HSP70 was added 10 minutes before the addition of FITC-labelled HSP70. After staining with FITC-labelled HSP70 for 30 minutes, cells were washed twice with PBS. Cells were then stained with 100 µl of propidium iodide (PI) (2 µg/ml) for 10 minutes and measured by flow cytometry.

5.5 Computational methods

5.5.1 Statistical tests and models for MFI

To compare the quantitative trait (MFI) between groups, the t-test and Analysis-of-Variance test were used. Non-parametric tests (e.g. Mann-Whitney-Wilcoxon and Kruskal-Wallis) were also applied to some data. Adjustment of p-values in case of

multiple comparisons was done using Tukey-Kramer's procedure. A linear model to explain MFI, accounting for the origin group (RESTART, TIMS or LTNP) and possible effects of genotype was fitted to the data. The genotype effects were estimated nested within the group of origin. For each SNP, the genotype was categorized into two groups: wild type vs. the other genotypes. Separate modelling was done for the HIV-1 positives and the healthy volunteers. In the analysis of the healthy volunteers, since there are no sub-groups, only the genotype effect was tested.

5.5.2 Level of significance

The level of significance was set to $\alpha=5\%$. Due to small sample size of some groups, robust levels of significant α' was derived from randomly permuted data sets as thresholds for significance in some of the statistical tests. The observed MFI measures were randomly allocated (permuted) to the study subjects and fitted to linear models as described above. The percentage of p-values (for specific term in the model equation) from 500 permutations were used as robust threshold value α' .

5.5.3 Statistical tools

R software version 2.3.1 was used to calculate the exact HWE p-values. All the other calculations were performed with SAS 9.1.

5.5.4 Haplotypes prediction and data analysis

The HapMap data were analyzed with the Haploview 3.2 software (Barret et al. 2005). The haplotype blocks were defined applying the confidence intervals algorithm (Gabriel et al. 2002), including only marker with minor allele frequency more than 5%. The PHASE 2.1 software (Stephens et al. 2001, 2005) was used to estimate haplotype pairs for each individual. Ten independent runs with different seed numbers were performed to account for seed-biased discrepancies in the haplotype assignments. The haplotype pair most often assigned to the individual was considered for the genotype-phenotype associations.

6. RESULTS

6.1 Binding of HSP70 to monocytes in PBMCs

HSP70 receptors are expressed on different cell types such as monocytes, DCs and fibroblasts. We analyzed the expression of HSP70 receptors on monocytes and the binding of HSP70 to these cells by flow cytometry. PBMC's were isolated from the blood of healthy volunteers. 5×10^5 cells were taken and stained with a PE-labeled anti-CD14 antibody and FITC-labeled HSP70 antibody. In parallel, PBMCs were stained with PE-labeled anti-mouse IgG_{2a}, an isotype control for CD14 antibody. To determine the specificity of HSP70 binding, a 10 fold excess of unlabeled HSP70 was added to the cells 10 minutes prior to the addition of FITC-labeled HSP70. CD14 expression and HSP70 binding were measured by flow cytometry as shown in Fig 7.

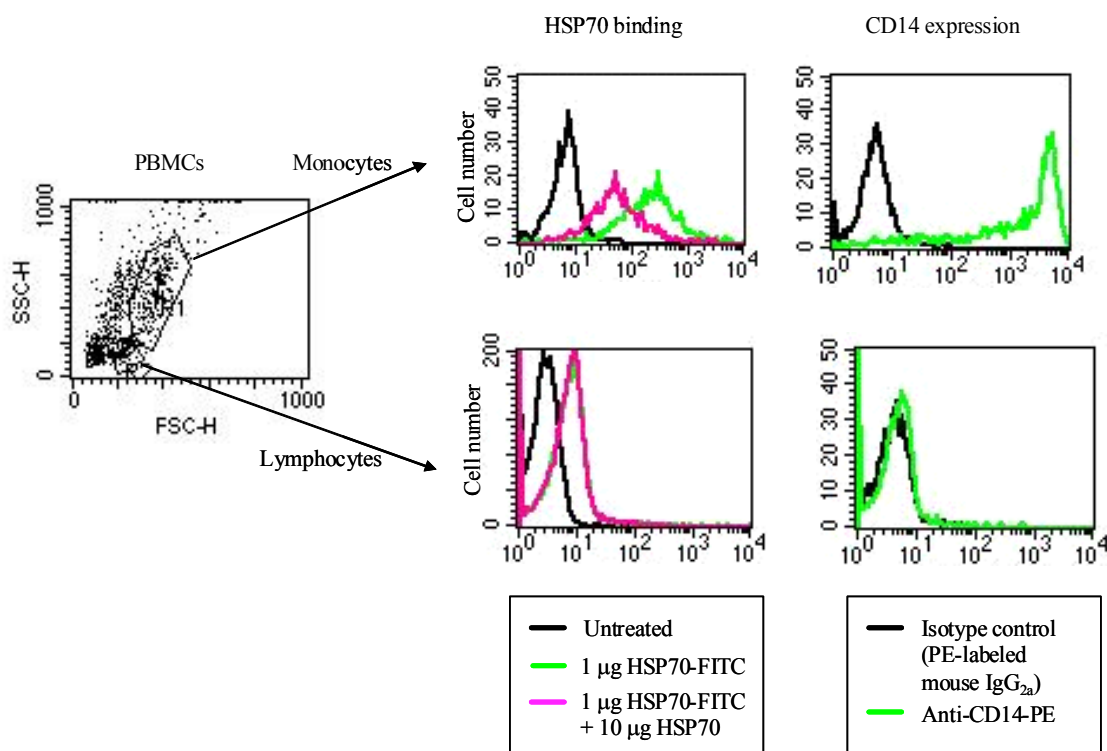


Fig 7. HSP70 binding study on PBMCs. Monocytes and lymphocytes among the PBMCs were gated and analyzed separately. The FSC and SSC indicate the forward scatter and side scatter of the cells in the dot plot. FSC correlates with the cell volume and SSC depends on the inner complexity of the cell. The histograms (left panel) show the binding of FITC-labeled HSP70 and furthermore its inhibition by excess of unlabeled HSP70. In the right panel the binding of PE-labeled anti-CD14 antibody and the respective isotype control (PE-labeled mouse IgG_{2a}) is shown.

There was a binding of FITC-labeled HSP70 to monocytes and this binding was inhibited by a 10-fold excess of unlabeled HSP70 as shown in Fig 7. Lymphocytes bound relatively little HSP70 compared to monocytes and there was no clear inhibition by a 10 fold excess of unlabeled HSP70. The gating of monocytes was confirmed by staining of the monocyte marker CD14 using a specific monoclonal antibody.

6.2 Expression of HSP70 receptors on monocytes

Several receptors including CD91 (Basu et al., 2001), LOX-1 (Delneste et al., 2002), TLR2 and TLR4 (Asea et al., 2002), as well as CD36 (Nakamura et al., 2002) are known to bind eukaryotic HSP70. Some of these receptors, such as CD91 and LOX-1, are believed to play an important role in channeling antigens bound to HSP70 into the MHC class I antigen-presentation pathway, a process known as cross-presentation (Heath and Carbone, 2001). Other receptors like TLR2 and TLR4 are implicated in mediating innate immune responses by HSP70 (Asea et al., 2002).

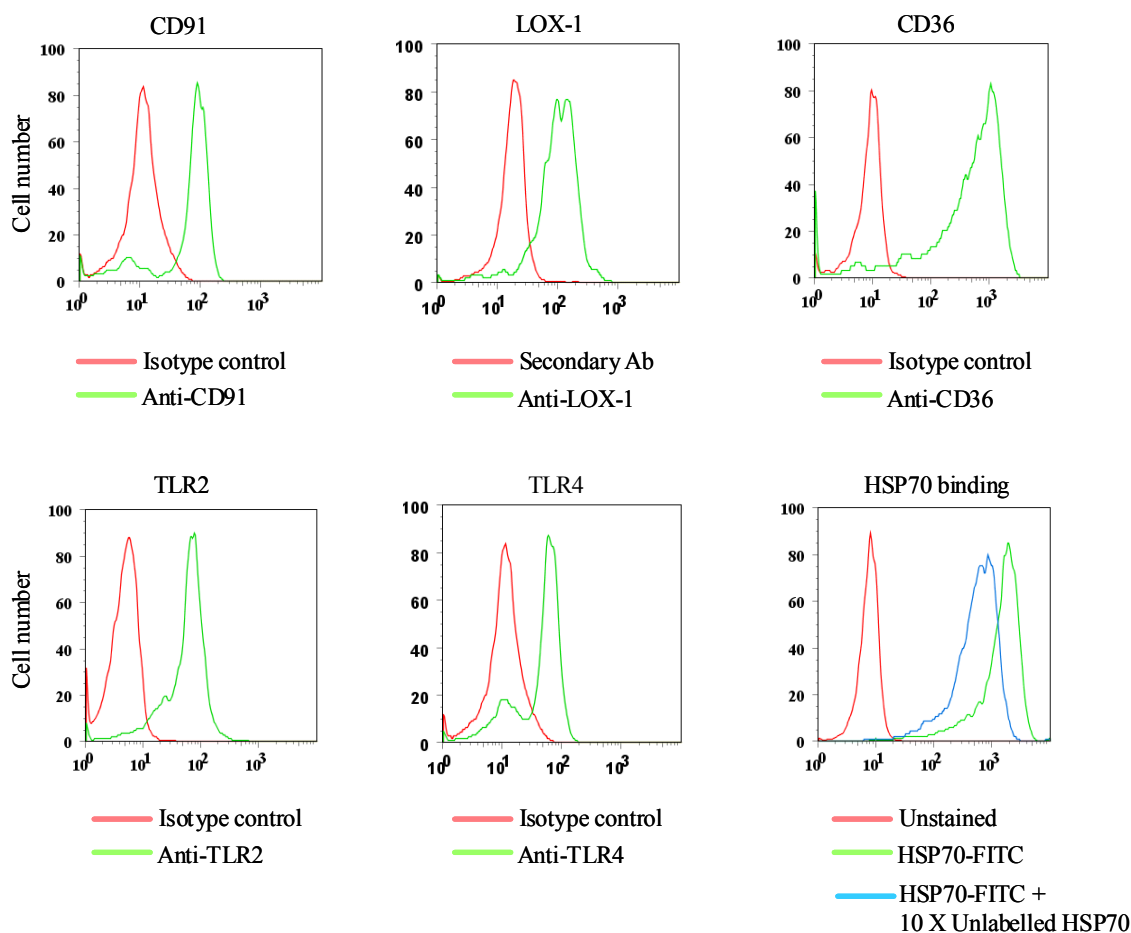


Fig 8. Expression of various HSP70 receptors on cell surface of monocytes. PBMCs were stained with a FITC-labeled anti-CD91 antibody, FITC-labeled anti-CD36 antibody, PE-labeled anti-TLR2 antibody, FITC-labeled anti-TLR4 antibody and anti-LOX-1 antibody (and a FITC-labeled goat anti-mouse IgG secondary antibody) and expression of these receptors on cell surface of monocytes was analyzed by flow cytometry after gating the monocyte population within PBMCs. In parallel PBMCs were stained with FITC-labeled HSP70. Expression of CD91, LOX-1, CD36, TLR2 and TLR4 on cell surface of monocytes and the HSP70 binding is shown by the green curve in the respective figures. The stainings of isotype controls for the antibodies against CD91, CD36, TLR2 and TLR4 and the secondary antibody staining for the primary anti-LOX-1 antibody is shown by a red curve in the respective figures. The inhibition of HSP70 binding by 10-fold excess of unlabeled HSP70 is shown by the blue curve.

We wanted to determine, if the expression of these HSP70 receptors on monocytes correlates with the binding of HSP70 to these cells. PBMCs from blood of each healthy

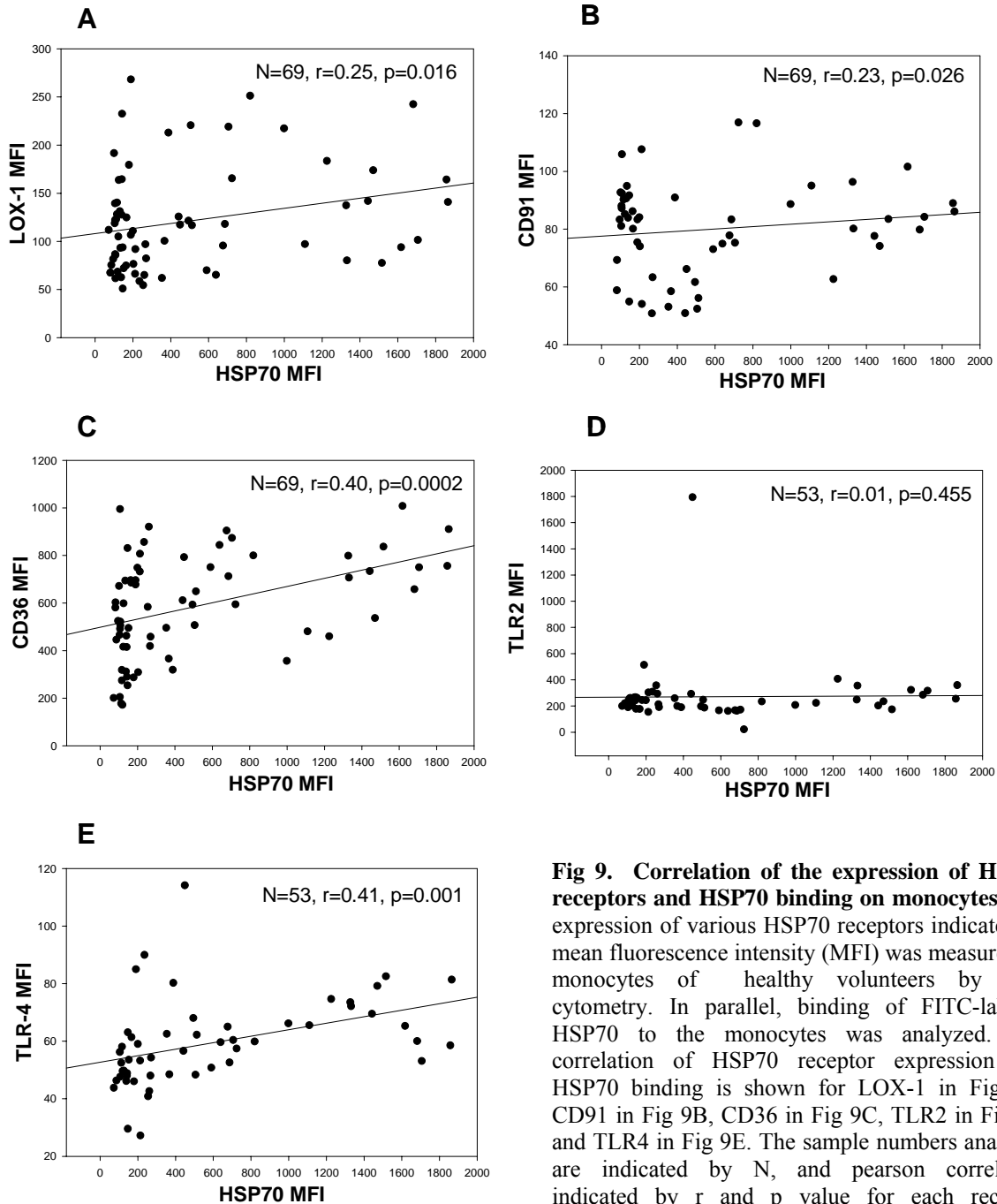


Fig 9. Correlation of the expression of HSP70 receptors and HSP70 binding on monocytes. The expression of various HSP70 receptors indicated by mean fluorescence intensity (MFI) was measured on monocytes of healthy volunteers by flow cytometry. In parallel, binding of FITC-labeled HSP70 to the monocytes was analyzed. The correlation of HSP70 receptor expression and HSP70 binding is shown for LOX-1 in Fig 9A, CD91 in Fig 9B, CD36 in Fig 9C, TLR2 in Fig 9D and TLR4 in Fig 9E. The sample numbers analyzed are indicated by N, and Pearson correlation indicated by r and p value for each receptor analyzed is given at the top of respective figures.

individual were isolated and stained with the antibodies for the various HSP70 receptors, such as LOX-1 (anti-LOX-1 antibody and a FITC-labeled goat anti-mouse IgG secondary antibody), CD91 (FITC-labeled anti-CD91 antibody), CD36 (FITC-labeled anti-CD36 antibody), TLR2 (PE-labeled anti-TLR2 antibody), and TLR4 (FITC-labeled anti-TLR4 antibody). Similarly, the PBMCs from each individual were stained with the isotype controls for CD91 (FITC-labeled anti-mouse IgG₁), CD36 (FITC-labeled anti-mouse IgM), TLR2 (PE-labeled mouse-IgG_{2a}) and TLR4 (FITC-labeled mouse-IgG₁). For the LOX-1 staining, the FITC-labeled goat anti-mouse IgG secondary antibody was used as a control. In parallel the PBMCs from the same individual were stained with FITC-labeled HSP70. Again, the specificity of HSP70 binding to PBMCs from each individual was

evaluated by an adding excess of unlabeled HSP70 prior to the addition of the FITC-labeled HSP70. The stainings were then measured by flow cytometry. The expression of CD91, LOX-1, CD36, TLR2, and TLR4 on monocytes is exemplified in Fig 8. Similarly, binding of HSP70 to monocytes is shown in Fig 8. Inhibition of FITC-labeled HSP70 binding to monocytes by unlabeled HSP70, in Fig 8 indicates the specific binding of HSP70 to monocytes. The amount of HSP70 binding was compared to levels of HSP70 receptors expression on cell surface in order to correlate expression of HSP70 receptors and HSP70 binding.

The correlation of HSP70 receptor expression and HSP70 binding is shown in Fig 9A to 9E. The results indicate a significant but moderate correlation of HSP70 binding and the expression of LOX-1 (Fig 9A), and CD91 (Fig 9B), CD36 (Fig 9C), and TLR4 (Fig 9E). The best correlation was found between TLR4 expression and HSP70 binding ($r=0.41$). However, there was no correlation of HSP70 binding to TLR2 expression (Fig 9D). This suggests that most of the HSP70 receptors on the cell surface of monocytes could participate in binding of HSP70.

6.3 Expression of CD91 in HIV-infected individuals

The expression of CD91 has been shown to be increased in HIV-infected LTNPs compared to disease progressive patients on HAART therapy (Stebbing et al., 2003), HIV-exposed but seronegative subjects compared to their seropositive partners (Kebba et al., 2005) and advanced slow melanoma progressors compared to patients with rapidly advancing metastatic disease (Stebbing et al., 2004). It was hypothesized that increased expression of CD91 in these subjects could be responsible for better presentation of viral or tumor antigens to T cells and thereby leading to a favourable immune response. We analyzed the expression of CD91 in a cohort of LTNP and two groups of disease progressing patients (from TIMS and RESTART studies). Frozen PBMCs obtained from these patients were thawed to room temperature and approximately 5×10^5 cells were taken for each staining of the flow cytometry analysis. Cells were co-stained with PE-labeled anti-CD14 antibody and FITC-labeled anti-CD91 antibody. Similarly cells in another tube were co-stained with isotype controls for CD91 (FITC-labeled anti-mouse IgG₁) and CD14 (PE-labeled anti-mouse IgG_{2a}). PBMC were then gated for lymphocytes and monocytes and the MFI of CD91 was evaluated on CD14⁺ monocytes. CD91 expression was found to be significantly increased in the LTNP group compared to TIMS ($p=0.0004$) and RESTART ($p=0.0296$) groups (Fig 10).

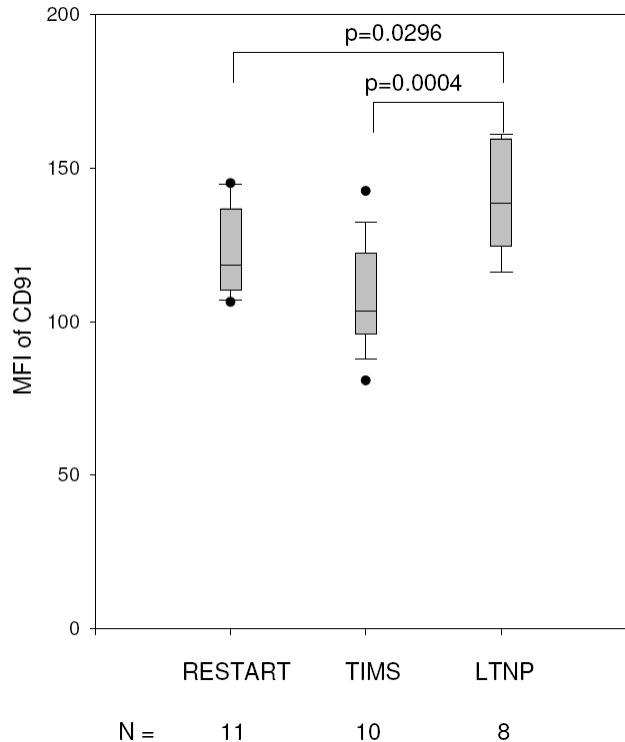


Fig 10. Increased CD91 expression on monocytes of HIV-infected LTNP. PBMCs were stained with FITC-labeled anti-CD91 and PE-labeled anti-CD14 antibodies. The MFI of CD91 on CD14⁺ monocytes was determined by flow cytometry. The CD91 expression in LTNP and disease progressing groups are indicated by box plot. A box plot is a graphical display that involves a five-numbers summary of a distribution of values, consisting of the minimum value, the lower quartile, the median, the upper quartile, and the maximum value. The dots above and below each box plot indicate the outliers. N indicates the number of patients in the respective group. The differences between the groups were analyzed by a t test.

6.4 Genotyping of CD91 promoter and exon 3 polymorphisms in HIV-infected individuals

A polymorphism in the promoter region of CD91 at -25 position has been described by (Schulz et al., 2002) to be associated with a higher CD91 mRNA expression in monocytes. CD91 exon 3 polymorphism has been shown to be associated with breast cancer and Alzheimer's disease (Baum et al., 1998); (Benes et al., 2003). The genotyping of the CD91 promoter and exon 3 polymorphisms was done by AS-PCR. The genotyping of the exon 3 polymorphism and promoter polymorphism for 5 samples is exemplified in Fig 11. The results were then cross-checked for these 5 samples by sequencing of PCR products and the genotype was confirmed to be the same as obtained by AS-PCR. The genotype of all the remaining samples was then determined by AS-PCR.

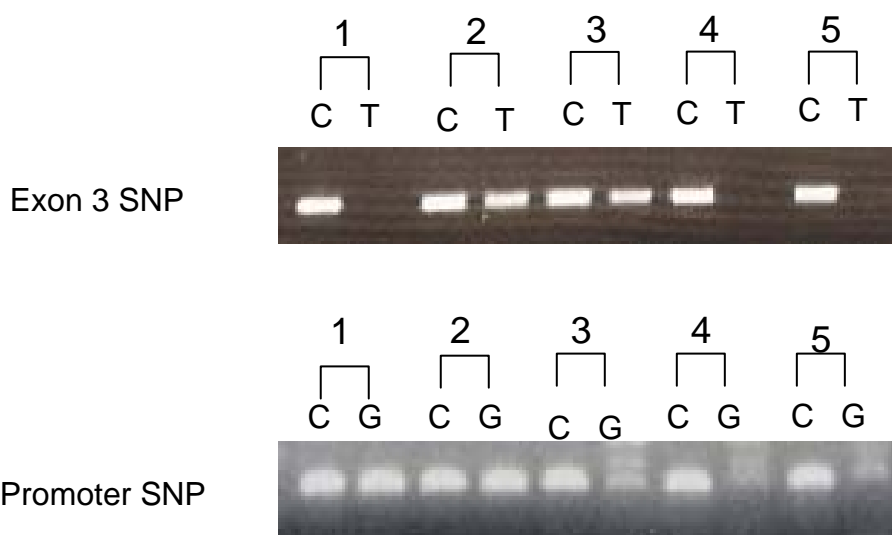


Fig 11. AS-PCR of the CD91 exon 3 (766 C>T) and promoter (-25 C>G) polymorphisms. AS-PCR reactions for both the alleles of the CD91 exon 3 polymorphism and the promoter polymorphism were performed for 5 samples with specific primers. The PCR products obtained were then run on a 1.5% agarose gel. The presence of band for an allele indicates the presence of that allele in the sample and the absence of the band indicates the absence of that allele.

The genotype distribution and allele frequencies for the CD91 promoter (-25 C>G) polymorphism in the LTNPs (N=8) and the patient control groups, TIMS (N=10) and RESTART (N=11) is shown in Table 2. There was no G allele carrier in the RESTART group. Hence, the Hardy-Weinberg equilibrium (HWE) for RESTART group could not be determined.

Table 2. Genotype distribution and allele frequencies of CD91 promoter polymorphism in the HIV cohort

Group	N	Allele Frequencies		CD91 Promoter SNP			Exact Test for HWE p-value
		C	G	C/C	C/G	G/G	
RESTART	11	1	0.00	11	--	--	--
TIMS	10	0.75	0.25	6	3	1	0.480
LTNP	8	0.94	0.06	7	1	--	1.000

The genotype distribution and allele frequencies of the CD91 exon 3 (766 C>T) polymorphism in the LTNPs and the patient control groups, TIMS and RESTART is shown in Table 3. There was no individual with homozygous T allele in the TIMS group. HWE was not observed for the genotype distribution in RESTART group.

Table 3. Genotype distribution and allele frequencies of CD91 exon 3 polymorphism in the HIV cohort

Group	N	Allele Frequencies		CD91 exon 3 SNP			Exact Test for HWE p-value
		C	T	C/C	C/T	T/T	
RESTART	11	0.91	0.09	10	--	1	0.048*
TIMS	10	0.85	0.15	7	3	--	1.000
LTNP	8	0.75	0.25	5	2	1	0.385

* HWE was not observed

6.5 Effect of CD91 promoter and exon 3 polymorphism on CD91 cell surface expression on monocytes in HIV cohort

We had observed an increased expression of CD91 on the cell surface of monocytes in LTNP compared to the patient control groups, RESTART and TIMS. To test if the promoter and exon 3 polymorphisms of CD91 gene have an influence on the CD91 expression level in the HIV cohort, the mean and standard deviation of the CD91 MFI measured in samples of each group were distributed according to the promoter and exon 3 genotype as shown in Table 4. Linear regression analysis was carried out to determine a genetic association of these polymorphisms with the CD91 expression. No significant effect was found of the G allele of the promoter polymorphism on CD91 expression within the TIMS group ($p=0.8692$). For the LTNP G-carrier, no statistic analysis was performed because only one subject carried the G allele. Thus no genetic effect was observed for CD91 promoter polymorphism on CD91 gene expression.

Table 4. Mean and standard deviation of CD91 expression distributed according to CD91 promoter and exon 3 genotype.

Group	Promoter						Exon3					
	C/C			C/G & G/G			C/C			C/T & T/T		
	N	Mean	(SD)	N	Mean	(SD)	N	Mean	(SD)	N	Mean	(SD)
HIV-1+												
Restart	11	121.96	(15.05)	0			10	122.33	(15.81)	1	118.70	(---)
TIMS	6	106.45	(15.77)	4	108.30	(22.92)	7	99.70	(12.63)	3	124.68	(16.72)
LTNP	7	137.37	(18.38)	1	160.11	(---)	5	131.28	(17.75)	3	155.10	(8.77)
Total	24	122.58	(19.37)	5	118.66	(30.51)	22	117.16	(19.35)	7	136.80	(20.42)

Interestingly, the presence of T allele in exon 3 (766 C>T) was associated with an increased CD91 expression on the cell surface of monocytes as shown in Fig 12. There was a significant increase of CD91 expression in TIMS group in the presence of T allele of exon 3 ($p=0.024$). A similar but borderline effect was observed in LTNP ($p=0.040$) if a robust threshold for significance of $\alpha'=0.033$ (obtained from permuted data sets) was applied. Since there was only one sample with T allele in the restart group, the genetic effect was not tested.

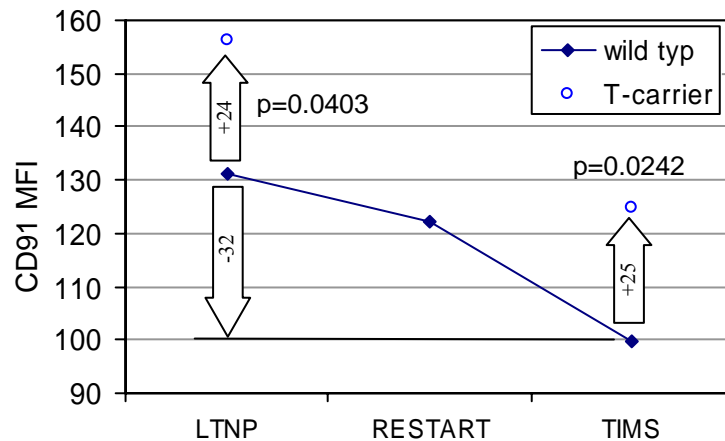


Fig 12. Increased expression of CD91 on monocytes in the presence of the T allele of the exon 3 polymorphism. The CD91 MFI values obtained in the presence of wild type C carrier is shown for all three groups analyzed. Furthermore increase in MFI values with the presence of T allele is indicated for LTNP and TIMS group. There was only one sample in the restart group carrying T allele and hence it is not indicated. The significance of the effect of T allele is indicated by p value.

6.6 Expression of CD91 mRNA in HIV cohort

In the HIV cohort, there was a significant increase of CD91 expression at protein level in LTNP group compared to the disease progressing TIMS and RESTART groups. To study this effect at mRNA level, total RNA was isolated from PBMCs of the HIV cohort. There was very limited material available and hence RNA could only be obtained from a few samples in the HIV cohort. Real-time PCR was performed for the samples where RNA was obtained and the CD91 and CD14 expression at mRNA level was determined using a Taqman gene expression assay. GAPDH served as an internal control. Expression of CD91 mRNA was determined by relative quantitation method, $2^{-\Delta\Delta C_t}$ (Livak and Schmittgen, 2001). At first the CD91 mRNA expression (ΔC_t) was normalized to the internal control, GAPDH. Similarly the CD14 mRNA expression (ΔC_t) was normalized to the internal control, GAPDH. Afterwards, to get the CD91 expression in CD14 positive monocytes, the CD91 mRNA expression was normalized to CD14 mRNA expression in every sample ($\Delta\Delta C_t$). Two samples in the LTNP group showed elevated levels of CD91 expression compared to TIMS and RESTART group (Fig 13 A). To further evaluate if this increase in CD91 mRNA expression is the result of increased number of monocytes in these samples, the CD91 and CD14 mRNA expression levels were correlated with each other. A significant correlation between CD91 and CD14 mRNA expression was observed in these samples (Fig 13 B) suggesting an increase number of monocytes in these samples.

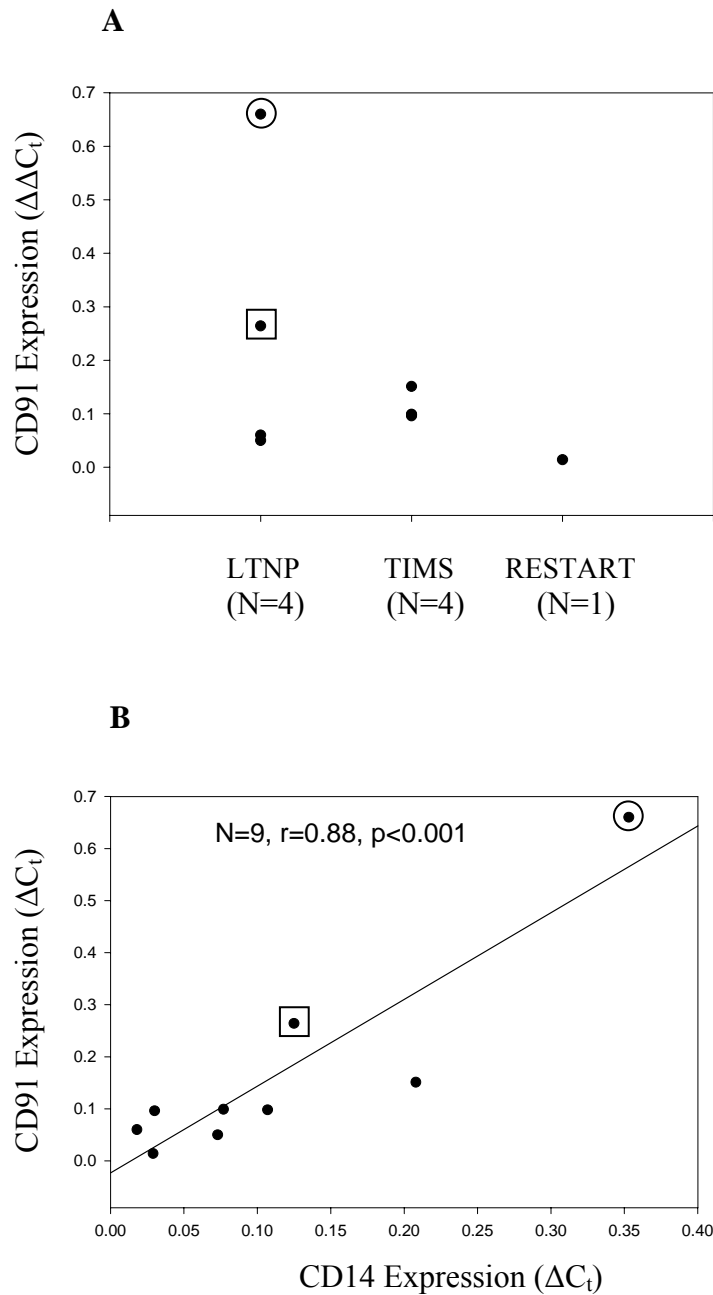


Fig 13. Analysis of CD91 and CD14 mRNA expression in samples of the HIV cohort. (A) The CD91mRNA expression ($\Delta\Delta C_t$) of the samples analyzed in the HIV cohort is shown. N indicates the number of samples analyzed in each group. (B) Expression of CD91 mRNA (ΔC_t) and CD14 mRNA (ΔC_t) determined for nine samples of the HIV cohort were correlated with each other and the correlation coefficient ($r=0.88$, $p=0.001$) was determined by pearson correlation test. Two LTNP samples showing high expression of CD91 indicated by square box and a circle (A) show a close correlation to CD14 expression levels (B).

6.7 Genotyping of CD91 promoter and exon 3 polymorphisms in healthy volunteers

The genotypes of CD91 promoter polymorphism and exon 3 polymorphism were determined in samples from healthy volunteers as explained for samples in the HIV

cohort. No individual with the GG genotype of the promoter polymorphism was found among the 102 samples analyzed. The genotype distribution and allele frequencies are shown in Table 5. The genotype distribution of promoter polymorphism was observed to be in HWE.

Table 5. Genotype distribution and allele frequencies of CD91 promoter polymorphism in HIV cohort

Group	N	Allele Frequencies		CD91 Promoter SNP			Exact Test for HWE p-value
		C	G	C/C	C/G	G/G	
Healthy Volunteers	102	0.92	0.08	86	16	--	1.000

The genotype distribution and allele frequencies of the exon 3 polymorphism in healthy volunteers are shown in Table 6. The genotype distribution of exon 3 polymorphism was observed to be in HWE.

Table 6. Genotype distribution and allele frequencies of CD91 exon 3 polymorphism in healthy volunteers

Group	N	Allele Frequencies		CD91 exon 3 SNP			Exact Test for HWE p-value
		C	T	C/C	C/T	T/T	
Healthy Volunteers	102	0.85	0.15	73	28	1	0.689

6.8 Analysis of the effects of the CD91 promoter and exon 3 polymorphism on the CD91 cell surface expression on monocytes in healthy volunteers

To test if the genetic effect of the CD91 polymorphisms could be observed in normal healthy volunteers, the CD91 MFI values were plotted against the genotypes of CD91 promoter and exon 3 polymorphism. Linear regression analysis was carried out to determine a genetic association of these polymorphisms with the CD91 expression. No increase in CD91 expression was observed on the cell surface of CD14⁺ monocytes with the presence of G allele of CD91 promoter polymorphism (p=0.325). There was also no effect of the exon 3 polymorphism on CD91 expression in healthy volunteers (p=0.293). The genetic effect of CD91 exon 3 polymorphism on CD91 expression which we observed in some of the HIV-1 infected groups seems to be disease specific and may occur in response to HIV-1 infection.

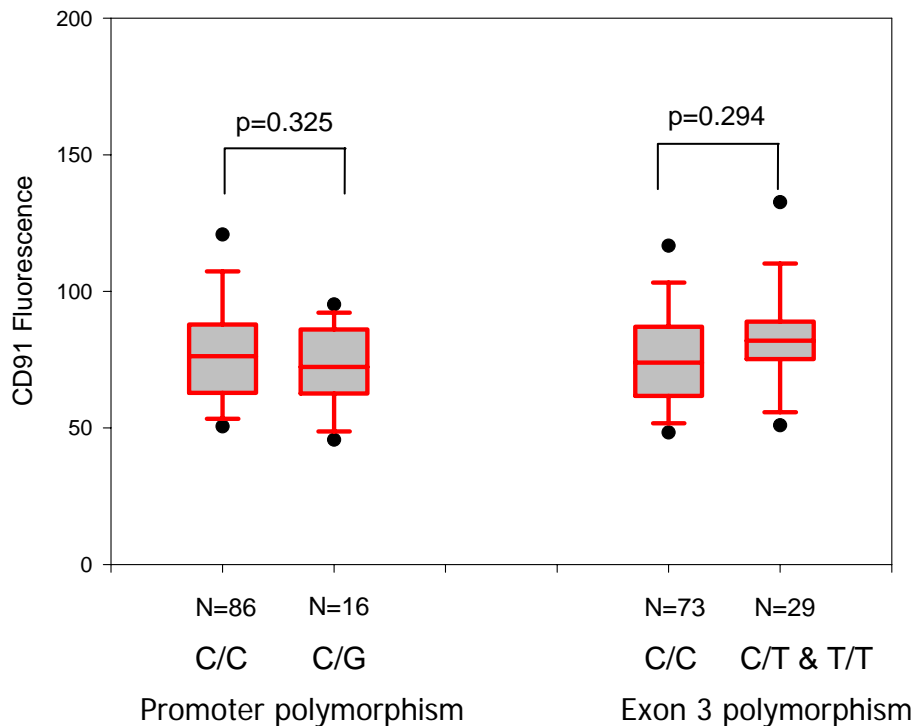


Fig 14. Analysis of the influence of the CD91 promoter and exon 3 polymorphisms on CD91 cell surface expression. CD91 expression was measured on monocytes of 102 healthy volunteers by FACS analysis. The CD91 MFI values for the samples with C/C genotype and C/G genotype of promoter polymorphism were plotted in a box plot. There was no individual with GG genotype. Similarly, the CD91 MFI values for the samples with genotype C/C and C/T, T/T together of the exon 3 polymorphism were plotted in a box plot. Since there was only one individual with TT genotype, it was not possible to produce box plot independently. N indicates the numbers of samples with the particular genotype.

6.9 Analysis of the effects of the CD91 promoter and exon 3 polymorphism on CD91 mRNA expression in healthy volunteers

Schulz and colleagues had reported an increase in CD91 expression at mRNA level with the presence of CD91 promoter (-25 C>G) polymorphism in healthy volunteers (Schulz et al., 2002). We found no influence of the CD91 promoter and exon 3 polymorphisms on CD91 protein expression in our study of healthy volunteers. To further test, if there is an influence of these polymorphisms at mRNA level, we isolated the total RNA from PBMCs of 34 healthy volunteers and performed real-time PCR analysis using a Taqman gene expression assay. Expression of CD91 mRNA was determined by relative quantitation method, $2^{-\Delta\Delta Ct}$ (Livak and Schmittgen, 2001). We detected no influence of the CD91 promoter polymorphism (Fig 15A) and CD91 exon 3 polymorphism (Fig 15B) on CD91 mRNA expression. Expression of CD91 and CD14 mRNA were correlated with each other to test if the differences in CD91 expression are due to the difference in the number of monocytes in each sample as shown in Fig 15C. There was a significant correlation of CD14 and CD91 expression ($r=0.92$, $p<0.001$) indicating that the differences in CD91 mRNA expression could be due to number of monocytes.

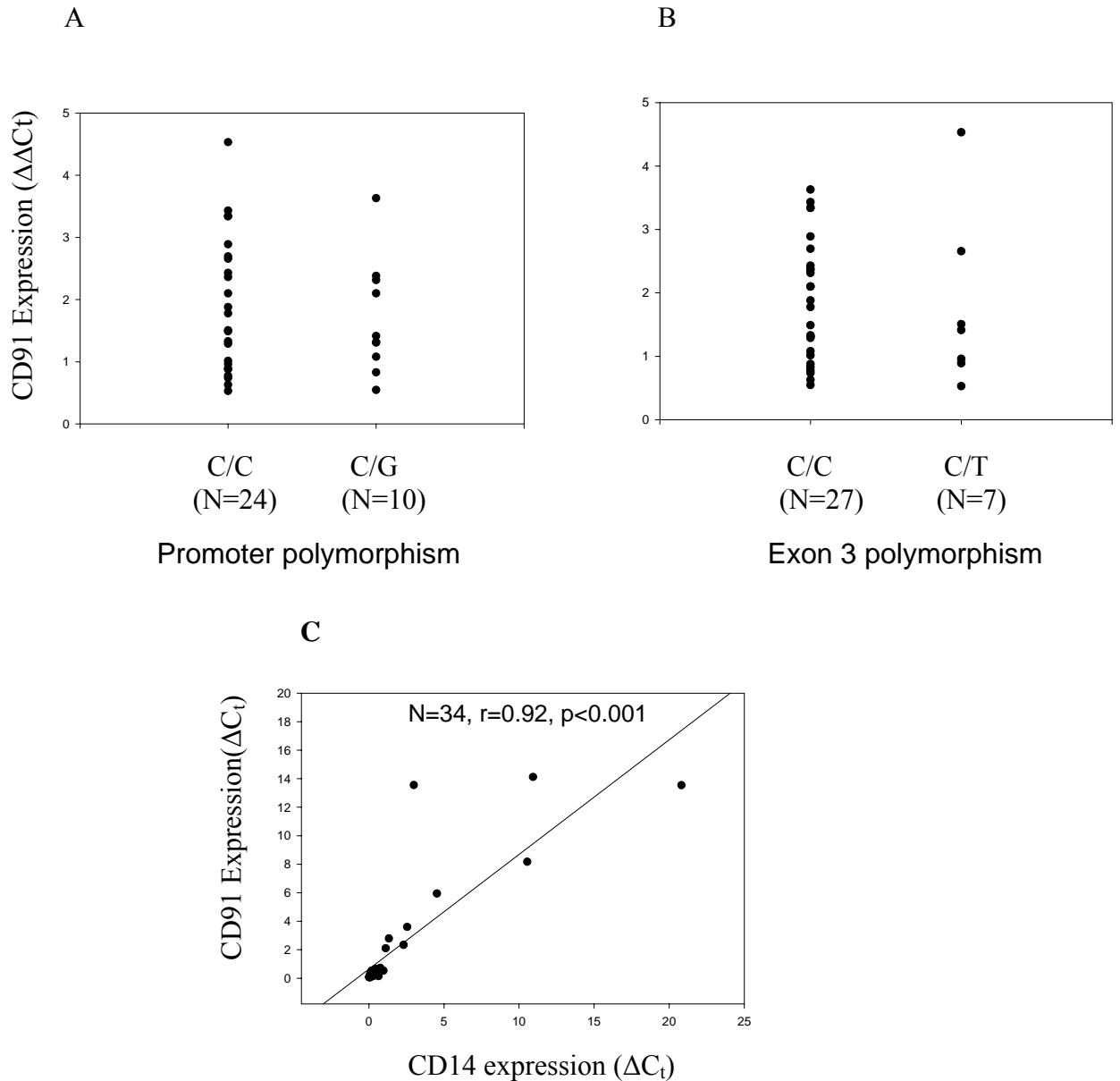


Fig 15. Analysis of CD91 and CD14 mRNA expression in healthy volunteers. The CD91 mRNA expression ($\Delta\Delta C_t$) of the samples analyzed in the healthy volunteers for the promoter polymorphism (A) and the exon 3 polymorphism (B) is shown. N indicates the number of samples analyzed in each group. Expression of CD91 mRNA (ΔC_t) and CD14 mRNA (ΔC_t) determined for 34 samples in healthy volunteers were correlated with each other and the correlation coefficient ($r=0.88$, $p=0<001$) was determined by pearson correlation test

6.10 Analysis of HapMap data for LRP1 (CD91) gene

We found a significant effect of exon 3 polymorphism on CD91 cell surface expression on monocytes in TIMS group and a similar but borderline effect in LTNP group. Since exon 3 polymorphism encodes a synonymous polymorphism, it may not be directly responsible for the effect on CD91 expression but is strongly associated with the CD91 expression. Five additional SNPs were analyzed within the gene. The SNPs were selected

to tag all haplotypes with at least 5% frequency within the HapMap Caucasian population as follows: The chromosomal region spanning the entire LRP1 gene and approximately 12 kb flanking region on either side of the gene was chosen for HapMap analysis. From the HapMap database (data release version 22 from March 2007, www.hapmap.org) the SNP genotype data representative of the Caucasian population for the selected genomic region was downloaded and analyzed by haploview software.

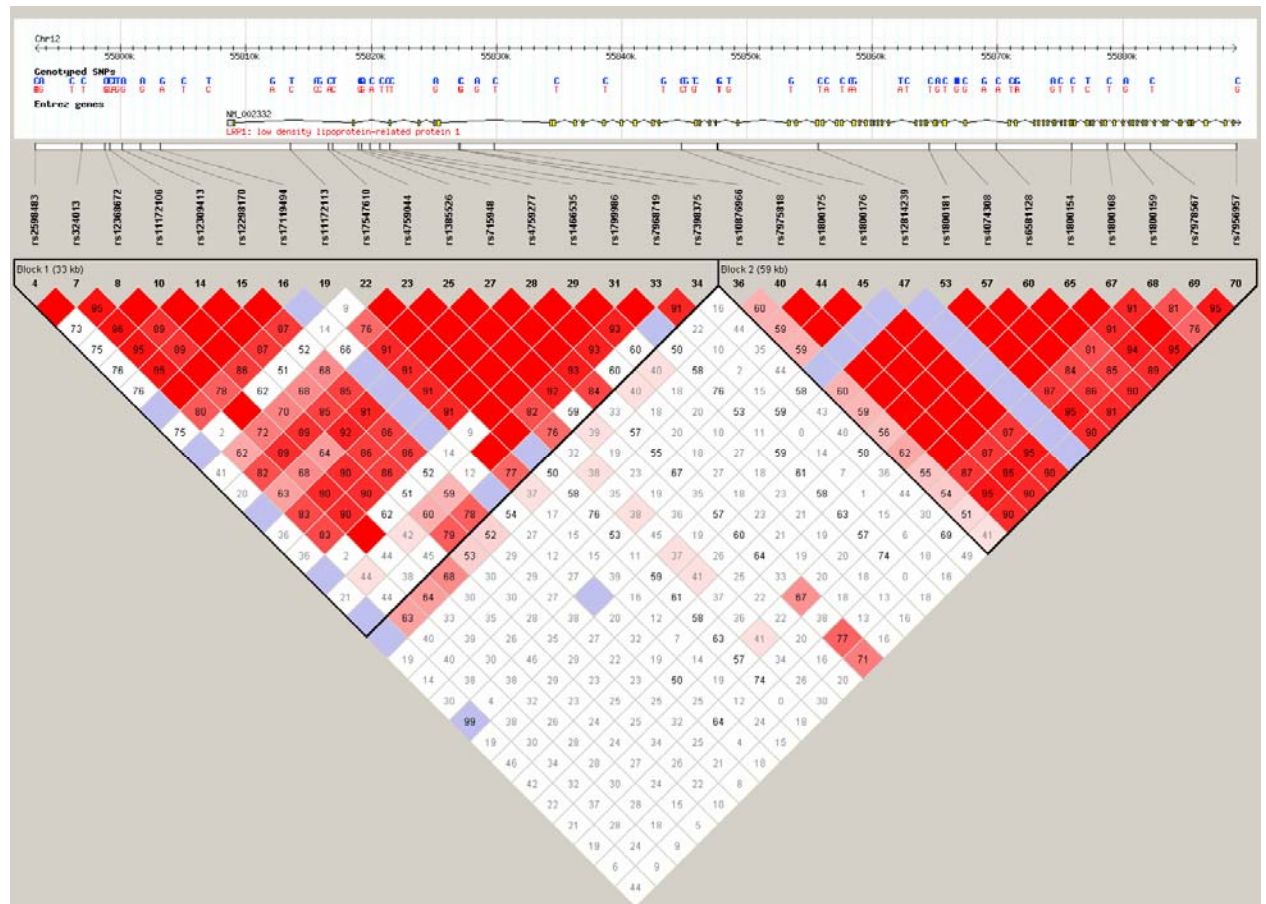


Fig 16. Display of LD for the chromosomal region containing LRP1 gene. LD among the markers within the LRP1 gene and a small genomic region surrounding the gene was analyzed. The color scheme is representing the strength of pair-wise LD in terms of D' as follows: red- strong LD (D' of 1), white – no LD (D' of 0) and the variations in between are represented in with different depth of pink and the exact D' values are given in percents. The blue color marks regions where the calculation of LD was not possible. The triangle indicates region of strong LD called as LD block. There are two blocks obtained for the LRP1 gene. An info track is displayed on top of the LD blocks giving the information regarding the region of chromosome being analyzed and genotyped SNPs in this region and also the genes that are present in the region.

Two recombinant blocks of strong LD were observed that include all the markers in the analyzed region (Fig 16). The haplotype structure within this region was analyzed (Fig 17). Since the exon 3 polymorphism occurred in the first block of analyzed region, detailed study of the haplotypes in this region was considered for analysis. Five haplotype tagging SNPs (htSNPs) were selected for the first block to differentiate between the frequent haplotypes ($> 4.9\%$) observed in the first block.

CD91 Tag 10 - rs11172106
 CD91 Tag 23 - rs4759044
 CD91 Tag 27 - rs715948
 CD91 Tag 31 - rs1799986 (CD91 exon 3 polymorphism)
 CD91 Tag 34 - rs7398375



Fig 17. Partial list of haplotypes generated for the LRP1 gene containing region. The frequency of haplotypes estimated from the HapMap dataset of Caucasian population is shown on right hand side of each haplotype. The numbers above represents the order of tag SNPs along the chromosome region analyzed responsible for tagging each haplotype. Lines between the two blocks show the most common crossings from one block to the next, with thicker lines showing more common crossings than the thinner ones. The value shown below the crossing lines is the multilocus D prime, which is a measure of LD between two blocks. The closer to zero the value is, the greater the amount of historical recombination between the two blocks. For our study, the haplotypes in the first block with at least close to 5% frequency were chosen for analysis as indicated by a red line. For the second block, only two major haplotypes were chosen as indicated by the red line. The htSNPs (tag 10, tag 23, tag 27, tag 31- exon 3 polymorphism, tag 34 for the first block and tag 67 for the second block) that are sufficient to differentiate between these haplotypes are indicated by red boxes.

For the second block, two major haplotypes were chosen for analysis and one tag SNP was sufficient to differentiate between these two major haplotypes. The reference SNP ID number for this tag SNP (tag 67) was rs1800168. The chosen tag SNPs were used to assess the genetic variability in our HIV cohort and healthy volunteers (Caucasian origin) and to study the effect of these SNPs and haplotypes on CD91 expression.

6.11 Genotyping of the tag SNPs in the first block of the CD91 gene

The AS-PCR method was tested for all the tag SNPs in the first block of the CD91 gene. 5 samples were sequenced and the genotype of each tag SNP for these samples was determined. For all the tag SNPs except tag 34, we obtained a mix of heterozygous and homozygous genotypes as shown in Table 7. The AS-PCR conditions were then tested to reproduce the sequence results of the same samples and after standardization, the same conditions were used to determine the genotype of remaining samples. For tag 34 SNP, we sequenced 25 samples, but we did not find any heterozygous genotype. We tested different AS-PCR conditions for tag 34, but again there was no heterozygous genotype. It was possible that these methods were not working for this SNP and hence the alleles could not be differentiated. Finally, we performed RFLP method and observed the heterozygous genotype for tag 34 across several sample. We repeated the RFLP method for several samples and it was reproducible.

Table 7. Validation of genotypes of tag SNPs by sequencing and AS-PCR methods in 5 samples

Sample number	Tag 10 SNP		Tag 23 SNP		Tag 27 SNP		Tag 34 SNP	
	Sequencing	AS-PCR	Sequencing	AS-PCR	Sequencing	AS-PCR	Sequencing	AS-PCR
1	C/C	C/C	T/T	T/T	A/A	A/A	C/C	C/C
2	C/G	C/G	C/T	C/T	G/A	G/A	C/C	C/C
3	C/G	C/G	C/T	C/T	G/G	G/G	C/C	C/C
4	C/C	C/C	C/T	C/T	G/A	G/A	C/C	C/C
5	C/C	C/C	C/C	C/C	G/A	G/A	C/C	C/C

Genotyping of tag 10 SNP was determined by AS-PCR. All the groups were observed to be in HWE. The genotype distribution and allele frequencies are shown in Table 8.

Table 8. Genotype distribution and allele frequencies of the CD91 Tag 10 polymorphism in the HIV cohort and healthy volunteers

Group	N	Allele Frequencies		CD91 Tag 10			Exact Test for HWE p-value
		C	G	C/C	C/G	G/G	
HIV-1 Positives							
RESTART	11	0.68	0.32	4	5	2	1.000
TIMS	10	0.70	0.30	5	4	1	1.000
LTNP	8	0.59	0.41	4	3	1	1.000
Healthy Volunteers	102	0.64	0.36	42	47	13	1.000

Table 9. Genotype distribution and allele frequencies of the CD91 Tag 23 polymorphism in the HIV cohort and healthy volunteers

Group	N	Allele Frequencies		CD91 Tag 23			Exact Test for HWE p-value
		C	T	C/C	C/T	T/T	
HIV-1 Positives							
RESTART	11	0.68	0.32	5	5	1	1.000
TIMS	10	0.40	0.60	3	2	5	0.082
LTNP	8	0.31	0.69	1	3	4	1.000
Healthy Volunteers	92	0.40	0.60	14	45	33	1.000

Table 10. Genotype distribution and allele frequencies of the CD91 Tag 27 polymorphism in the HIV cohort and healthy volunteers

Group	N	Allele Frequencies		CD91 Tag 27			Exact Test for HWE p-value
		A	G	A/A	G/A	G/G	
HIV-1 Positives							
RESTART	11	0.27	0.73	--	6	5	0.505
TIMS	10	0.30	0.70	1	4	5	1.000
LTNP	8	0.50	0.50	3	2	3	0.199
Healthy Volunteers	100	0.34	0.66	10	49	41	0.508

Genotyping of tag 23 SNP was done by AS-PCR. The genotype distribution and allele frequencies are shown in Table 9. Genotyping of tag 27 in HIV cohort was done by AS-PCR. There was no homozygous individual for A allele in the RESTART group. The genotype distribution and allele frequencies are shown in Table 10. Genotyping of tag 34 SNP was done by restriction fragment length polymorphism (RFLP) method. The enzyme used for the digestion of PCR product was Rsa1, which cuts in the presence of C allele but not the G allele as shown in Fig 18. The genotype distribution and allele frequencies for tag 34 SNP are shown in Table 11.



Fig 18. Genotyping of tag 34 SNP by RFLP method. The enzyme used the analysis of tag 34 SNP by RFLP method was Rsa1. As indicated in the figure, the enzyme cuts the C allele but not the G allele. The enzymatic digestion of the PCR product carrying tag 34 SNP of 5 samples is indicated in the gel picture. The genotype determined for these 5 samples is indicated above the lane of each sample.

Table 11. Genotype distribution and allele frequencies of the CD91 Tag 34 polymorphism in the HIV cohort and healthy volunteers

Group	N	Allele Frequencies		CD91 Tag 34			Exact Test for HWE p-value
		C	G	C/C	C/G	G/G	
HIV-1 Positives							
RESTART	11	0.62	0.38	4	7	--	0.480
TIMS	10	0.75	0.25	5	5	--	1.000
LTNP	8	0.68	0.32	4	2	2	0.217
Healthy Volunteers	102	0.75	0.25	54	44	4	0.294

6.12 Analysis of the effect of independent tag SNPs on CD91 protein expression in the HIV cohort

The genotypes obtained for the tag SNPs in the first block of CD91 gene for the samples in the HIV cohort were plotted against their CD91 MFI values on cell surface of monocytes as shown in Fig 19. We did not observe any significant effect of these SNPs on CD91 expression.

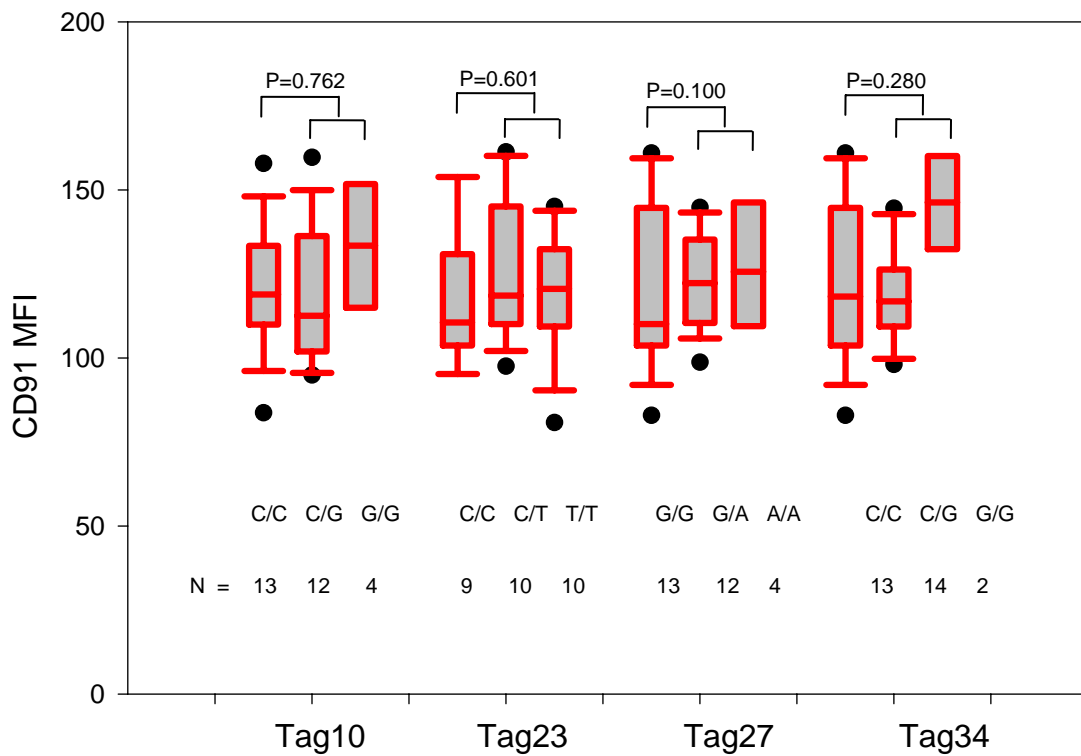


Fig 19. Effect of tag SNPs in the first block of CD91 gene on CD91 expression in the HIV cohort. Genotypes obtained for all the tag SNPs were analyzed independently to observe any effect on CD91 expression on cell surface of monocytes. N indicates the number of samples with the given genotype. For the statistical analysis of the genetic effect of individual SNP on CD91 expression, the genotype was categorized into two groups: wild type vs. the other genotypes. Statistical analysis was done by linear regression model and is indicated by p values.

6.13 Analysis of the effect of independent tag SNPs on CD91 protein expression in the healthy volunteers

The genotypes of the tag SNPs in the first block of CD91 gene for healthy volunteers were plotted against their CD91 MFI values on cell surface of monocytes as shown in Fig 20. No significant effect of these SNPs was observed on the CD91 expression in healthy volunteers.

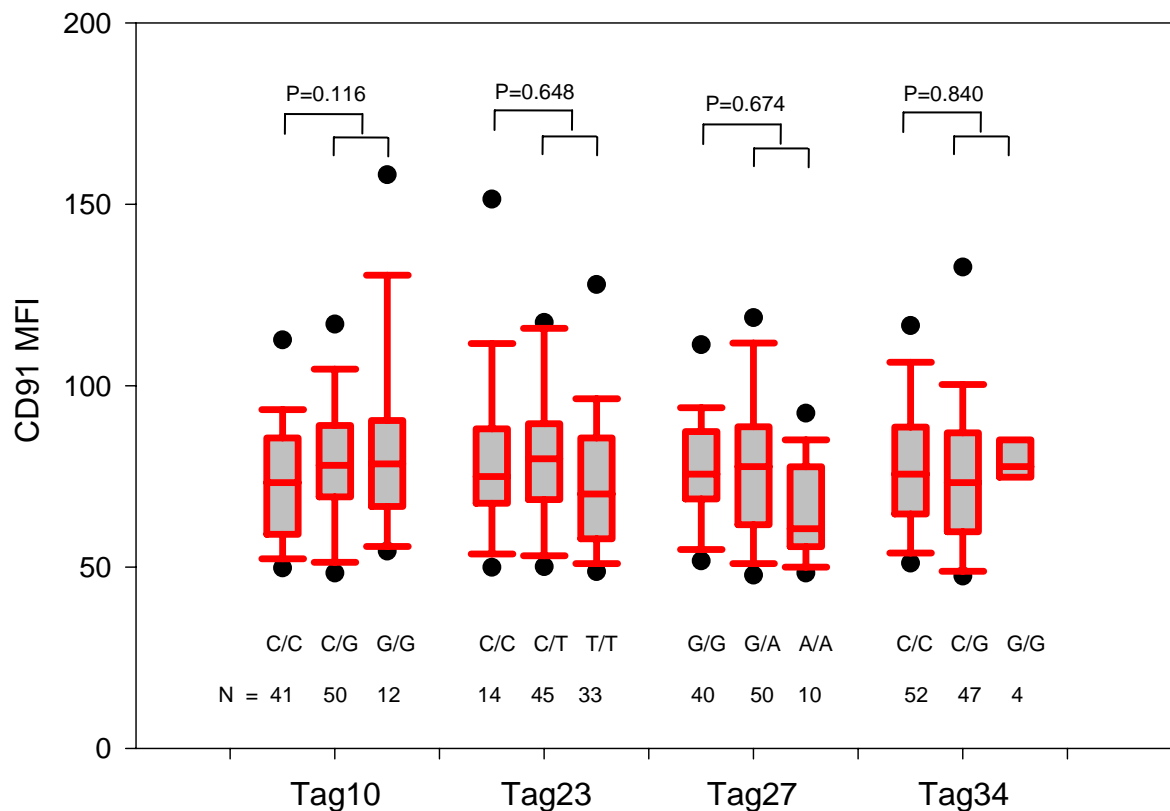


Fig 20. Effect of tag SNPs in the first block of the CD91 gene on CD91 expression in healthy volunteers. Genotypes obtained for all the tag SNPs were analyzed independently to observe any effect of these SNPs on the CD91 expression on cell surface of monocytes. N indicates the number of samples with the given genotype. Statistical analysis for the genetic effects of these SNPs on CD91 expression was done by linear regression model and is shown by p values. For the statistical analysis, the genotypes were categorized into two groups: wild type and the other genotypes.

6.14 Generation of haplotypes

The genotypes obtained for all tag SNPs and the genotypes of promoter polymorphism and exon 3 polymorphism were analyzed by phase version 2.1 software (Stephens and Donnelly, 2003; Stephens et al., 2001) to estimate the haplotypes. The haplotypes were also estimated with HAP webserver (Halperin and Eskin, 2004) and the haplotypes obtained were similar to those obtained with phase software. The list of the most frequent haplotypes and their frequency observed in our study population of healthy volunteers and HIV cohort is indicated in Fig 21.

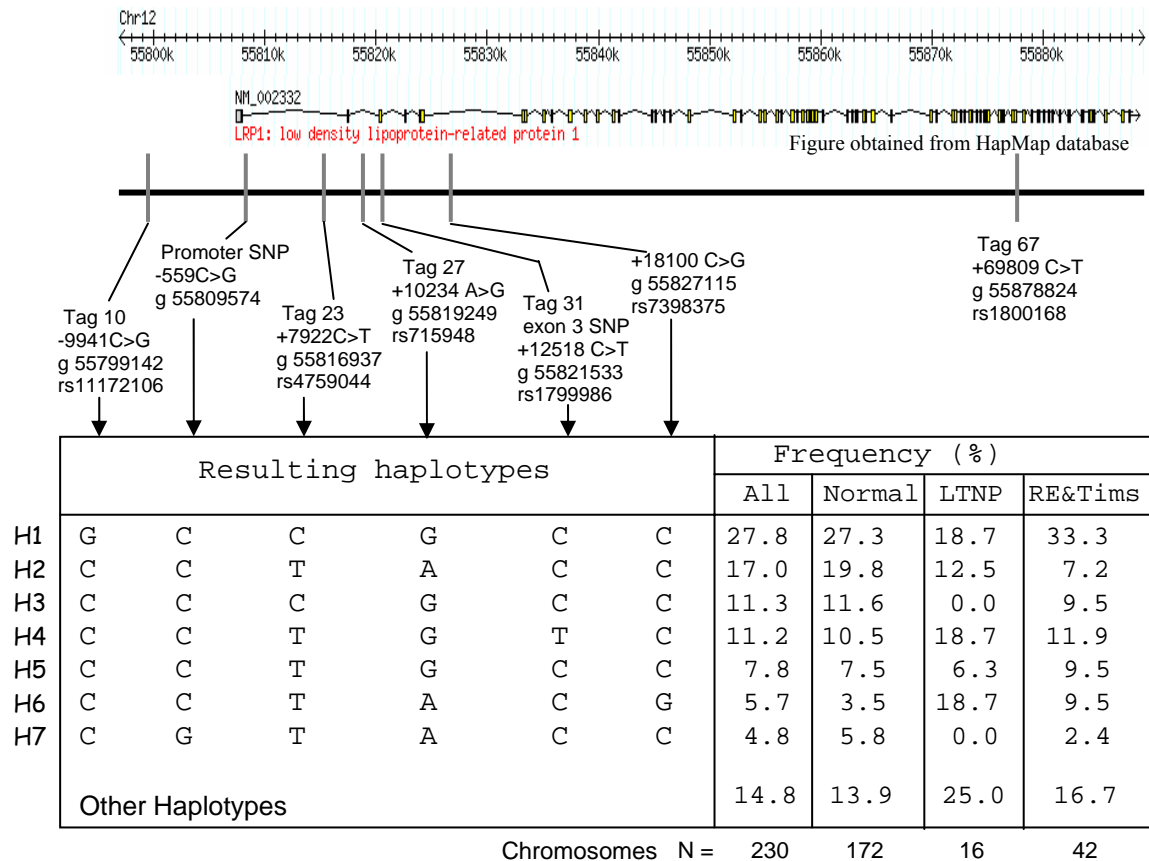


Fig 21. Genomic location, identity of SNP tags for CD91 and their resulting haplotypes and frequencies. The chromosomal location of the CD91 gene and the position of tag SNPs in the gene are indicated. The resulting polymorphism of each SNP and their NCBI reference SNP number is also indicated. The arrow indicates the position of each SNP in the estimated haplotypes. H1 to H7 represent the most frequent haplotypes estimated for CD91 gene in all the samples including the healthy volunteers and the HIV cohort. The frequencies of each haplotype for different groups analyzed are also indicated. N represents the total number of chromosomes analyzed.

We then compared the haplotype frequencies obtained with our samples of healthy volunteers (Caucasian population) to the haplotype frequencies of the HapMap Caucasian population. The most frequent haplotype H1 (27.8%) obtained in our samples was similar to the most frequent one in the HapMap Caucasian population (24.9%). However, three haplotypes H2 (17%), H3 (11.3%) and H4 (11.2%) were over-represented compared to the HapMap Caucasian population, 8.7%, 5% and 4% respectively and one haplotype H6 (5.7%) was under-represented compared to the HapMap Caucasian population (17%).

6.15 Effect of CD91 haplotypes on CD91 expression in HIV cohort and healthy volunteers

The haplotypes generated for the first block of the CD91 gene in HIV cohort and healthy volunteers were analyzed for their effect on CD91 expression. The haplotypes were plotted against their MFI values of CD91 on the cell surface of monocytes in HIV cohort (Fig 22) and healthy volunteers (Fig 23). There was no obvious effect of these haplotypes on CD91 expression in HIV cohort and the healthy volunteers as shown in Fig 22 and

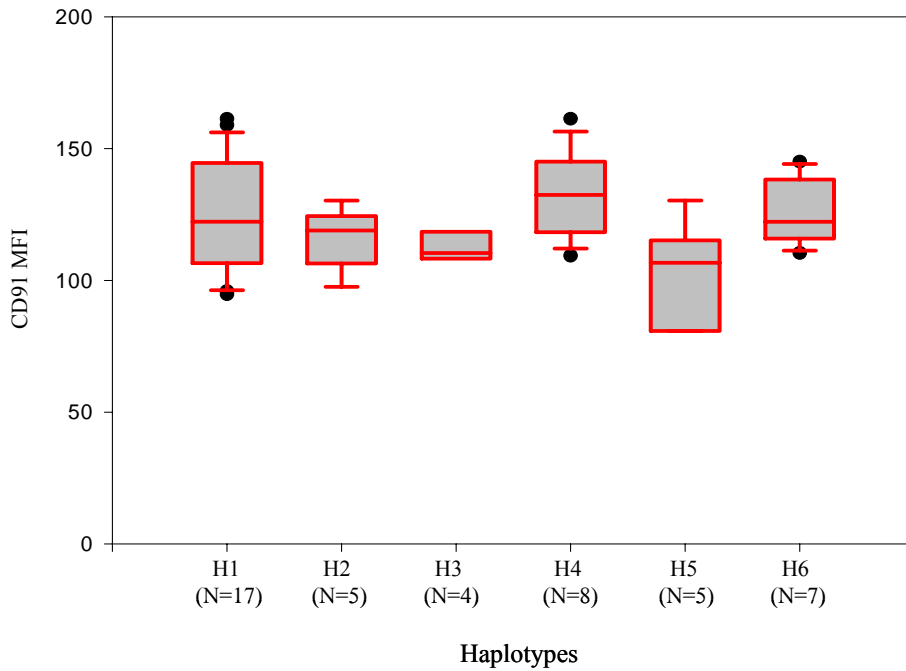


Fig 22. Effect of CD91 haplotypes on CD91 expression in HIV cohort. The MFI of CD91 measured on monocytes of HIV cohort were plotted according to the presence of 6 haplotypes (H1, H2, H3, H4, H5 and H6) observed in this group. There was only one individual with H7 haplotype and hence it could not be plotted. N indicated the number of chromosomes with a particular haplotype.

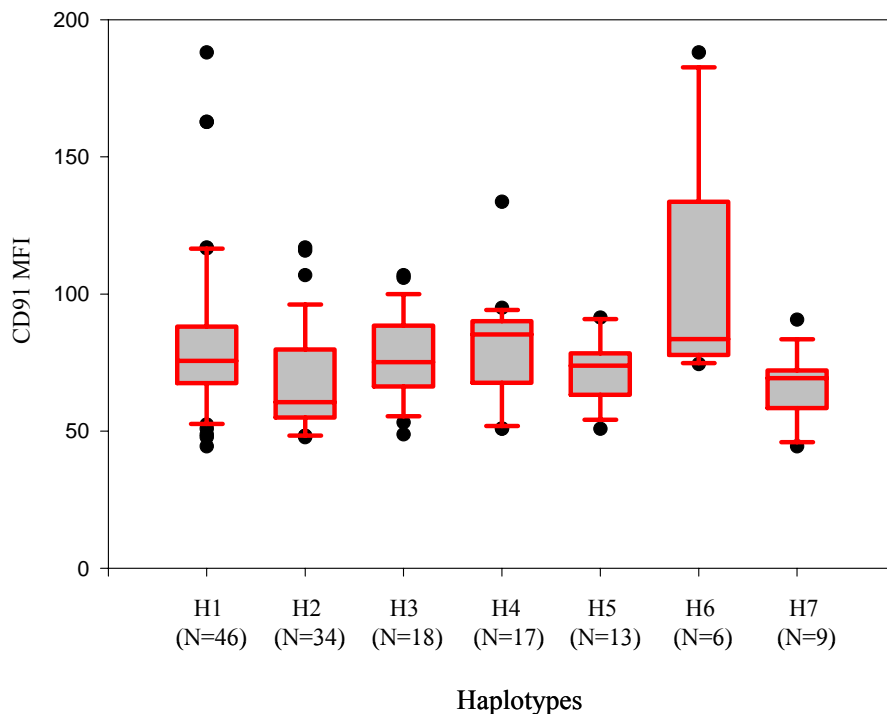


Fig 23. Effect of CD91 haplotypes on CD91 expression in healthy volunteers. CD91 MFI measured on monocytes of healthy volunteers were plotted according to the presence of 7 haplotypes (H1, H2, H3, H4, H5, H6 and H7) observed within these individuals. N indicated the number of chromosomes with a particular haplotype.

Fig 23 respectively. Also the sample number is too low to detect subtle differences by statistical analysis.

6.16 Genotyping of the tag SNP in second block of the CD91 gene

Genotyping of tag 67 SNP was done by AS-PCR. The genotype distribution for all the three groups in the HIV cohort and the healthy volunteers is shown in Table 12.

Table 12. Genotype distribution and allele frequencies of CD91 Tag 67 polymorphism in the HIV cohort and healthy volunteers

Group	N	Allele Frequencies		CD91 Tag 67			Exact Test for HWE p-value
		C	T	C/C	C/T	T/T	
HIV-1 Positives							
RESTART	11	0.25	0.75	2	4	5	0.538
TIMS	10	0.30	0.70	1	4	5	1.000
LTNP	8	0.36	0.64	1	2	5	0.385
Healthy Volunteers	94	0.30	0.70	7	42	45	0.626

6.17 Analysis of the effect of tag 67 SNP on CD91 protein expression in the HIV cohort and healthy volunteers

The genotypes of the tag 67 SNP in the second block of the CD91 gene were plotted against their CD91 MFI values on cell surface of monocytes for the HIV cohort (Fig 24A) and the healthy volunteers (Fig 24B). There was no influence of CD91 Tag 67 SNP on CD91 expression in HIV cohort (Fig 24A) and healthy volunteers (Fig 24B).

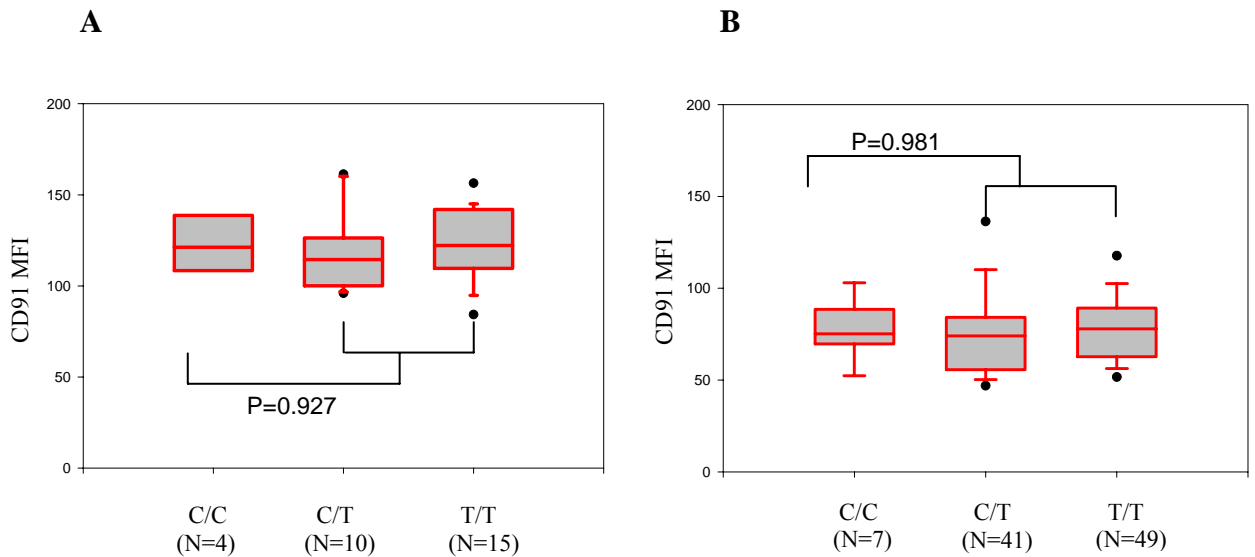


Fig 24. Influence of tag 67 SNP on CD91 expression in HIV cohort and healthy volunteers. Tag 67 SNP was genotyped in all the groups of HIV cohort and healthy volunteers and the CD91 expression on monocytes obtained for these individuals were plotted against individual genotypes in a box plot. (A) The effect of tag 67 genotypes on CD91 expression for HIV cohort is shown. (B) The effect of tag 67 genotypes on CD91 expression in healthy volunteers is shown. Statistical analysis for the genetic effect of tag 67 SNP on CD91 expression in HIV cohort and healthy volunteers was done by linear regression model and is shown by p values.

6.18 Genotyping of CD91 exon 3 polymorphism from serum DNA of LTNPs

In our analysis of LTNP samples, we found an increased frequency of T allele of the CD91 exon 3 polymorphism in LTNP group (0.25, N=8) compared to the frequencies obtained for disease progressive groups (0.12, N=21) TIMS and RESTART. To further increase the number of samples of LTNP group, we obtained serum samples of new LTNP patients from Dr. J. Stebbing (Department of Immunology, Imperial College, Chelsea and Westminster Hospital, London). Genomic DNA from the serum sample was obtained by proteinase K / SDS lysis method. A PCR product carrying the exon 3 SNP region was amplified for all the samples and the genotypes for exon 3 SNP was determined by sequencing. The genotype distribution and allele frequencies for the CD91 exon 3 polymorphism in these additional LTNP samples are shown in Table 13.

We then compared the T allele frequencies of CD91 exon 3 genotype of all the LTNP samples with the disease progressive group. More occurrence of T allele was observed in LTNP group (0.20, N=22) compared to the disease progressive group (0.12, N=21). However the differences of T allele frequencies between the LTNP group and disease progressive groups were not statistically significant ($p=0.383$).

Table 13. Genotype distribution and allele frequencies of CD91 exon 3 polymorphism obtained from LTNP serum samples.

Group	N	Allele Frequencies		CD91 exon 3 SNP		
		C	T	C/C	C/T	T/T
LTNP	14	0.82	0.18	10	3	1

6.19 Study of CD91 expression in rhesus macaques

In humans, CD91 expression has been described to be augmented on monocytes of HIV-1 infected LTNPs compared to patients with chronically suppressed HIV-1 by highly active anti-retroviral therapy (HAART) (Stebbing et al., 2003). In the HIV cohort, we observed an increased expression of CD91 on monocytes of LTNPs compared to HIV-1 infected disease progressing groups (TIMS & RESTART). However, in humans it is impossible to evaluate whether high CD91 expression in LTNPs is noticeable before HIV infection or occurs after infection. An animal model such as rhesus macaque that develops an AIDS-like disease upon infection with simian immunodeficiency virus (SIV), allows for studying the CD91 expression before and after SIV infection. SIV vaccination trials in rhesus macaques at the Primate Center, Göttingen gave us an opportunity to obtain blood for the analysis of CD91 expression in rhesus macaques before and after SIV infection.

6.20 CD91 expression on CD14 positive cells in rhesus macaques before SIV infection

Groups of animals were vaccinated or mock vaccinated and then challenged with SIV and another group (naïve) was not vaccinated but challenged with SIV. These experiments were designed for other purposes but we obtained blood from these animals for the analysis of CD91 expression on monocytes. Therefore, we can not reveal details on the vaccination protocols here and we did not intend to specifically evaluate the effect of the vaccination in the CD1 expression. Blood was collected at two different time points before the SIV infection and at different time intervals after the infection as shown by a cartoon in Fig 25.

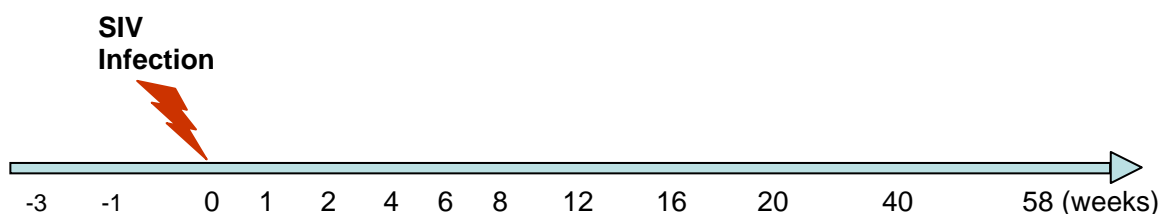


Fig 25. Schematic representation of different time points of CD91 expression analysis in rhesus macaques. Blood was collected at two intervals before the SIV infection and at different time points after the infection.

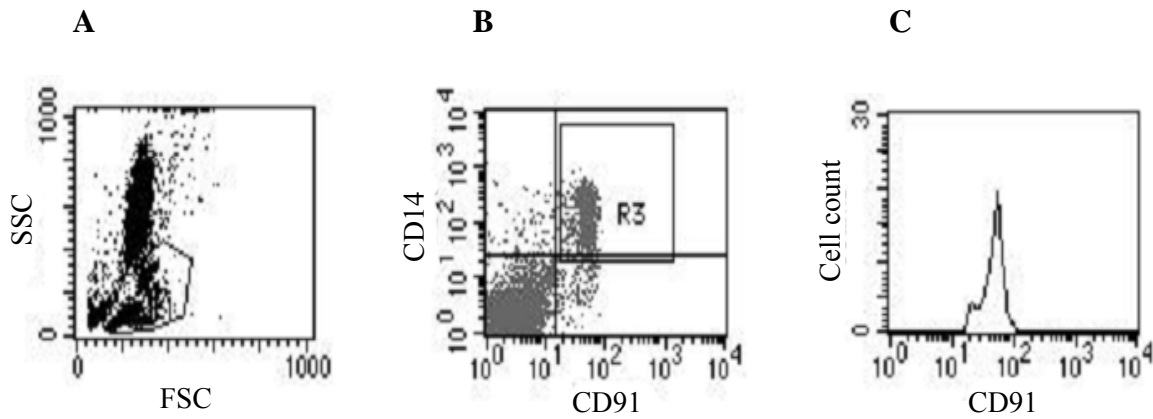


Fig 26. Measurement of CD91 expression on CD14 positive monocytes. (A) The population of lymphocytes and monocytes are gated based on forward and side scatter properties. (B) The PE-labeled CD14 positive cells appear in the upper left quadrant and FITC-labeled CD91 positive cells appear in the lower right quadrant. The CD14 and CD91 double positive cells appear in the upper right quadrant and cells in the lower left quadrant are negative for both CD14 and CD91. A further gate is created for CD14 and CD91 double positive cells. (C) The peak indicates the MFI of CD91 on CD14 positive cells.

The blood samples were co-stained with PE-labeled anti-CD14 antibody and FITC-labeled anti-CD91 antibody. Samples were processed as explained in the methods section and CD91 and CD14 expression was measured by flow cytometry. For measurement of CD91 expression, at first live PBMCs (i.e. lymphocytes and monocytes) were gated by forward scatter (FSC) and side scatter (SSC) characteristics followed by a second gating of CD14⁺ monocytes. The MFI of CD91 was evaluated on the CD14⁺ monocytes (Fig 26). The CD91 expression measured at two different time points before SIV challenge correlated well ($r = 0.63$) as determined by pearson correlation (Fig 27A).

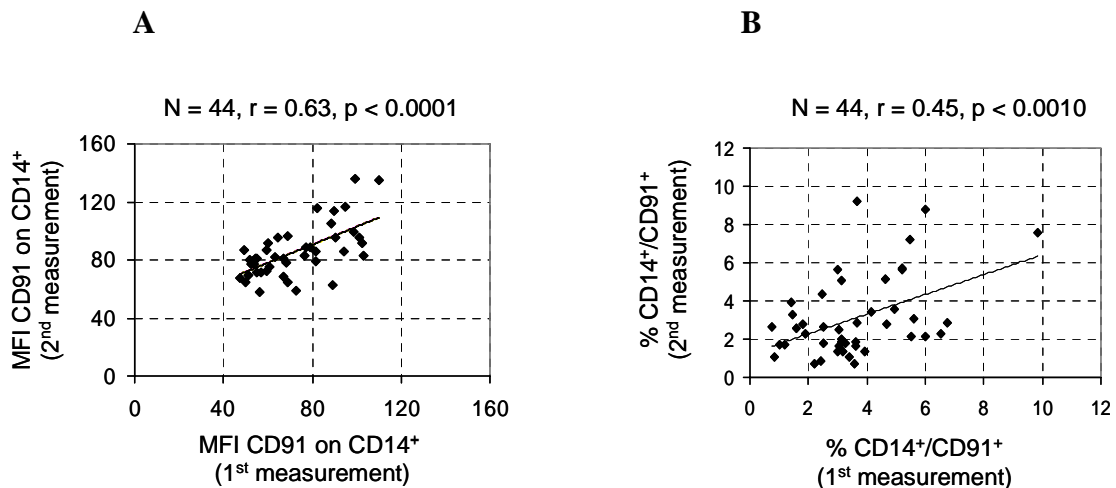


Fig 27. Correlation of CD91 expression on CD14⁺ cells and the percentage of CD14/CD91 double positive cells measured at two different time points in rhesus macaques before infection. (A) CD91 expression on CD14 positive cells was measured at two different time points and the MFI of CD91 obtained were correlated with each other. (B) The percentage of CD14 and CD91 double positive cells measured at these time points were correlated. The correlation was analyzed by pearson correlation test. The number of animals analyzed (N) and the pearson correlation coefficient is indicated above the figures.

However, the CD91 expression level varied between the individual animals. Furthermore, we evaluated the proportion of CD14 and CD91 positive cells among the PBMCs. The percentage of CD14 and CD91 double positive cells correlated less between the two measurements ($r = 0.45$, Fig 27B) before infection. This suggests that the CD91 expression on monocytes shows indeed an inter-individual variation but is quite stable for individual animals.

6.21 Expression of CD91 and proportion of CD14/CD91 positive cells in the course of SIV infection

Blood was obtained from rhesus macaques at different time points after infection as shown in Fig 25. The rhesus macaques analyzed in the experiment belonged to three categories. Some animals were not vaccinated but challenged with SIV (naïve infected), some animals that were mock-vaccinated and then challenged with SIV and some animals were vaccinated and then challenged with SIV. These groups were not designed for the CD91 expression studies, but they were evaluated separately. A gradual decrease of CD91 expression on CD14⁺ monocytes was observed with time after the SIV infection as shown for all the animals from three groups combined (all infected) in Fig 28A. The gradual decrease of CD91 expression on CD14⁺ monocytes was still evident even when the obtained data was evaluated according to the animals in three groups (naïve, mock vaccinated and vaccinated) as shown in Fig 28A. This suggests that the vaccination did not interfere with the CD91 expression observed on CD14⁺ monocytes in these animals. However, this evaluation was not the purpose of the study. The proportion of CD14/CD91 double positive cells showed a more variable pattern in the time course after infection (Fig 28B).

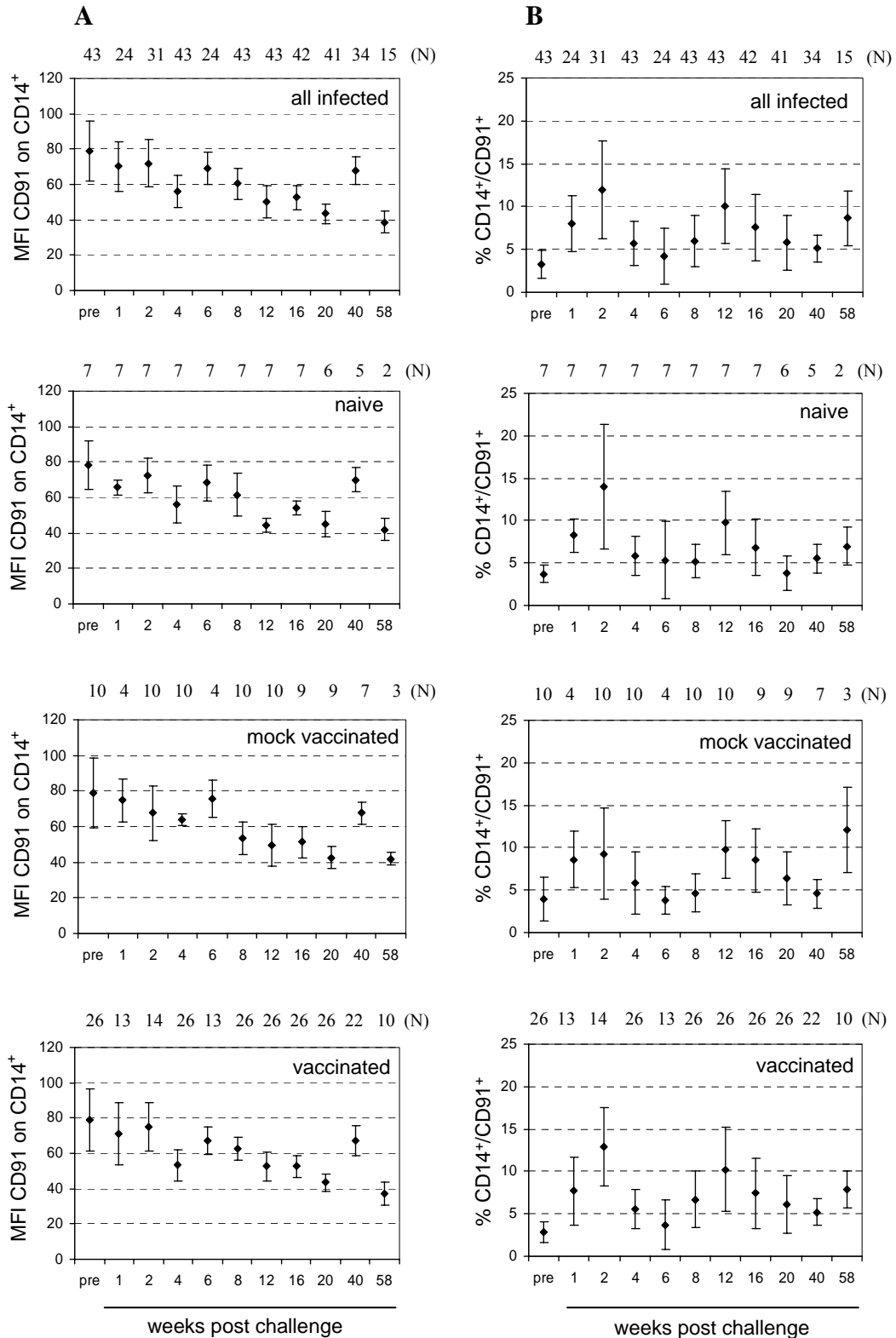


Fig 28. Expression of CD91 and percentage of CD14/CD91 double positive cells before SIV infection and at different time points after infection. (A) MFI (mean \pm SD) of CD91 expression on CD14 positive cells were plotted for all infected animals together and separately for the animals categorized into three groups of the vaccination trials (naïve, mock-vaccinated and vaccinated) at different time points indicated. The mean and standard deviation of two CD91 expression values before infection were combined together. N indicates the number of animals analyzed at the different time points. (B) The mean percentage of

CD14/CD91 double positive cells ($\% \pm \text{SD}$) obtained at indicated time points for all animals together and independently for the animals categorized into three groups of the vaccination trials are shown.

6.22 Expression of CD91 and proportion of CD14/CD91 positive cells in non-infected rhesus macaques

In the experimental group, two animals remained uninfected after the challenge with SIV, one of which belonged to the naïve group and the other to the vaccinated group. The general pattern of CD91 expression on monocytes and the proportion of CD14/CD91 double positive cells was not different to the infected animals. This observation, although only for two animals, challenges the hypothesis that the CD91 expression decreases in the course of infection.

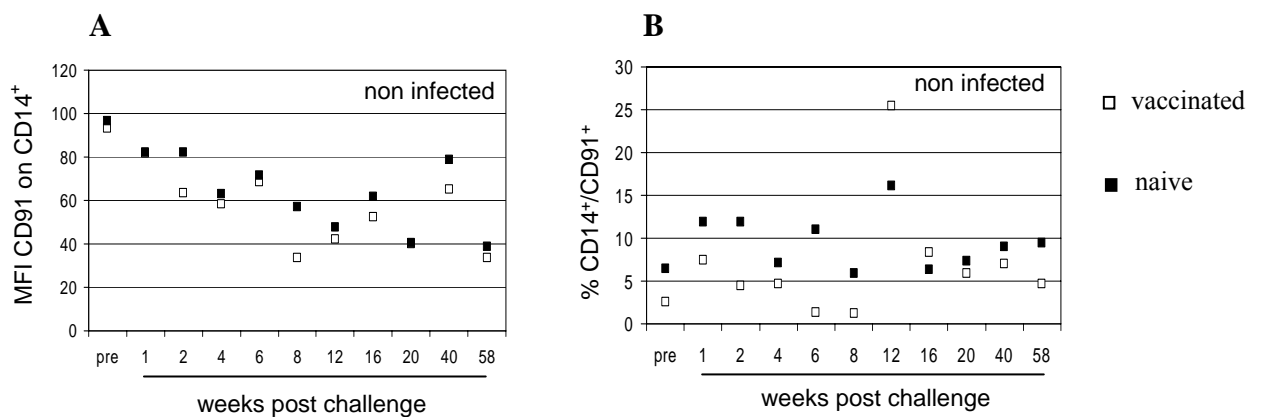


Fig 29. Expression of CD91 and percentage of CD14/CD91 double positive cells before SIV infection and at different time points after infection in non-infected animals. (A) MFI of CD91 expression on CD14 positive cells before and at different time points after SIV infection for both the uninfected animals is shown. One animal indicated by open square belonged to vaccinated group and the other indicated by closed square belonged to naïve group. (B) The percentage of CD14/CD91 double positive cells before and at different time points after SIV infection for both the uninfected animals is shown.

6.23 Expression of CD91 and proportion of CD14/CD91 positive cells in different groups of rhesus macaques.

Five LTNP rhesus macaques were obtained as a result of some rare events in SIV vaccination studies in the Primate Center, Göttingen. They were also used for the CD91 expression studies. Blood was obtained from the LTNP animals and CD91 expression was measured on CD14 positive monocytes. Similarly, the CD91 expression on CD14 monocytes was measured for animals from a non-experimental group and naïve experimental group before being challenged with SIV. Interestingly, an increased expression of CD91 on CD14 positive monocytes in LTNP was observed, when compared to the CD91 expression in disease progressive group (animals challenged with SIV) (Fig 30A). The non-experimental group which was housed under different condition than the experimental animals showed the highest expression of CD91 among these groups due to husbandry as shown in Fig 30A. Inversely, the disease progressing group showed the highest percentage of CD14/CD91 double positive cells among all the groups analyzed as shown in Fig 30B. The proportion of CD14/CD91 double positive cells

among the other groups was not very different from each other (Fig 30B). Thus, the CD91 expression level could be influenced by other factors such as psychosocial conditions during experimentation.

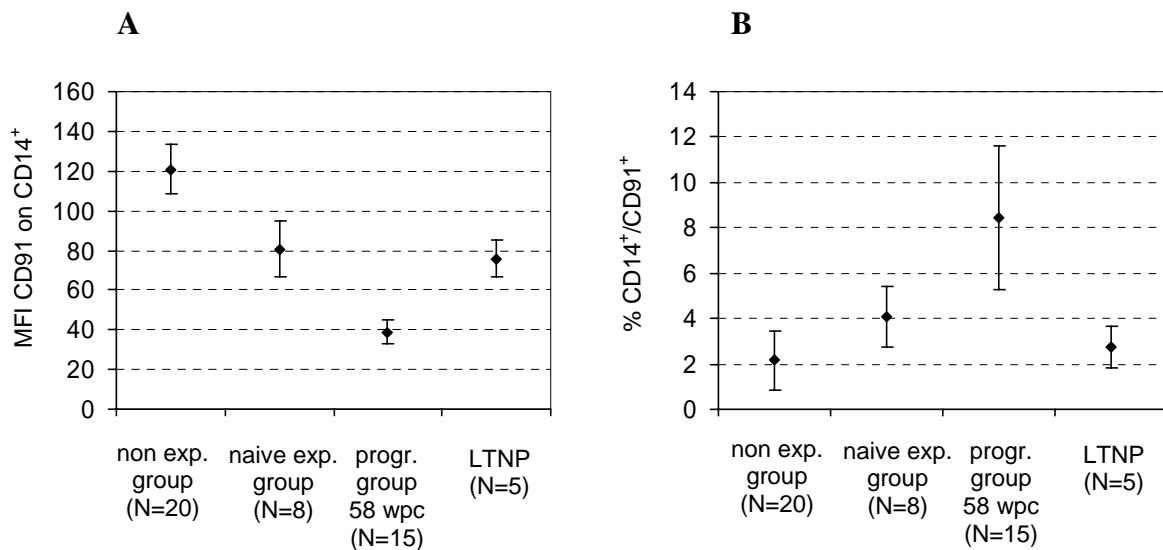


Fig 30. Expression of CD91 and percentage of CD14/CD91 double positive cells in different groups of rhesus macaques. (A) MFI (mean \pm SD) of CD91 expression on CD14 positive cells in non-experimental group, naïve experimental group, disease progressive group and LTNP is shown. The number of animals analyzed is indicated by N. (B) The percentage of CD14/CD91 double positive cells determined in the above mentioned animals is shown.

6.24 Screening for polymorphisms in CD91 promoter region of rhesus macaque

We screened the promoter region 600 bp above the codon start site of the CD91 gene to check for the presence of unknown polymorphisms. In the CD91 promoter region of uninfected control rhesus macaques (N=14) that were sequenced, we observed a polymorphism (-703 C>G) that occurred in 3 of the samples. This polymorphism is represented in the sequences shown in Fig 31.

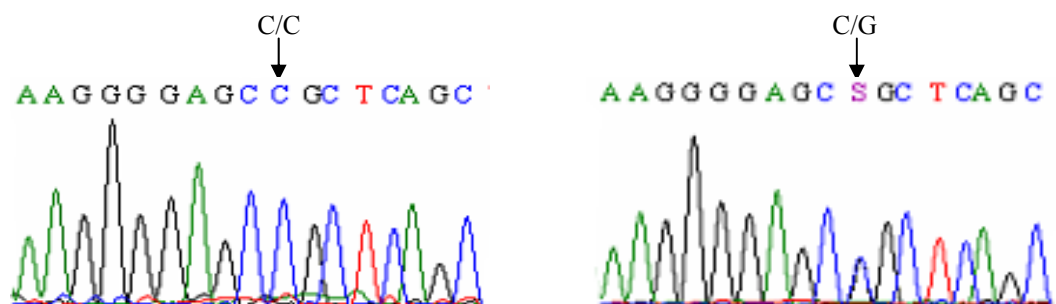


Fig 31. Promoter polymorphism of CD91 in rhesus macaques. The polymorphism in the promoter region of CD91 gene in rhesus macaque determined by sequencing is shown. The homozygous wild type alleles (C/C) and heterozygous alleles (C/G) are indicated.

We then genotyped the DNA samples of rhesus macaques infected with SIV for this promoter polymorphism. The genotypes and allele frequencies of this promoter polymorphism is shown in Table 14.

Table 14. Genotypes of CD91 promoter polymorphism in rhesus macaques

Rhesus macaques group	N	Allele Frequencies		CD91 Promoter polymorphism		
		C	G	C/C	C/G	G/G
SIV infected	36	0.79	0.21	23	11	2
Uninfected controls	14	0.89	0.11	11	3	-

We then tested the effect of the promoter polymorphism on CD91 expression before infection with SIV in SIV-infected group and the uninfected rhesus macaques group. The genotypes of CD91 promoter polymorphism were plotted against the pre-infected MFI values of CD91 for the SIV-infected group (Fig 32A) and genotypes of uninfected controls were plotted against their CD91 MFI values (Fig 32B). There was no influence of the promoter polymorphism on CD91 expression in non-experimental group ($p=0.707$) and SIV infected group (0.665) found. However, more samples of the G/G genotype would be required for a definitive analysis.

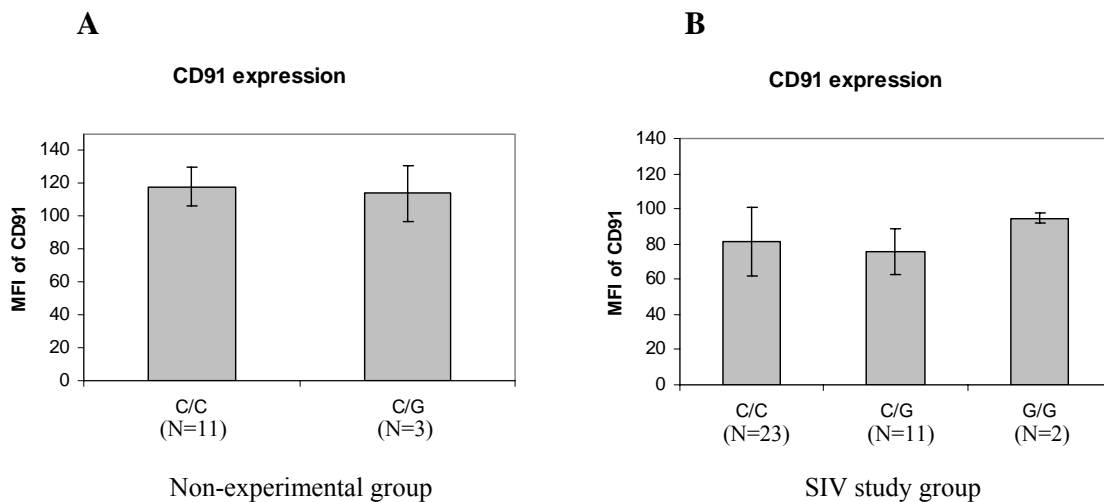


Fig 32. Evaluation of influence of CD91 promoter polymorphism on CD91 expression in rhesus macaques. (A) The MFI values of CD91 for the animals in the non-experimental group were plotted against their genotypes of promoter polymorphism. There was no animal homozygous for G allele in this group. (B) The MFI values of CD91 obtained before the infection with SIV for the animals in the SIV-infected group were plotted against their genotypes of CD91 promoter polymorphism. N indicates the number of animals with the particular genotype.

6.25 Genomic organization and selected SNPs of the OLR1 (LOX-1) gene

The OLR1 gene (LOX-1) is located on the p arm of chromosome 12. Three SNPs within the gene were chosen for genotyping after HapMap analysis which has been discussed in detail in chapter 6.10 for CD91. As indicated in the Fig 33, one of these SNPs is present in 3'UTR (tag 27), one in exon 4 (tag 36) and the other one in intron 2 (tag 45). The SNP in the exon 4 (rs11053646) and 3'UTR region (rs1050283) of this gene have been shown previously to be associated with myocardial infarction (Mango et al., 2003; Tatsuguchi et al., 2003). The exon 4 SNP leads to a change in amino acid from lysine to asparagine.

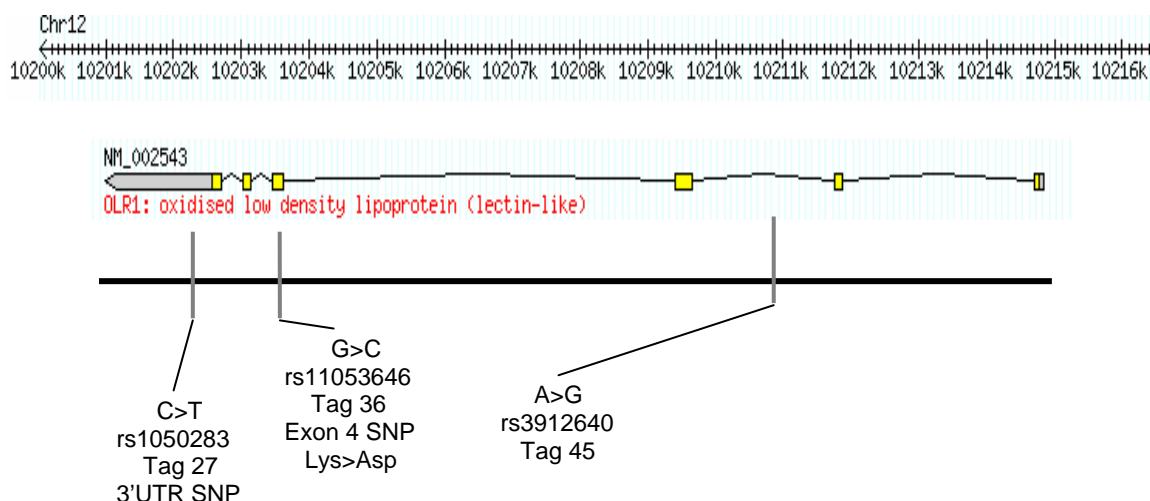


Fig 33. Genomic organization of the OLR1 (LOX-1) gene. This figure was generated by haploview software after loading the chromosomal location information of the LOX-1 gene obtained from HapMap database. The location of the gene on chromosome 12 is shown. The exons in the gene are indicated by boxes and the introns by a thin line. The location of three selected SNPs and their SNP reference numbers, and tag numbers are shown. The amino acid substitution caused by exon 4 SNP is also indicated.

6.26 LD plot and HapMap haplotypes of the OLR1 gene

For the chromosomal region containing the OLR1 gene, the SNP genotype data representative of the Caucasian population was downloaded from the HapMap database (data release version 22 from March 2007, www.hapmap.org). A single block of strong LD was observed that include all markers in the analyzed region (Fig 34). The haplotype structure within this region was analyzed (Fig 35). htSNPs were selected to differentiate between all haplotypes occurring with at least 5% frequency within the HapMap Caucasian population (Fig 35). Three SNPs (rs1050283, tag 27 - 3'UTR polymorphism; rs11053646, tag 36 - exon 4 polymorphism and rs1050283, tag 45) tagged the frequent haplotypes (>5%) observed in the OLR1 gene (Fig 35) and were used to assess the genetic variability in the OLR1 region in our healthy volunteers.

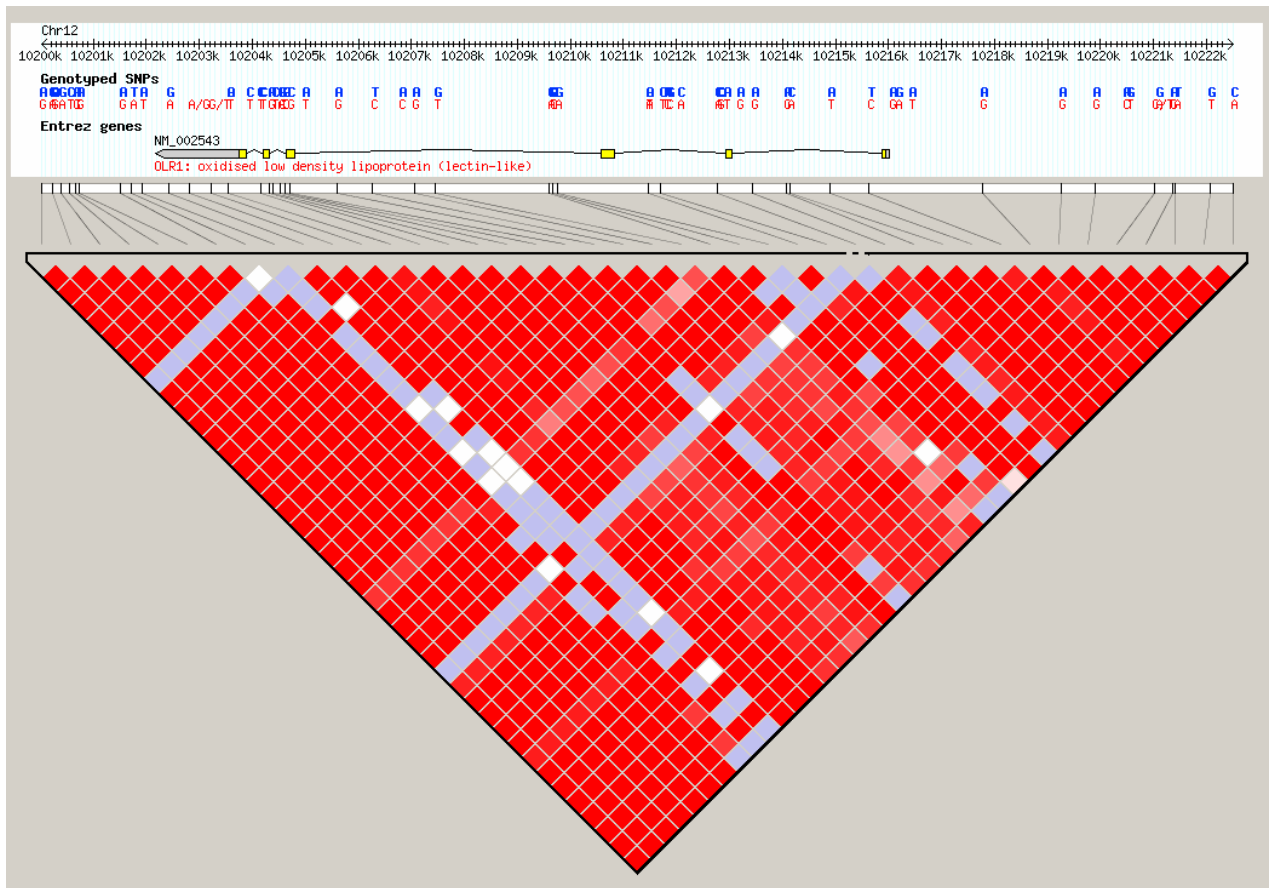


Fig 34. LD in the chromosomal region containing OLR1 gene. LD among the markers within the LOX-1 gene and a small region surrounding the gene was analyzed. The color scheme is representing the strength of pair-wise LD in the terms of D' as follows: red- strong LD (D' of 1), white – no LD (D' of 0) and the variations between are represented in with different depth of pink. The blue color marks regions where the calculation of LD was not possible. The triangle indicates region of strong LD (so called LD-block) that 95% of the informative markers are in high LD. An info track is displayed on top of the LD block giving the information regarding the region of chromosome being analyzed and genotyped SNPs in this region and also the genes that are present in the region.

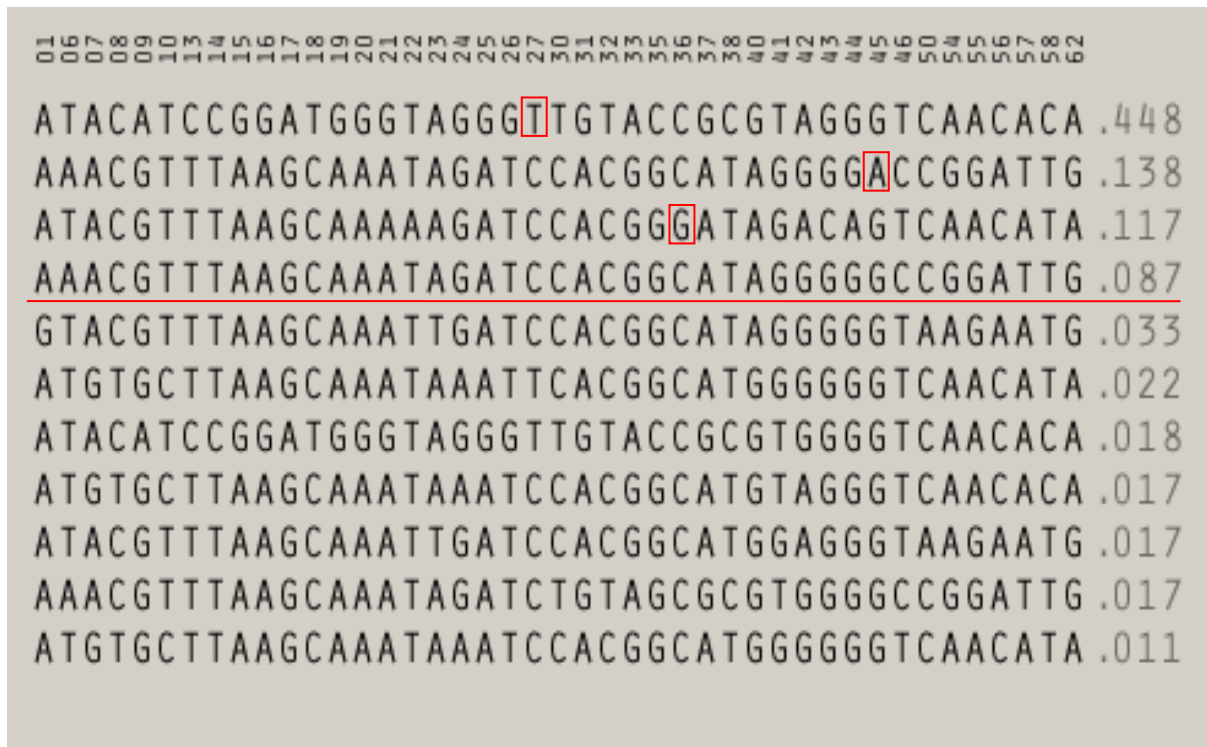


Fig 35. Partial list of haplotypes generated for the OLR1 gene containing chromosomal region. The frequency of haplotypes is represented on right hand side of the image. The number represents the order of tag SNPs along the chromosome region analyzed responsible for tagging each haplotype. The haplotypes with at least 5% frequency were chosen for analysis indicated by a red line. The htSNPs (tag 27, 3'UTR polymorphism; tag 36, exon 4 polymorphism and tag 45) that are sufficient to differentiate between these haplotypes are indicated by red boxes.

6.27 Genotype distribution and allele frequencies of LOX-1 SNPs

Genotyping of the LOX-1 exon 4 SNP (tag 36) in the HIV cohort and healthy volunteers was performed by AS-PCR. The genotype distribution and allele frequencies are shown in Table 15. The genotype of LOX-1 3'UTR SNP (tag 27) was determined by sequencing the SNP region for all samples. No individual was homozygous for the T allele observed in LTNP group. The genotype distribution and allele frequencies are shown in Table 16. Genotyping for tag 45 SNP was performed by AS-PCR. There was no sample with a homozygous T genotype. The genotype distribution and allele frequencies are shown in Table 17.

Table 15. LOX-1 exon 4 genotypes of HIV-infected individuals and healthy volunteers

Group	N	Allele Frequencies		LOX-1 exon 4 SNP			Exact Test for HWE p-value
		G	C	G/G	G/C	C/C	
HIV-1 Positives							
RESTART	11	0.95	0.05	10	1	--	1.000
TIMS	10	0.90	0.10	9	--	1	0.052
LTNP	8	0.94	0.06	7	1	--	1.000
Healthy Volunteers	74	0.93	0.07	65	8	1	0.277

Table 16. LOX-1 3'UTR genotypes of HIV-infected individuals and healthy volunteers

Group	N	Allele Frequencies		LOX-1 3'UTR SNP			Exact Test for HWE p-value
		C	T	C/C	C/T	T/T	
HIV-1 Positives							
RESTART	11	0.50	0.50	2	7	2	0.581
TIMS	10	0.60	0.40	4	4	2	0.573
LTNP	8	0.63	0.37	2	6	--	0.440
Healthy Volunteers	74	0.50	0.50	19	36	19	0.818

Table 17. LOX-1 Tag 45 genotypes of HIV-infected individuals and healthy volunteers

Group	N	Allele Frequencies		LOX-1 Tag 45			Exact Test for HWE p-value
		C	T	C/C	C/T	T/T	
HIV-1 Positives							
RESTART	11	0.77	0.23	6	5	--	1.000
TIMS	10	0.85	0.15	7	3	--	1.000
LTNP	8	0.81	0.19	5	3	--	1.000
Healthy Volunteers	74	0.82	0.18	48	26	--	0.107

6.28 Effect of LOX-1 SNPs on LOX-1 expression

LOX-1 receptor expression is upregulated by Ox-LDL and other pro-atherogenic factors in the arteries of hypertensive, dyslipidemic, and diabetic animals (Chen et al., 2000); (Chen et al., 2001a);(Nagase et al., 1997). Upregulation of LOX-1 has been identified in atherosclerotic arteries of several animal species and humans (Mehta et al., 2006). The LOX-1 exon 4 SNP and 3'UTR polymorphisms have been shown to be associated with an increased risk of acute myocardial infarction (Tatsuguchi et al., 2003);(Mango et al., 2003). However, it is not known, if these polymorphisms have an influence on LOX-1 expression. We tested the effect of these polymorphisms on LOX-1 expression. We found no effect of these polymorphisms on LOX-1 expression on cell surface of monocytes in healthy volunteers as shown in Fig 36.

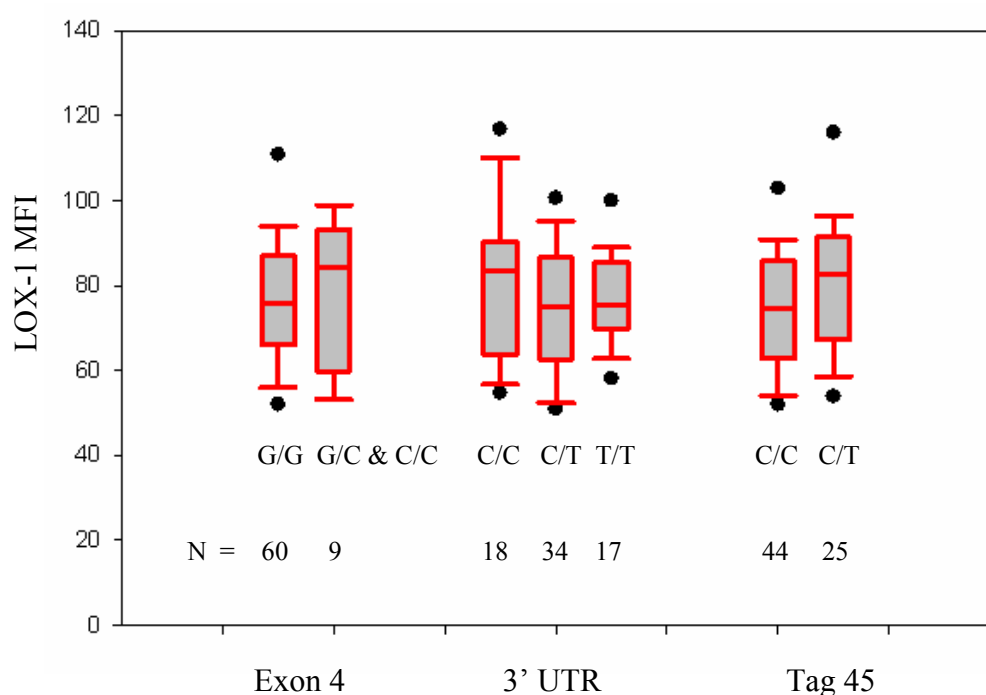


Fig 36. Effect of LOX-1 exon 4, 3'UTR, and tag 45 SNPs on LOX-1 expression. LOX-1 expression was measured on monocytes of 69 healthy volunteers by flow cytometry. The MFI of LOX-1 for the genotypes of LOX-1 SNPs obtained with FACS analysis were plotted in a box plot. The genotypes represented in the figure are G/G and G/C & C/C together (there was only one sample with C/C genotype and it was combined with G/C genotypes) of LOX-1 exon 4 polymorphism, genotype C/C, C/T and T/T of LOX-1 3'UTR polymorphism, and genotype C/C and C/T (the T/T genotype was not observed) of LOX-1 tag 45 SNP. N indicates the numbers of samples with the respective genotypes.

6.29 Generation of LOX-1 haplotypes

When the three SNPs (exon 4, 3'UTR and tag 45) in LOX-1 were analyzed independently, they did not have any effect on LOX-1 expression. However other SNPs that are represented in the LOX-1 haplotypes may influence its expression. The genotype data obtained for the three SNPs from healthy volunteers were analyzed by phase version 2.1 software (Stephens and Donnelly, 2003; Stephens et al., 2001) to estimate the haplotypes. The haplotypes were also estimated with HAP webserver (Halperin and

Eskin, 2004) and the haplotypes obtained were similar to those obtained with phase software. The list of the most frequent haplotypes and their frequency observed in our study population is indicated in Fig 37.

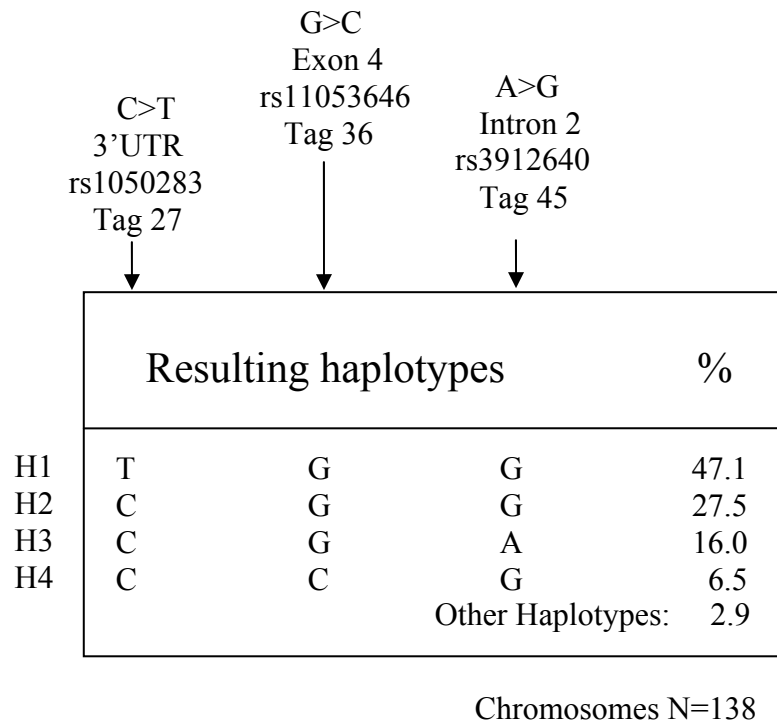


Fig 37. The tag SNPs analyzed for LOX-1 and their resulting haplotypes and frequencies. The polymorphism of each tag SNP, their location in the gene and their NCBI reference SNP number is indicated. H1 to H4 represent the four most frequent haplotypes estimated with tag SNPs in healthy volunteers and their frequencies are indicated (%). N represents the number of chromosomes analyzed for generation of these haplotypes.

6.30 Effect of LOX-1 haplotypes on LOX-1 expression

The haplotypes of LOX-1 were generated from LOX-1 SNPs (exon 4, 3'UTR and tag 45) genotype data of healthy volunteer individuals. The presence of each haplotype in these individuals was analyzed for its effect on LOX-1 expression. The haplotypes of healthy volunteers were plotted against their MFI values of LOX-1 on cell surface of monocytes as shown in Fig 38. There was no influence of LOX-1 haplotypes on LOX-1 expression.

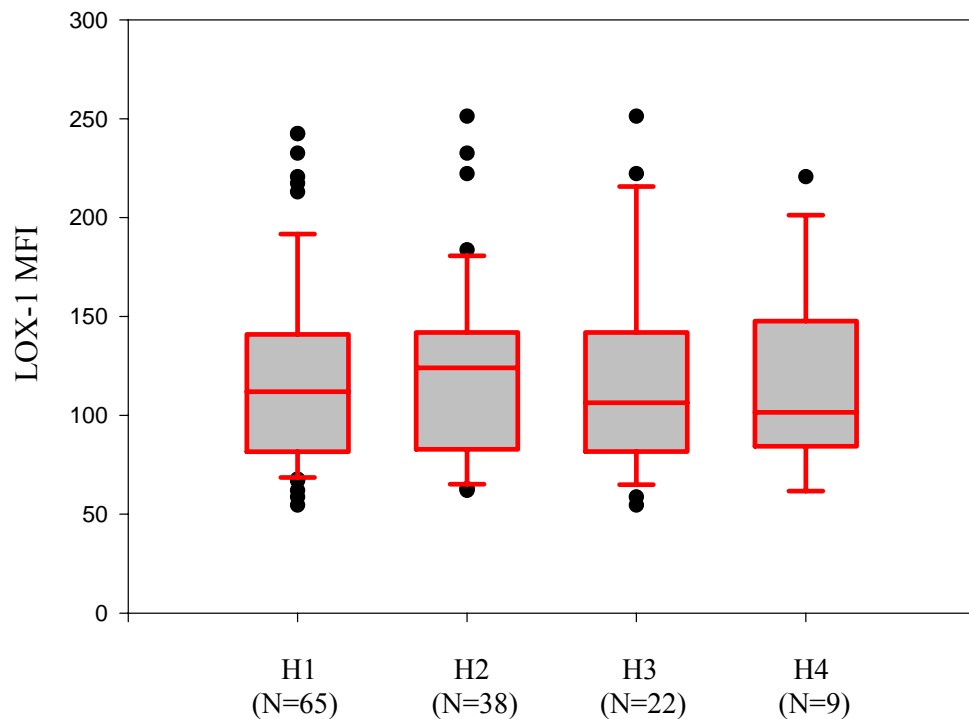


Fig 38. Effect of LOX-1 haplotypes on LOX-1 expression. LOX-1 expression (LOX-1 MFI) measured on monocytes of healthy volunteers were plotted according to the presence of the four major haplotypes (H1, H2, H3 and H4) observed within these individuals. N indicates the number of chromosomes with a particular haplotype.

6.31 Generation of a full-length cDNA for LOX-1

A polymorphism in the exon 4 region (501 C>G, rs11053646, tag 36) of LOX-1 gene leads to a change of amino acid from lysine to asparagine in the ligand binding domain of the protein. Substitution of certain lysine residues with alanine in the ligand binding domain of LOX-1 leads to reduced binding of Ox-LDL to LOX-1 as shown by biochemical analyses (Chen et al., 2001b). We wanted to determine, if the exon 4 SNP causing a substitution of a lysine residue affects the binding of HSP70 to LOX-1. cDNA obtained from RNA of different human tissues (stomach, testis, brain and PBMCs) were analyzed for the amplification of full-length LOX-1 cDNA. A PCR was performed with LOX-1 F and LOX-1 R primers and the products obtained were run on a 1.5% agarose gel. Multiple bands were observed from all the tested cDNA samples (Fig 39). The uppermost band was cut out from each lane and the PCR product was extracted and sequenced. The remaining bands were not analyzed. Sequence results were compared to the LOX-1 reference sequence in the NCBI database and confirmed as LOX-1 full-length and LOX-1 exon 5 splice variant lacking exon 5 cDNA (Mango et al., 2005).

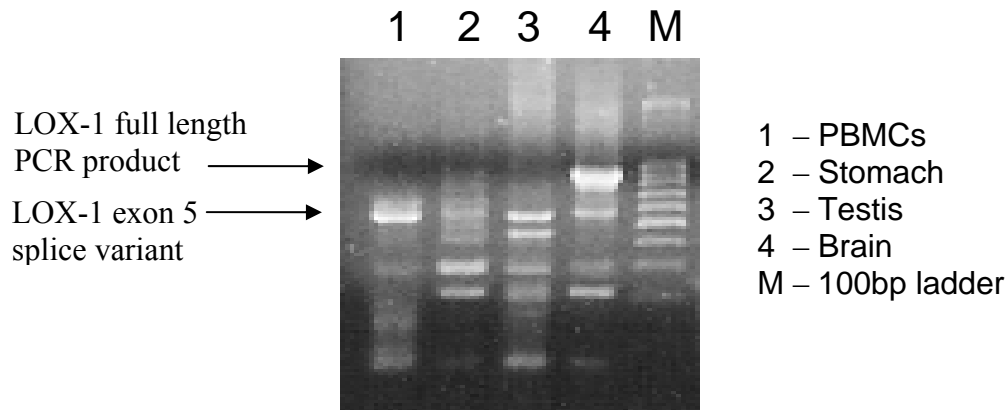


Fig 39. Full-length PCR product of LOX-1 cDNA. cDNA obtained from different tissues (PBMCs, stomach, testis and brain) were tested for the amplification of full-length LOX-1. The uppermost band in lane 4 was confirmed as LOX-1 full-length PCR product. The uppermost band in lane 1 and lane 3 were confirmed as LOX-1 exon 5 splice variant. The other bands were not analyzed.

6.32 Generation of exon 4 SNP mutant by SDM

The sequence of full-length LOX-1 cDNA amplified from brain cDNA was not polymorphic for LOX-1 exon 4 SNP. We decided to introduce the exon 4 SNP mutation by PCR-based SDM as described in the methods section (Fig 3 in methods section). The PCR was performed on LOX-1 cDNA by a primer pair (LOX-1 Ex 4 SDM F / LOX-1 cDNA R) that would introduce a LOX-1 exon 4 SNP mutation and synthesize the PCR product spanning part of exon 4 and upto the stop codon of LOX-1 cDNA (Fig 40A – Lane 1). The other primer pair (LOX-1 cDNA For / LOX-1 Ex5 Rev) used synthesized a PCR product spanning the LOX-1 start codon to end of LOX-1 exon 5 region (Fig 40A – Lane 2). The PCR products obtained (Fig 40A - lanes 1 and 2) were purified by PCR purification columns and were then mixed together in equal ratio. These PCR products had overlapping sequences and hence served as primers for amplification of mixture of full-length wild type LOX-1 and full-length exon 4 mutant LOX-1 PCR products. The PCR was performed for 12, 15 and 18 cycles and the product was checked on 1.5% agarose as shown in Fig 40B. A single band of expected size (892 bp) was obtained.

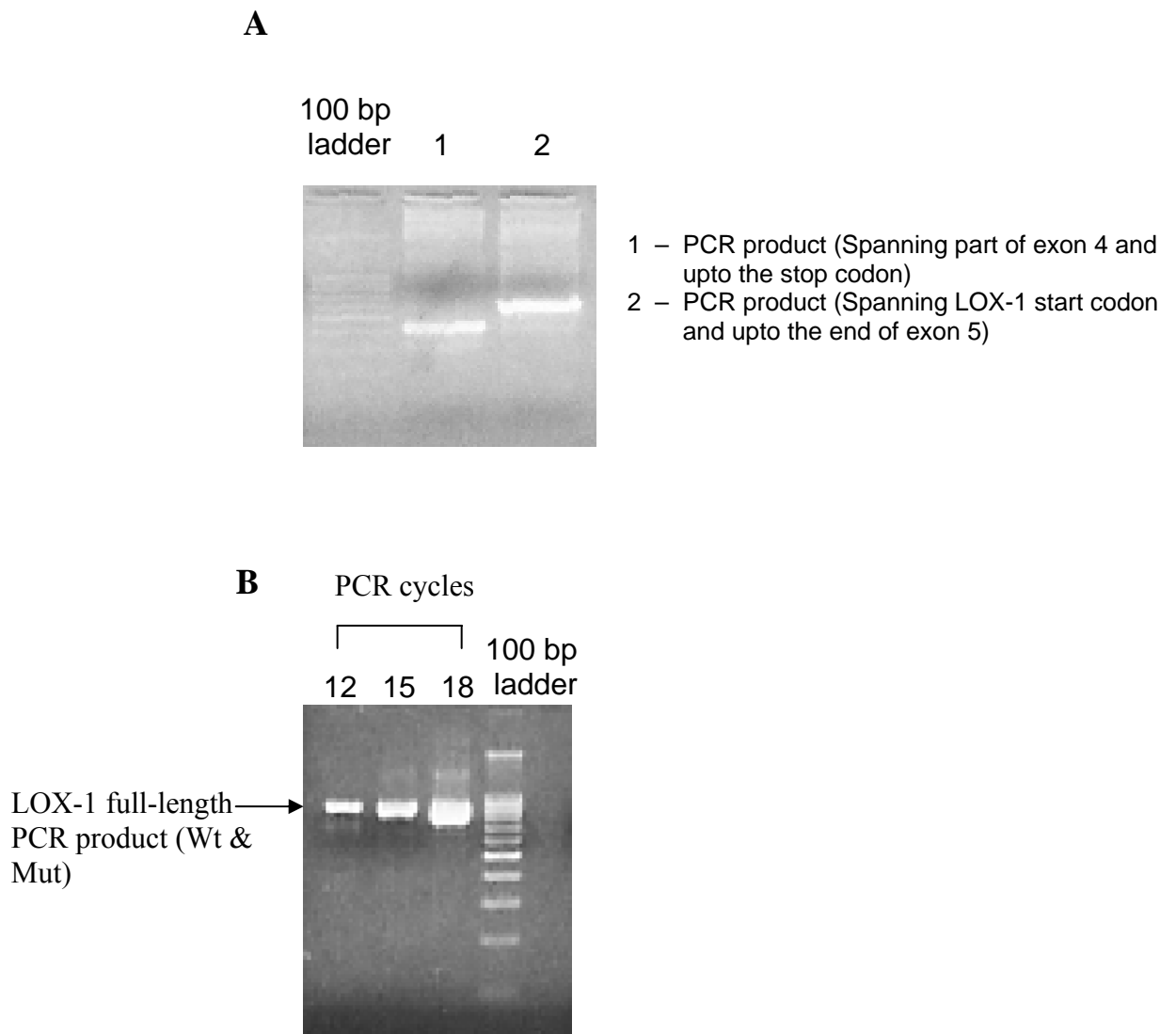


Fig 40. Introduction of exon 4 SNP mutation by PCR based SDM. (A) LOX-1 exon 4 SNP mutation (G>C) was introduced by performing a PCR by a mutagenic primer carrying a exon 4 SNP mutation (C). Two PCR products were obtained with overlapping sequences and these overlapping regions served for primer extension and synthesis of LOX-1 full-length PCR product. (B) PCR was performed for 12, 15 and 18 cycles and LOX-1 full-length PCR product carrying a mixture of LOX-1 Wt and LOX-1 Mut (exon 4 SNP) were obtained.

6.33 Generating constructs of LOX-1 Wt and LOX-1 Mut

PCR products obtained for LOX-1 Wt and LOX-1 Mut had to be confirmed for the presence of exon 4 SNP and also cloned into mammalian expression vector to express the LOX-1 Wt and LOX-1 Mut proteins on the cell surface of a mammalian cell line. PCR products were directly cloned into a linearized mammalian expression vector (pcDNA 3.1/CT-GFP-Topo) containing 5'-T overhang. The clones were analyzed by sequencing

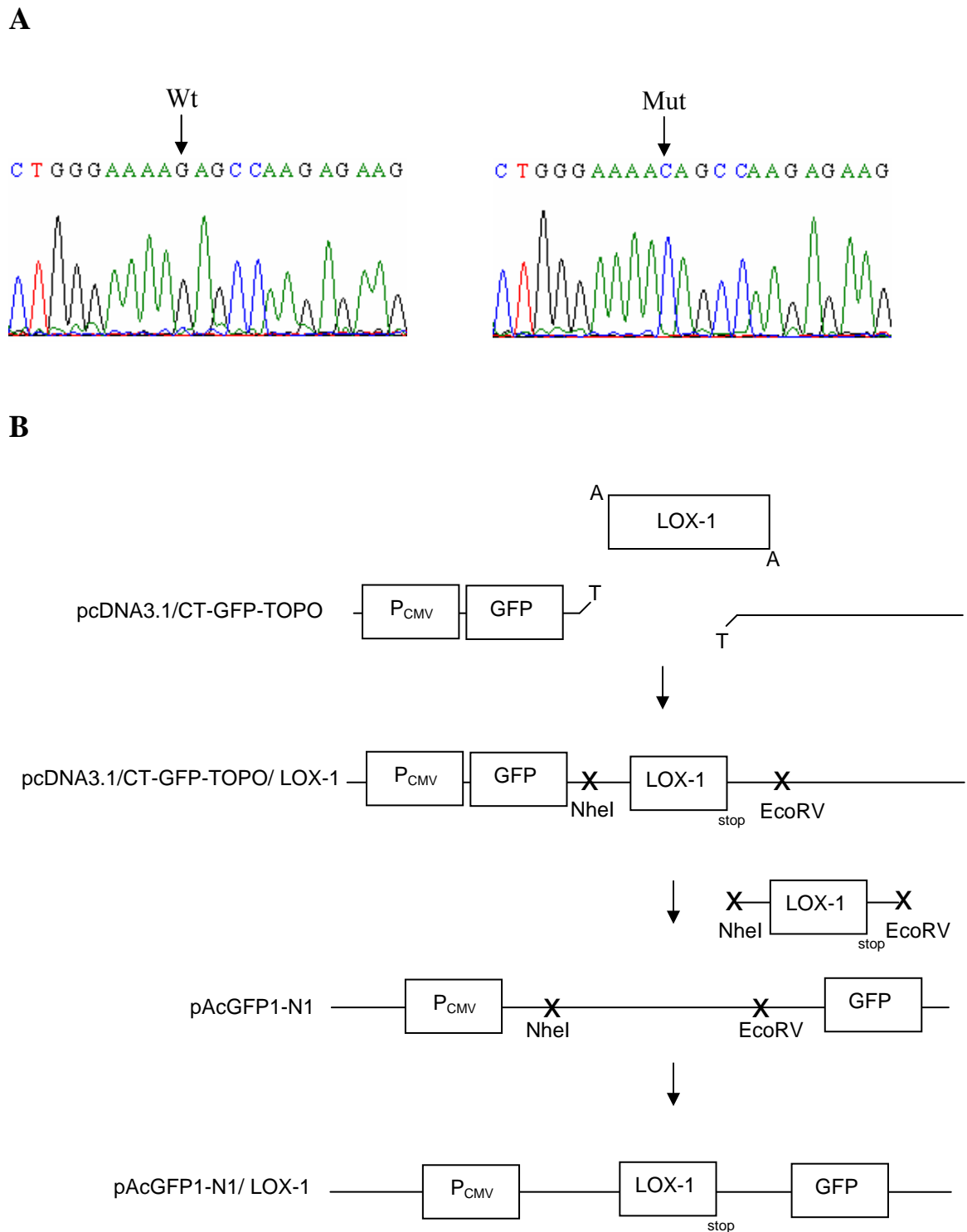


Fig 41. Generating LOX-1 Wt and LOX-1 Mut constructs. (A) PCR products of LOX-1 Wt and LOX-1 Mut cloned into pcDNA3.1/CT-GFP-TOPO vector containing 5'T overhang were confirmed by sequencing. (B) PCR products of LOX-1 Wt and LOX-1 Mut ligated with linearized pcDNA3.1/CT-GFP-TOPO vector containing 5'T overhang were then cut out with the restriction enzymes NheI and EcoRV and cloned into the NheI and EcoRV restriction sites in the pAcGFP1-N1 vector. Expression from both the vectors was driven by CMV promoter as indicated.

and the positive clones obtained (Fig 41A) were used for the transfection experiments. The expression of LOX-1 was not detectable from this vector in our initial transfection experiments. Therefore, the LOX-1 insert was then cut out from pcDNA 3.1/ CT-GFP-

Topo vector by Nhe 1 and EcoRV restriction enzymes and sub-cloned into Nhe 1 and EcoRV sites of the pAcGFP1-N1 expression vector (Fig 41B). There was no expression of green fluorescent protein (GFP)-LOX-1 fusion protein from pAcGFP1-N1 vector because of the presence of stop codon in the LOX-1 insert.

6.34 Analysis of LOX-1 expression and HSP70 binding in Chinese hamster ovary (CHO) cells

CHO cells were screened for endogenous LOX-1 expression and cell surface HSP70 binding to determine whether they would be suitable for transfection experiments with the LOX-1 constructs. CHO cells were stained with an anti-LOX-1 antibody for 30 minutes followed by FITC-labeled goat anti-mouse IgG secondary antibody for 20 minutes. In parallel, CHO cells were also stained with FITC-labeled HSP70. Expression of LOX-1 and HSP70 binding to cell surface of CHO cells was then analyzed by flow cytometry. No expression of LOX-1 was observed on cell surface of CHO cells as shown in Fig 42. It could be also possible that anti-human LOX-1 antibody used for detection of LOX-1 expression on CHO cells does not bind to hamster LOX-1, therefore it is most important that no HSP70 was bound by viable (PI negative) CHO cells as shown in Fig 42. Hence, CHO cells were suitable for LOX-1 Wt and exon 4 Mut transfections and evaluation of HSP70 binding to cell surface of LOX-1 Wt and exon 4 Mut transfected cells.

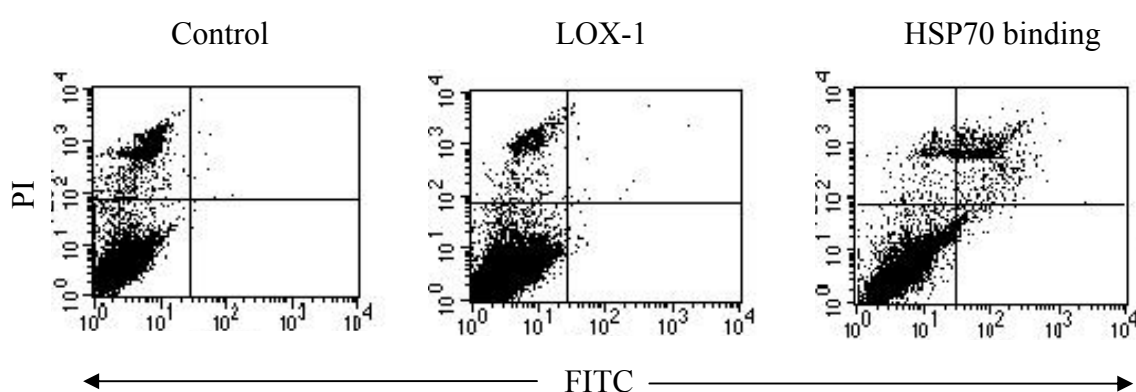


Fig 42. Evaluation of endogenous LOX-1 expression and HSP70 binding in CHO cells. Dot plots of CHO cells that were stained only with PI, with anti-LOX-1 antibody (and a FITC-labeled goat anti-mouse IgG secondary antibody) and PI, or with FITC-labeled HSP70 and PI are shown. The upper left quadrant indicates PI-stained cells, lower left quadrant indicates unstained cells, lower right quadrant indicates FITC-stained cells and upper right quadrant indicates both PI and FITC-stained cells.

6.35 Transient transfection of pAcGFP1-N1 / LOX-1 Wt and Mut constructs in CHO cells

CHO cells (2×10^5) were transiently transfected with $0.5 \mu\text{g}$ DNA each of pAcGFP1-N1 / LOX-1 Wt and Mut constructs using metafectene (a liposomal transfection reagent). After 24 hours, the cells were stained with an anti-LOX-1 antibody (and a FITC-labeled

goat anti-mouse IgG secondary antibody) and cell surface LOX-1 expression was measured by flow cytometry. Expression was detected for both the LOX-1 Wt and Mut protein as shown in Fig 43. Expression of LOX-1 Wt and Mut protein were then compared with each other and was found to be similar as shown in Fig 43.

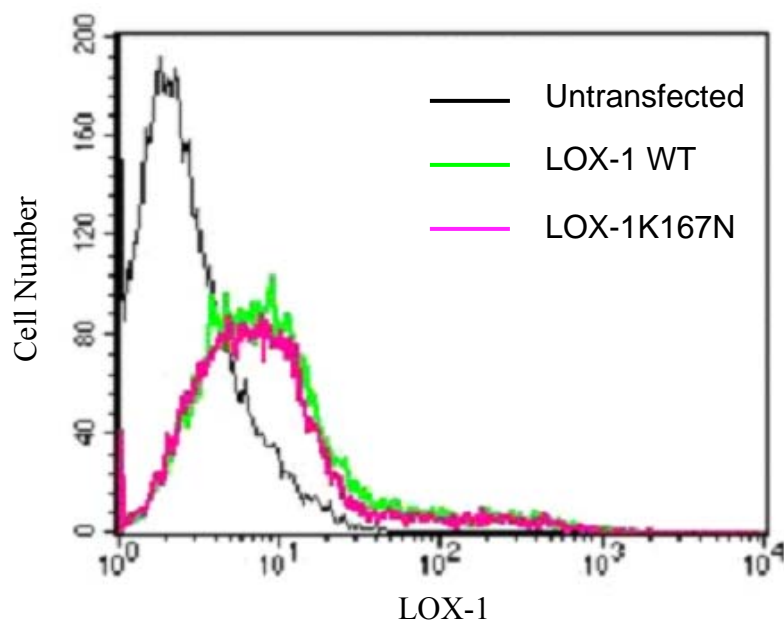


Fig 43. Similar expression levels of LOX-1 Wt and Mut proteins in transiently transfected CHO cells. CHO cells transiently transfected with pAcGFP1-N1 constructs carrying LOX-1 Wt and LOX-1 Mut insert were stained with an anti-LOX-1 antibody followed by a FITC-labeled goat anti-mouse IgG secondary antibody before LOX-1 expression on the cell surface was measured by flow cytometry. In parallel, untransfected CHO cells were stained with anti-LOX-1 and a FITC-labeled goat anti-mouse IgG secondary antibody and measured. The histograms of these measurements were overlaid on each other using cell quest software. The histogram overlay shows a low but similar expression level of the LOX-1 Wt and Mut proteins.

6.36 Evaluation of HSP70 binding to LOX-1 Wt and LOX-1 Mut transfected CHO cells

The polymorphism in the exon 4 (501 C>G) of LOX-1 gene leads to a change of an amino acid from lysine to asparagine in the ligand binding domain of the protein. The effect of this amino acid substitution on HSP70 binding was tested. 0.5 μ g DNA each of LOX-1 Wt and LOX-1 Mut constructs were transiently transfected independently into CHO cells (2×10^5 cells/well). 24 hours after transfection, the cells were stained with an anti-LOX-1 antibody (and a TC-conjugated goat anti-mouse IgG secondary antibody) and FITC-labeled HSP70. LOX-1 expression on the cell surface of CHO cells and HSP70 binding were measured by flow cytometry. Both the LOX-1 expression and HSP70 binding was observed on the cell surface of LOX-1 Wt and Mut transfected CHO cells (Fig 44).

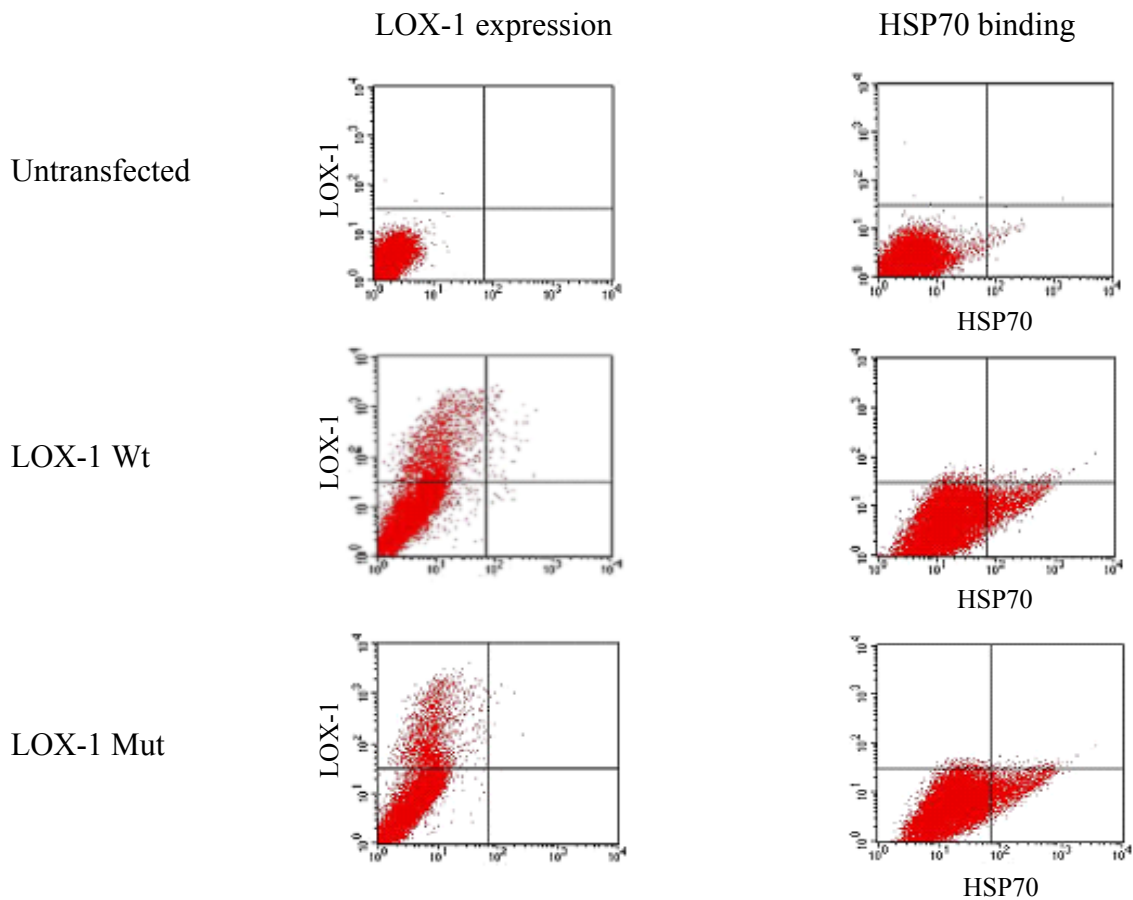


Fig 44. Expression of LOX-1 Wt and LOX-1 Mut in transiently transfected CHO cells and the binding of HSP70. CHO cells were transiently transfected with LOX-1 Wt and Mut constructs. Cells were then stained either with an anti-LOX-1 antibody (and a TC-conjugated goat anti-mouse IgG secondary antibody) or FITC-labeled HSP70. The dot plots obtained after flow cytometry for LOX-1 expression and HSP70 binding on cell surface of untransfected CHO cells, LOX-1 Wt transfected and LOX-1 Mut transfected CHO cells are shown.

6.37 Comparison of LOX-1 expression and HSP70 binding on LOX-1 Wt and LOX-1 Mut transfected CHO cells

To test if there was any quantitative difference in HSP70 binding to LOX-1 Wt and LOX-1 Mut transfected CHO cells, 0.5 μg DNA each of LOX-1 Wt and LOX-1 Mut constructs were transiently transfected into CHO cells (2×10^5 cells/well). After 24 hours, the cells were double stained with an anti-LOX-1 antibody (and a TC-conjugated goat anti-mouse IgG secondary antibody) and FITC-labeled HSP70 and expression of LOX-1 and HSP70 binding were measured simultaneously by flow cytometry. A reduced binding of HSP70 to the cell surface of CHO cells transfected with LOX-1 Mut compared to cells transfected with LOX-1 Wt was observed as indicated by mean fluorescence intensity values in the histograms in Fig 45A. In order to ascertain the effect of exon 4 polymorphism of LOX-1 on HSP70 binding, 10 independent experiments of HSP70 binding to cell surface of LOX-1 Wt and LOX-1 Mut transfected CHO cells were performed. A significant decrease of HSP70 binding to LOX-1 Mut protein ($p=0.016$;

Wilcoxon test) was observed as shown in Fig 45B. The expression of LOX-1 Wt and Mut did not differ from each other (Fig 45B).

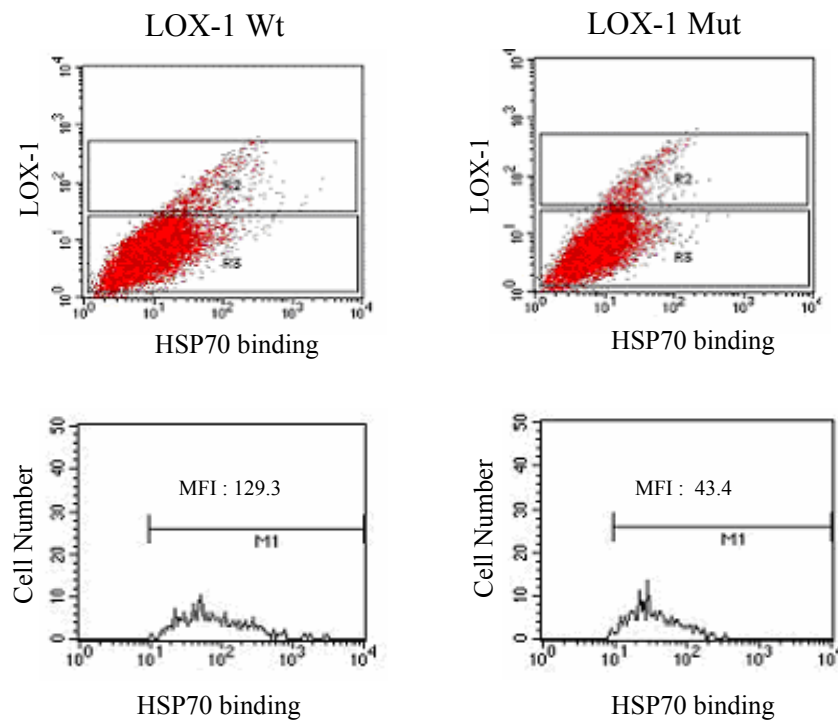


Fig 45A. MFI of HSP70 binding to LOX-1 Wt and LOX-1 Mut expressing CHO cells. CHO cells transiently transfected with LOX-1 WT and LOX-1 Mut constructs were co-stained with an anti-LOX-1 antibody (and a TC-conjugated goat anti-mouse IgG secondary antibody) and FITC-labeled HSP70. LOX-1 positive cells were gated and the MFI of HSP70 bound to LOX-1 Wt and LOX-1 Mut cells was determined as indicated in the histogram.

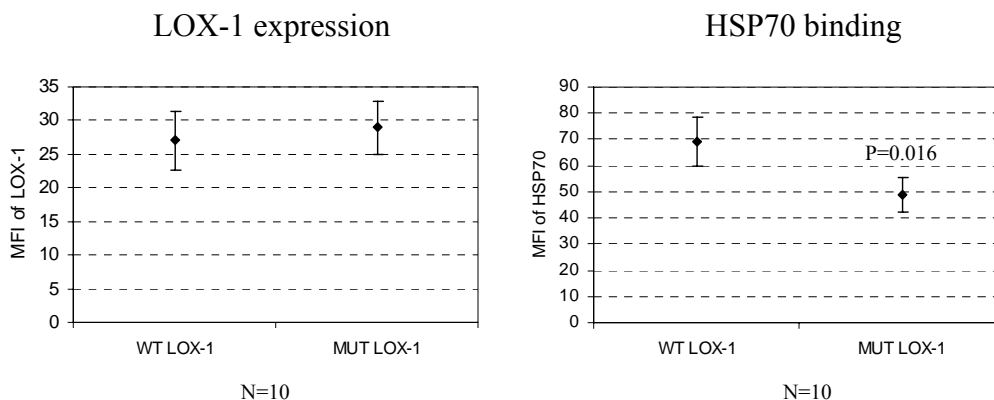


Fig 45B. Comparison of LOX-1 expression and HSP70 binding on LOX-1 Wt and LOX-1 Mut transfected CHO cells. The means and standard error of means (SEM) of LOX-1 expression of 10 independent transient transfection experiments of LOX-1 Wt and LOX-1 Mut constructs in CHO cells are shown. Similarly, the means and SEM of HSP70 bound to LOX-1 Wt and LOX-1 Mut transfected CHO cells in these 10 independent experiments are shown. The statistical analysis for the differences in LOX-1 Wt and LOX-1 Mut expression and the differences in HSP70 binding to LOX-1 Wt and LOX-1 Mut was done by Wilcoxon test.

6.38 Screening for LOX-1 Wt and LOX-1 Mut stable CHO cells

A difference in binding of HSP70 was observed between LOX-1 Wt and LOX-1 Mut transfected CHO cells. Stable cell lines expressing LOX-1 Wt and LOX-1 Mut protein would provide a further valuable tool to carry out functional studies of these proteins. For this purpose, CHO cells (2×10^5 cells/well) were independently transfected with 0.5 μ g DNA each of pAcGFPI-N1 vector, pAc LOX-1 WT and pAc LOX-1 Mut constructs for 48 hours. Cells were then grown in a selection medium containing G418 (1000 μ g/ml) for three weeks.

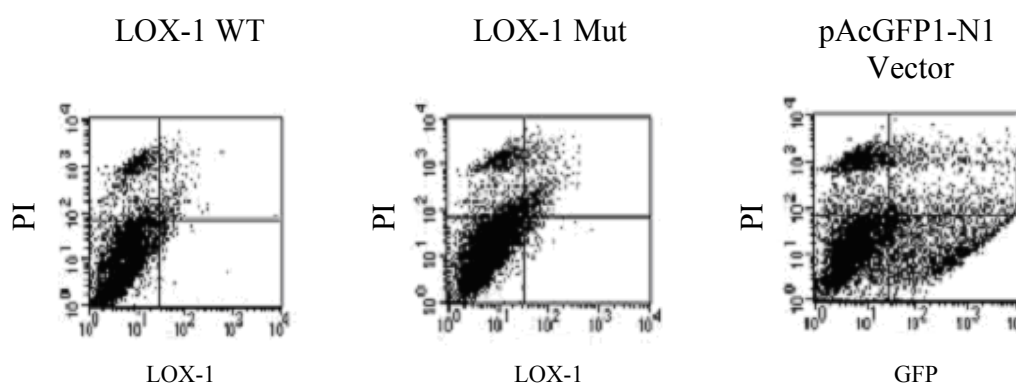


Fig 46. Screening for LOX-1 Wt and LOX-1 Mut stable colonies. Stable colonies of LOX-1 Wt and LOX-1 Mut obtained after 3 weeks of G418 selection were stained with anti-LOX-1 antibody (FITC-conjugated goat anti-mouse IgG secondary antibody) and analyzed by flow cytometry. Similarly stable colonies of pAcGFPI-N1 vector transfected CHO cells were analyzed by flow cytometry for cells expressing GFP. All cells were also stained with PI to differentiate between living and dead cells. No cells with LOX-1 expression were observed among the LOX-1 Wt and LOX-1 Mut colonies. Colonies of pAcGFPI-N1 vector transfected stable cells showed a population of GFP expressing cells.

Individual colonies obtained were then picked, expanded and screened for the LOX-1 expressing cells by staining the cells with anti-LOX-1 antibody (and a FITC-conjugated goat anti-mouse IgG secondary antibody) and analyzed by flow cytometry. No colonies with LOX-1 expressing cells were observed among the LOX-1 WT (Fig 46; Table 2.4) and the LOX-1 Mut (Fig 46; Table 18) stable transfectants. However, cells transfected with the pAcGFPI-N1 vector which expresses GFP were readily obtained (Fig 46; Table 18).

Table 18. Analysis of constitutively expressing LOX-1 Wt and LOX-1 Mut stable colonies

Stable transfection	No. of colonies analyzed	Positive colonies
pAcGFPI-N1/LOX-1Wt	23	0
pAcGFPI-N1/LOX-1 Mut	23	0
pAcGFPI-N1 Vector	26	15 (GFP expressing)

6.39 Analysis of LOX-1 expression and HSP70 binding in HT1080 cells

Stable cells expressing LOX-1 were not obtained with the constitutive expression system. It has to be noted that LOX-1 is reported to mediate the induction of apoptosis by Ox-LDL (Chen et al., 2004). Hence, it is possible that LOX-1 is toxic when it is expressed constitutively in the cells. This problem could be circumvented by having an inducible system where the expression of LOX-1 gene is turned on only in the presence of an inducer (doxycycline). Human HT1080 cells were tested for endogenous LOX-1 expression and HSP70 binding. The cells were stained with anti-LOX-1 antibody (and a FITC-labeled goat anti-mouse IgG secondary antibody) and in parallel with FITC-labeled HSP70. Expression of LOX-1 and HSP70 binding to cell surface of HT1080 cells was then analyzed by flow cytometry. There was no endogenous LOX-1 expression in HT1080 cells (Fig 47) and they did not bind to HSP70 (Fig 47). A stable HT1080 cell line carrying a regulatory pTet-on vector was obtained from Prof. Thomas Dierks (Department of Biochemistry, University of Göttingen). These cells were used for generating stable cells for inducible LOX-1 Wt and LOX-1 Mut expression.

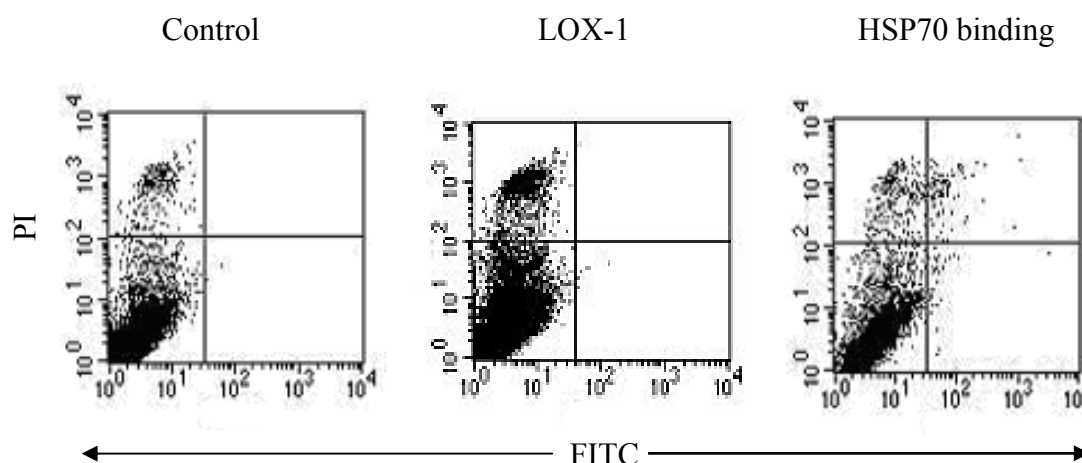
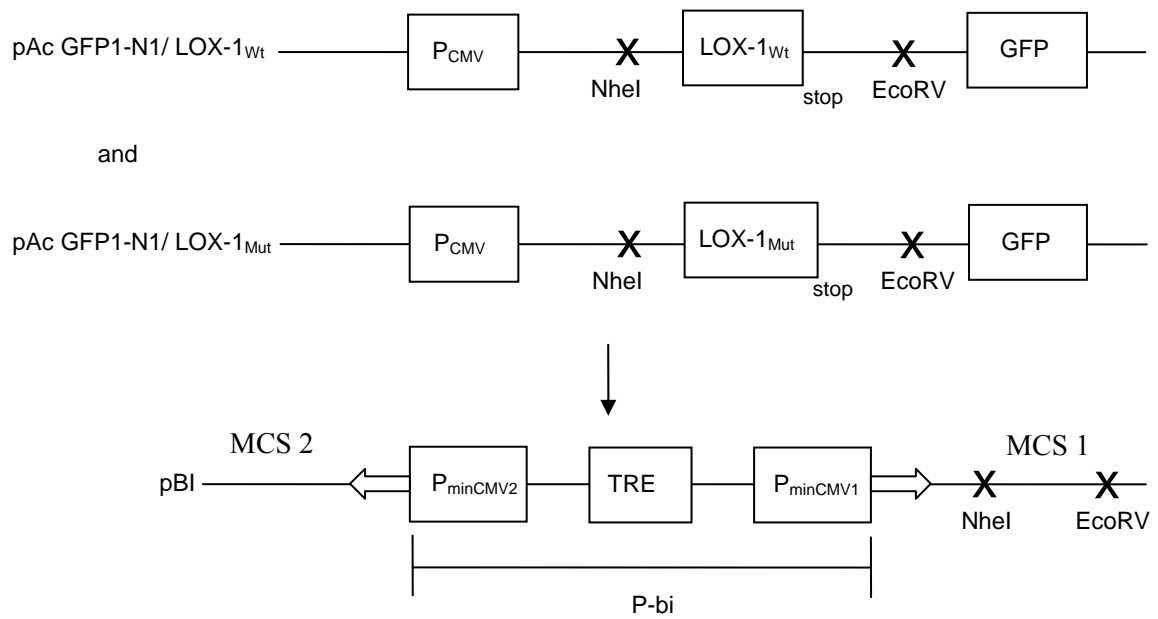


Fig 47. Evaluation of endogenous LOX-1 expression and HSP70 binding in HT1080 cells. The dot plots of HT1080 cells that were stained only with PI, with an anti-LOX-1 antibody (and a FITC-labeled goat anti-mouse IgG secondary antibody) and PI, or with FITC-labeled HSP70 and PI are shown. No expression of LOX-1 and no HSP70 binding was observed on cell surface of HT1080 cells.

6.40 Expression of LOX-1 Wt and LOX-1 Mut after induction by doxycycline

LOX-1 Wt and LOX-1 Mut inserts were cut out from their respective pAcGFP1-N1 vectors by Nhe 1 and EcoRV digestion and cloned into Nhe1 and EcoRV sites of pBI vector as shown in Fig 48A. The pBI vector does not contain a selection marker in the backbone. Therefore, pBI LOX-1 Wt and pBI LOX-1 Mut vectors were then separately cotransfected with a selection vector pPUR in a ratio of 10:1 (pBI LOX-1: pPUR) into a stable HT1080 cell line carrying a regulatory pTet-on vector. 48 hours after transfection, cells were grown in a selection medium containing puromycin (0.3 $\mu\text{g}/\text{ml}$) for three weeks. Stable cell clones obtained for pBI LOX-1 Wt and pBI LOX-1 Mut were then

A



B

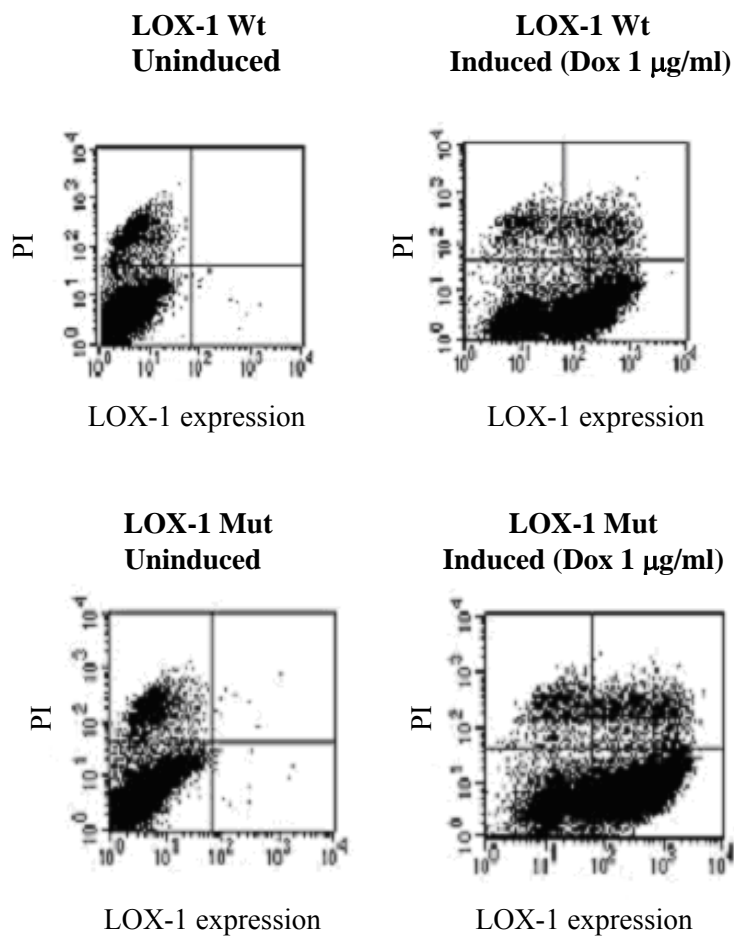


Fig 48. Generation of pBI/LOX-1 constructs and inducible expression of cell surface LOX-1 Wt and LOX-1 Mut in HT1080 cells. (A) LOX-1 Wt and LOX-1 Mut inserts were digested from NheI and EcoRV restriction sites in their respective pAcGFP-N1 vector and cloned separately into NheI and EcoRV

restriction sites of pBI vector. The pBI Tet vector contains the bidirectional promoter (P-bi) which is responsive to rtTA regulatory protein in the Tet-On system. The TRE (Tet-responsive element) is between two minimal CMV promoters (P_{minCMV}), which lack the enhancer that is part of the complete CMV promoter. Two multiple cloning sites are present (MCS 1 and MCS 2) which allows two genes to be expressed at the same time from the vector system. (B) LOX-1 Wt and LOX-1 Mut HT1080 doxycycline inducible cell clones were induced with 1 $\mu\text{g/ml}$ doxycycline for 16 hours. After induction, cells were stained with anti-LOX-1 antibody and a FITC-labeled goat anti-mouse IgG secondary antibody and cell surface expression of LOX-1 was measured by flow cytometry. All the cells were also stained with PI 10 minutes before the flow cytometric analysis. Cell surface expression of LOX-1 for the uninduced and induced LOX-1 Wt and LOX-1 Mut clones is shown.

screened for the expression of cell surface LOX-1 after induction with 1 $\mu\text{g/ml}$ of doxycycline in culture medium. Inducible cell clones were obtained both for LOX-1 Wt and LOX-1 Mut. The expression of LOX-1 after induction with 1 $\mu\text{g/ml}$ doxycycline for 16 hours for LOX-1 Wt clone and LOX-1 Mut clone is shown in Fig 48B.

6.41 Control of LOX-1 Wt and LOX-1 Mut protein expression levels by different induction conditions

Doxycycline inducible cell clones obtained for pBI/LOX-1 Wt and pBI/LOX-1 Mut transfectants were analyzed for the LOX-1 expression. Cells from individual clones were either left uninduced (control) or induced with doxycycline. After the treatment, cells were harvested and stained with anti-LOX-1 antibody and FITC-labeled goat anti-mouse IgG secondary antibody and analyzed by flow cytometry. Inducible cell clones of LOX-1 Mut showed higher expression levels of the LOX-1 on cell surface compared to LOX-1 expression on cell surface of LOX-1 Wt clones with the same induction condition. Hence, the expression level of LOX-1 between LOX-1 Wt and LOX-1 Mut clones was

Table 19. Analysis of pBI/LOX-1 Wt and pBI/LOX-1 Mut clones

Clones	DOX ($\mu\text{g/ml}$) 16 hours	% of positive cells		LOX-1 Mean	
		Uninduced	Induced	Uninduced	Induced
LOX-1 Wt 1	0.5	2.15	78.38	10.04	181.06
LOX-1 Wt 2	0.5	0.52	70.10	6.56	110.41
LOX-1 Wt 3	0.5	6.27	80.64	15.59	168.58
LOX-1 Wt 4	1	3.22	76.93	11.71	143.65
LOX-1 Wt 5	1	0.99	84.23	8.39	148.42
LOX-1 Wt 6	1	0.92	74.18	7.63	131.71
LOX-1 Mut 1	0.5	8.58	75.06	18.74	281.57
LOX-1 Mut 2	0.5	4.24	50.13	16.78	393.74
LOX-1 Mut 3	0.5	8.98	90.55	26.24	524.54
LOX-1 Mut 4	1	4.28	67.91	12.10	334.52
LOX-1 Mut 5	1	3.27	58.87	6.77	390.68
LOX-1 Mut 6	1	4.86	66.91	9.88	364.62

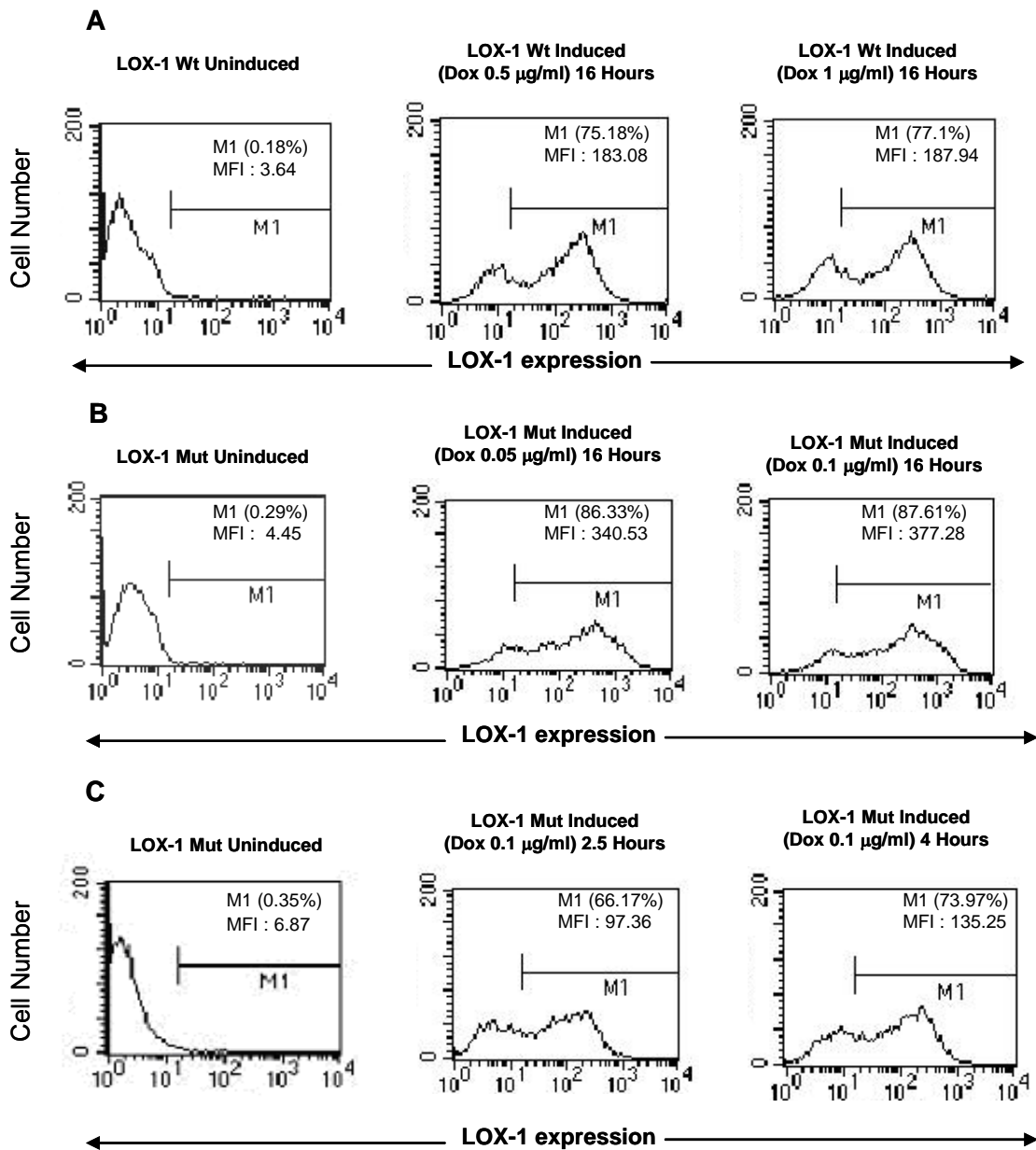


Fig 49. Controlling cell surface expression of LOX-1 by varying induction conditions. (A, B) A LOX-1 Wt stable cell clone was induced for 16 hours with 10-fold higher amount of doxycycline (0.5 $\mu\text{g/ml}$ and 1 $\mu\text{g/ml}$) than that used for LOX-1 Mut stable cell clone (0.05 $\mu\text{g/ml}$ and 0.1 $\mu\text{g/ml}$ for 16 hours). Cells were stained with anti-LOX-1 antibody (and a FITC-labeled goat anti-IgG mouse secondary antibody) and LOX-1 expression was measured by flow cytometry. Mean values of LOX-1 expression and percentage of positive cells obtained for uninduced and induced LOX-1 Wt and LOX-1 Mut cell clones are indicated in the figures. (C) A LOX-1 Mut stable cell clone was induced with 0.1 $\mu\text{g/ml}$ doxycycline for 2.5 and 4 hours. Cells were then stained with anti-LOX-1 antibody and cell surface LOX-1 expression was measured by flow cytometry. Mean values of LOX-1 expression and percentage of positive cells obtained for uninduced and induced LOX-1 Mut stable cell clone are indicated in the figures.

different with the same induction conditions. However, for further functional studies of the LOX-1 Wt and LOX-1 Mut proteins, it was valuable to obtain similar expression levels of both proteins. The summary of the clones analyzed is given in Table 19.

The amount of doxycycline used for induction of LOX-1 Mut clones was reduced compared to LOX-1 Wt clones. Mean expression values of LOX-1 Mut protein was higher even when 2-fold and 10-fold lower concentration of doxycycline was used compared to doxycycline amount used for induction of LOX-1 Wt protein, (Fig 49A and B). Increase of doxycycline concentration did not greatly influence the mean values of LOX-1 expression for both LOX-1 Wt and LOX-1 Mut clones (Fig 49A and B, Table 20). Since increase of doxycycline concentration did not greatly affect the expression levels of LOX-1, induction time was varied to test the expression levels of LOX-1. Furthermore, it made more sense to use LOX-1 Mut clones and test if the LOX-1 expression levels could be reduced in these clones. The induction time was reduced for LOX-1 Mut clone and induction was tested for 2.5 hours and 4 hours using the same concentration of doxycycline. There was reduced expression of LOX-1 Mut protein on the cell surface after short duration of inductions of 2.5 and 4 hours with doxycycline as shown in Fig 49C and Table 20. Hence, it was possible to reduce the amount of cell surface LOX-1 expression on LOX-1 Mut clone by changing the induction time and these cells can be used in the future for HSP70 binding studies.

Table 20. Summary of induction conditions for LOX-1 Wt and LOX-1 Mut clones taken from Fig 2.17

LOX-1 Wt			LOX-1 Mut		
Time	Doxycycline (µg/ml)	MFI	Time	Doxycycline (µg/ml)	MFI
16 hours	0.5	183.08	16 hours	0.05	340.53
16 hours	1	187.94	16 hours	0.1	377.28
			4 hours	0.1	135.25
			2.5 hours	0.1	97.36

6.42 Differences in induction of protein but not mRNA of LOX-1 in LOX-1 Wt and LOX-1 Mut clones

The higher expression of LOX-1 Mut protein on cell surface of LOX-1 Mut inducible cell clones could be due to increased transcription of LOX-1 Mut gene. Three independent clones each for LOX-1 Wt and LOX-1 Mut were tested for their LOX-1 mRNA expression and in parallel the expression of cell surface LOX-1 was also measured. 1 million cells were seeded in a 10 cm dish and cells were either left un-induced (normal medium) or induced with 1 µg/ml doxycycline for 24 hours. Cells were harvested and for each clone a portion of cells were analyzed for LOX-1 cell surface expression by flow cytometry and another portion was used for RNA preparation and cDNA synthesis. For flow cytometry analysis, cells were stained with anti-LOX-1 antibody and a FITC-labeled goat anti-mouse IgG secondary antibody and cell surface LOX-1 expression was measured by flow cytometry. For analysis of LOX-1 mRNA expression, real-time PCR was performed on the cDNA of each clone by SYBR green reagent. GAPDH was used as an endogenous control to normalize for the differences in cDNA amount across each sample. The amount of LOX-1 mRNA expression was determined by relative quantitation method (Livak and Schmittgen, 2001) in comparison to the internal control,

GAPDH. There was a difference in protein expression level observed between the LOX-1 Wt and LOX-1 Mut clones (Fig 50A) but less so at the mRNA level (Fig 50B).

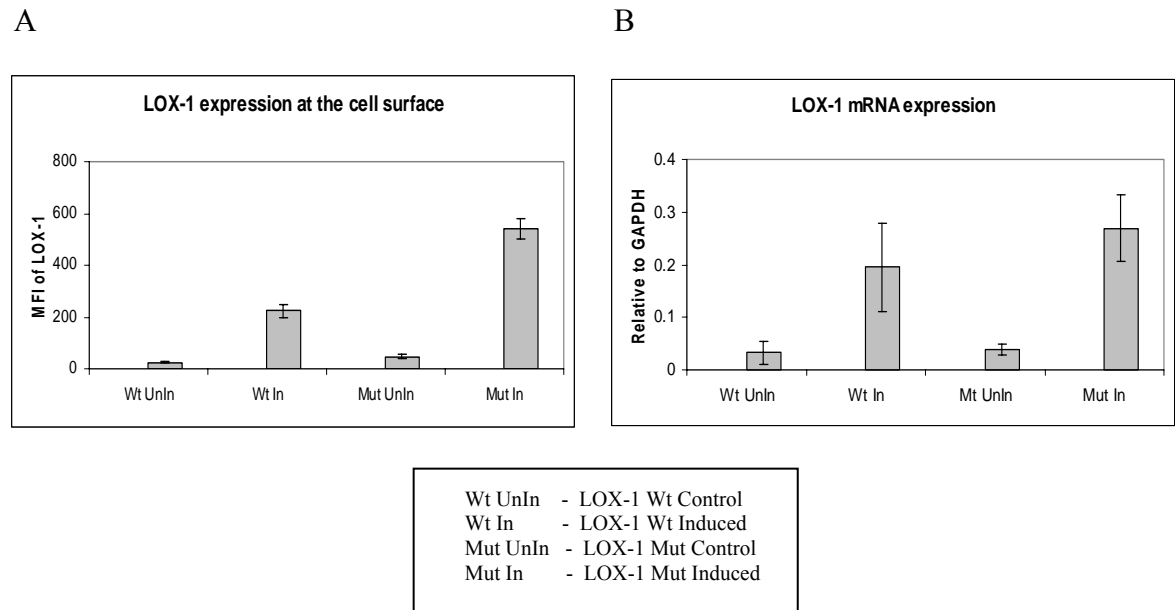


Fig 50. Induction of cell surface LOX-1 and LOX-1 mRNA in LOX-1 Wt and LOX-1 Mut clones by doxycycline. (A) Cell surface expression of LOX-1 for LOX-1 Wt control, LOX-1 Wt induced (1 μ g/ml doxycycline, 24 h), LOX-1 Mut control and LOX-1 Mut induced (1 μ g/ml doxycycline, 24 h) clones was measured by flow cytometry after staining the cells with an anti-LOX-1 antibody and a FITC-labeled goat anti-mouse IgG secondary antibody. The mean (\pm SD) of LOX-1 cell surface expression of three independent clones is shown. (B) The clones analyzed for cell surface LOX-1 expression were also analyzed for LOX-1 mRNA expression by real-time PCR using SYBR green reagent. The primers used for LOX-1 were LOX-1 cDNA For and Rev. The mean (\pm SD) of LOX-1 mRNA expression of three independent clones is shown.

7. Discussion

7.1 Analysis of HSP70 binding to its receptors on monocytes

Extracellular HSP70 has been found to play a role in both innate and adaptive immune responses (Srivastava, 2002). Many of these effects of HSP70 are mediated through cell surface receptors. Such receptors include including CD91 (Basu et al., 2001), LOX-1 (Delneste et al., 2002), TLR2 and TLR4 (Asea et al., 2002), CD36 (Nakamura et al., 2002), CD40 (Becker et al., 2002), SR-A (Bervin et al., 2003), and CCR5 (Whittall et al., 2006). Studies have shown that HSP70 binds to CD91 (Basu et al., 2001; Binder et al., 2000) and LOX-1 (Delneste et al., 2002) and is involved in antigen cross-presentation through MHC class I pathway. The cross-presentation refers to the ability of certain antigen-presenting cells to take up, process and present extracellular antigens with MHC class I molecules to CD8 T cells. Very recently, (Zitzler et al., 2008) showed that the individual domains of HSP70 (nucleotide binding domain or ATPase domain and substrate binding domain) interact with distinct sites on the membrane of APCs indicating that at least distinct receptors exist on APC membrane for the HSP70 domains. Furthermore the authors showed that the substrate binding domain appears to be responsible for efficient cross-presentation mediated by HSP70. Hence, the existence of distinct receptors for individual domains of HSP70 on macrophages and DCs may correlate with the diverse functions that have been ascribed to HSP70. TLRs have been suggested to be involved in HSP-mediated signaling and activation of APCs but not in representation of HSP-chaperoned peptides. Asea and colleagues reported that recombinant HSP70 could signal through TLR2 and TLR4 with the involvement of CD14 (Asea et al., 2002). Vabulas and colleagues showed a TLR4-mediated signaling effect of HSP70 (Vabulas et al., 2002). However, there has been serious concern regarding role of TLRs in HSP70 mediated signaling (Gao and Tsan, 2003a; Gao and Tsan, 2003b), because TLRs are well documented ligands for bacterial LPS and LPS contamination is common during recombinant protein preparation in bacteria. To circumvent major LPS contaminations various strategies have been used. One of these was the inhibition of LPS with the LPS-specific inhibitor polymyxine B (PmB), and the other was the heat sensitivity of HSP versus heat insensitivity of LPS. However, these controls were not sufficient to completely exclude the contribution of LPS to HSP-mediated stimulation because low amounts of LPS revealed to be heat sensitive and inhibition of LPS by PmB was not complete (Wallin et al., 2002). To circumvent these LPS contaminations, HSP70, HSP90 and gp96 purified from eukaryotic tissues were used in a few studies. HSP70 purified from liver was shown to induce the maturation of DC and to activate cytokine release in macrophages (Basu et al., 2000). Furthermore, a better insight into a possible function of HSP as endogenous danger signals was obtained by employing transgenic eukaryotic cell lines that overexpress HSP or express HSP as membrane bound cell surface proteins (Todryk et al., 1999); (Chan et al., 2007). Cell surface HSP including HSP60 and HSP70 were shown to induce the maturation of APC and the production of cytokines by APC leading to enhanced NK and T cell activation in vitro (Todryk et al., 1999) (Gehrmann et al., 2003) (Osterloh et al., 2007). Using such systems HSP were shown to modulate immune cell functions in the absence of bacterial LPS. Initially, CD40 was reported to bind mycobacterial HSP70 but not mammalian HSP70 (Wang et al., 2001). Later studies showed that macrophages expressing CD40, specifically bind human HSP70 and uptake the HSP70 bound peptide (Becker et al., 2002). Recently, chemokine receptor CCR5 was shown to bind mycobacterial HSP70 (Whittall et al., 2006).

In our study, we wanted to determine if HSP70 preferentially binds to some or several of these receptors on the cell surface of monocytes, which could indicate the relative importance of these receptors in HSP70 binding. We measured the expression of CD91, LOX-1, CD36, TLR2 and TLR4 on cell surface of monocytes. The correlation of HSP70 binding to the expression of these receptors on monocytes indicated a significant but moderate correlation of HSP70 binding and the expression of LOX-1, CD91, CD36, and TLR4. The best correlation was found between TLR4 expression and HSP70 binding and there was no correlation of HSP70 binding to TLR2 expression. This suggests that several HSP70 receptors on the cell surface of monocytes could participate in binding of HSP70 and mediate innate and adaptive immune responses.

7.2 Expression of CD91 on cell surface of monocytes in HIV cohort

CD91 is a rather widely expressed protein and plays a dual role in endocytosis and signal transduction (Herz and Strickland, 2001). In vessel walls, the interaction of CD91 with growth factors and tissue plasminogen activator (tPA) influence vessel development and integrity, tone and grade of permeability (Boucher et al., 2003; Nassar et al., 2004). In neuronal tissue, CD91 influences the ion channel function and also the amyloid precursor protein (APP) processing (May et al., 2004; Waldron et al., 2006). It is involved in the endocytosis of a broad range of ligands, including protease/protease inhibitor complexes and chylomicron remnants (Herz and Strickland, 2001). It has also been shown to be important for phagocytosis of apoptotic cells and embryonic development (Su et al., 2002). The importance of CD91 in a variety of diseases has been shown by its ability to mediate the uptake of HIV-1 Tat protein, apolipoprotein E4, APP, and amyloid β -protein (Liu et al., 2000). CD91 has also been recently demonstrated to bind and internalise α -defensins in a saturable and dose-dependent manner. The α -defensins are secreted from stimulated CTLs in a rare minority of individuals infected with HIV-1 but with no evidence of progressive disease termed as LTNPs. The study also showed that α -defensins have an anti-HIV property (Zhang et al., 2002).

An increased expression of CD91 has been described on monocytes of HIV-1 infected LTNP (Stebbing et al., 2003), HIV-1 exposed but seronegative individuals (Kebba et al., 2005), and advanced melanoma slow progressors (Stebbing et al., 2004). High levels of CD91 on professional antigen presenting cells could improve the cross-presentation of antigens to CTL and provide an advantage for the induction of CTL responses against viruses and tumors. Our comparison of the expression of CD91 on cell surface of monocytes in a small cohort of LTNP and two groups of disease progressing patients (from TIMS and RESTART studies) showed a significant increase of CD91 expression in LTNPs compared to the disease progressing patients. This result further underscores the assumption that increased CD91 expression on APCs may be beneficial during HIV-1 infection.

7.3 Genotype distribution of CD91 exon 3 polymorphism and its influence on CD91 expression

The $\epsilon 4$ allele of the APOE gene is a well recognized genetic susceptibility factor for late-onset AD. However, the mechanism by which APOE alleles affect disease development is not fully understood. The CD91 receptor is the main apoE receptor in the brain (Holtzman et al., 1995). CD91 is also responsible for the endocytosis of secreted APP (Knauer et al., 1996), another molecule central to the pathogenesis of AD. Besides the lipoprotein metabolism, CD91 is also involved in the coagulation-fibrinolysis balance (Bu et al., 1993) which relate to the development of atherosclerosis and also in tumor progression and invasion (Li et al., 1998). Therefore, polymorphisms affecting the function or expression of CD91 may thus influence the individual's risk to these diseases and have been studied in the respective cohorts.

The exon 3 polymorphism (766 C>T) of CD91 gene has been reported to be associated with Alzheimer's disease (AD), breast cancer (BC) and myocardial infarction (MI). Hollenbach and colleagues provided evidence of increased frequency of the C allele of CD91 exon 3 polymorphism in patients with AD (AD: C/T of 0.87/0.23; control: C/T of 0.80/0.20) (Hollenbach et al., 1998). Similarly, an increased frequency of the C allele of exon 3 polymorphism has been found among 157 patients with late-onset AD compared to controls (AD: C/T of 0.89/0.11; control: C/T of 0.80/0.20) in white Americans (Kang et al., 1997). The authors suggested that the polymorphism, predicted to be silent, may be in LD with a putative nearby AD susceptibility locus. In our study group of HIV cohort, we observed an increased occurrence of T allele in LTNP compared to the disease progressive group from TIMS and RESTART studies (LTNP: C/T of 0.75/0.25; TIMS & RESTART of 0.88/0.12). We increased the sample number of LTNP and analysed the exon 3 genotype in further 14 LTNPs. Though the occurrence of T allele was still higher in LTNPs (C/T of 0.80/0.20) when compared to the disease progressive group (TIMS & RESTART of 0.88/0.12), however the differences were not statistically significant ($p=0.383$). The T allele frequency of CD91 exon 3 polymorphism observed in our group of healthy volunteers was slightly lower (C/T of 0.85/0.15) than in other controls groups (Hollenbach et al., 1998; Kang et al., 1997).

Increase in CD91 expression has been described on monocytes of LTNPs (Stebbing et al., 2003). We then asked the question whether the T allele of exon 3 polymorphism is associated with expression CD91. Interestingly, the presence of T allele in exon 3 polymorphism was associated with increase in CD91 expression on cell surface of monocytes in subgroups of HIV-1 infected individuals. We found a significant effect of the exon 3 polymorphism (T allele) on CD91 expression on the cell surface on monocytes in the patients of the TIMS group ($p=0.0242$) and a similar but only borderline effect in the LTNP group ($p=0.0403$), if a robust threshold for significance of $\alpha'=0.033$ (obtained from permuted data sets) was applied. Since there was only one sample with T allele in the RESTART group, the genetic effect could not be tested. However, there was no effect of exon 3 polymorphism on CD91 expression in healthy volunteers ($p=0.293$). Since there was an increase in CD91 expression with the presence of exon 3 polymorphism in the HIV cohort, the genetic effect of CD91 exon 3 polymorphism on CD91 expression could be disease-specific and may occur in response to HIV infection or other external triggers. Furthermore, the exon 3 polymorphism did not influence the expression of CD91 mRNA in healthy volunteers. As the RNA sample was available only for few samples in HIV cohort, the effect of exon 3 polymorphism on CD91 mRNA expression

in HIV cohort could not be tested in depths. The exon 3 polymorphism is a silent mutation, which does not produce an amino acid change, and hence it is unclear how it influences the expression of the CD91 receptor.

The exon 3 SNP could be linked to a nearby SNP that could influence the expression of CD91. However it would be cumbersome to analyze all the SNPs located nearby exon 3 SNP to test if any of these influence the CD91 expression. With the help of HapMap database, it is possible to evaluate further SNPs and haplotypes for a CD91 gene (www.hapmap.org) that might be associated with CD91 expression. The HapMap is a catalog of common genetic variants that occur in human beings. It identifies these variations and their position in the DNA and its distribution among people in different parts of the world. The objective of the HapMap project is to identify most of the 10 million SNPs estimated to occur in the human genome. Genetic variants that are near each other tend to be inherited together. These regions of linked variants are known as haplotypes. In many parts of our chromosomes, just a handful of haplotypes are found in humans. The International HapMap Project is identifying these common haplotypes in four populations from different parts of the world. Samples examined are: (1) 90 individuals (30 parent-offspring trios) from Yoruba in Ibadan, Nigeria; (2) 90 individuals (30 trios) in Utah, USA, representing the Caucasian population; (3) 45 Han Chinese in Beijing, China; and (4) 44 Japanese in Tokyo, Japan. The HapMap is also identifying "tag" SNPs that uniquely identify these haplotypes. By testing an individual's tag SNPs by genotyping; it is possible to identify the collection of haplotypes in a person's DNA. For disease association studies, the haplotypes in individuals with a disease are compared to the haplotypes of a group of individuals without a disease (the controls). If a particular haplotype occurs more frequently in affected individuals compared with controls, one or number of SNPs in that haplotype could be responsible for the disease.

Recently evidence has been provided that synonymous SNPs can affect protein expression by alterations in the stability of the mRNA (Nackley et al., 2006). A previous report had shown that synonymous SNP can markedly affect mRNA secondary structure which can then have functional consequences on the rate of mRNA degradation (Duan et al., 2003). It is also possible that polymorphic alleles directly modulate protein translation through alterations in mRNA secondary structure, because protein translation efficiency is affected by mRNA secondary structure (Shalev et al., 2002). Very recently, it has been shown that a synonymous SNP in association with other SNPs in a haplotype alters the interaction of the ATP-binding cassette (ABC) transporter, ABCB1 with its substrates and inhibitors (Kimchi-Sarfaty et al., 2007). Thus, it is possible that the exon 3 SNP in association with other SNPs in a haplotype could itself influence the expression of CD91. However, at the moment no experimental data are available for the CD91 mRNA to support this hypothesis.

7.4 Genotype distribution of CD91 promoter polymorphism and its effect on CD91 expression

A polymorphism in the promoter region of CD91 (-25 C>G) has been described (Schulz et al., 2002). In this study of coronary patients with myocardial infarction, the authors found no changes in genotype distribution between coronary patients and control group (coronary patients: CC/CG of 0.87/0.13; control group: 0.87/0.13). However, a significant difference was found when the group was split according to clinical relevance,

taking the severity of coronary obstruction into account: patients with more than 2 atherosclerotically affected vessels were significantly carrying more frequent CG-genotype than patients with 2 or 1 affected vessels (0.185/0.104/0.043; $p < 0.02$). In our study group of HIV cohort we found a slightly decreased frequency of G allele in LTNPs compared to the disease progressing group (C/G of 0.94/0.06; TIMS & RESTART of 0.88/0.12). In healthy volunteers we observed a similar genotype distribution as observed in the control group of (Schulz et al., 2002) (CC/GG of 0.84/0.16) discussed above.

The CD91 promoter polymorphism (-25 C>G) leads to a creation of a new GC-box, that is recognized by the constitutively expressed SP1 transcription factor (Schulz et al., 2002). Investigation of CD91 gene expression with respect to this polymorphism by (Schulz et al., 2002), showed that carriers of G allele had a higher CD91 mRNA expression in human monocytes. In contrast to this observation, we did not observe any influence of CD91 promoter polymorphism on mRNA expression of CD91 in CD14 positive monocytes of healthy volunteers. There was very limited material available for the HIV cohort and hence RNA could only be obtained for few samples. Therefore, the influence of promoter polymorphism on CD91 mRNA expression in HIV cohort could not be analyzed in detail. Our analysis of the promoter polymorphism influence on CD91 mRNA expression in monocytes of healthy volunteers did not show any effect on the CD91 expression. Furthermore, we did not observe any effect of CD91 promoter polymorphism on CD91 cell surface expression on monocytes of HIV cohort and the healthy volunteers. Since CD91 promoter polymorphism did not influence the expression of CD91 at mRNA or the receptor level, it is not responsible for the increased expression of CD91 observed in LTNPs compared to the disease progressing groups (TIMS & RESTART).

7.5 Evaluation of additional SNPs of CD91 gene determined from the HapMap database

We found a significant effect of the exon 3 polymorphism (T allele) on CD91 expression on the cell surface on monocytes in subgroups of HIV-1 infected individuals. Since exon 3 SNP does not cause any amino acid substitution, it is possible that the exon 3 SNP in association with other SNPs in a haplotype influences the expression of CD91. There are some reports showing that haplotypes represented by some SNPs have an influence on gene expression. Very recently, it has been shown that the promoter region of the human platelet-derived growth factor α -receptor (PDGFRA) gene contains a total of 10 polymorphic sites that give rise to 5 distinct haplotypes, and of these one haplotype was associated with the expression of PDGFRA (Toepoel et al., 2008). Another study had shown that a SNP in the IL-10 gene and a haplotype linked with that SNP were associated with higher IL-10 expression levels (Kingo et al., 2005).

We determined additional SNPs within the CD91 gene and also looked at the haplotypes that could influence or are associated with CD91 expression. We obtained two major blocks within the CD91 gene indicating that there is a recombination event occurring with the gene. The first block spanned the region of CD91 gene containing exon 3 SNP and therefore detailed analysis of first block containing exon 3 SNP was considered. The SNPs that identify the haplotypes are referred to as tag SNPs. The five tag SNPs represented in the first block were tag 10, tag 23, tag 27, tag 31 (exon 3 polymorphism) and tag 34. We found a variation in frequency of polymorphic allele of tag 23, tag 27 and

tag 34 in LTNP group compared to the disease progressive group. However, we did not observe any influence of these SNPs on CD91 expression in HIV cohort and the healthy volunteers. The tag 67 SNP in the second block of CD91 gene also did influence the expression of CD91 in HIV cohort and healthy volunteers. Since these independent SNPs did not influence the expression of CD91, it is unlikely that the most frequent haplotypes tagged by these SNPs could influence the expression of CD91. However, it is still possible that exon 3 genotype could be associated with some minor haplotypes in the HIV cohort that could influence the CD91 gene expression, which warrants further investigation or it could be by itself responsible for the effect on CD91 expression as discussed above.

7.6 CD91 expression on monocytes of SIV-infected Rhesus macaques

In humans, CD91 expression is increased on monocytes of HIV-infected LTNPs compared to HIV-infected patients on HAART therapy (Stebbing et al., 2003). In our studies we found a significant increase in CD91 expression in LTNPs compared to the disease progressing patients (from TIMS and RESTART studies). However, it is impossible to evaluate if selective advantage of high CD91 expression on monocytes in LTNPs is predisposed or occurs after the infection. We were interested to determine whether the CD91 expression on monocytes is altered during the course of HIV disease. We had the opportunity to obtain the blood samples from rhesus macaques in SIV vaccination trials at the Primate Center, Göttingen. We analyzed the CD91 expression on monocytes before infection and at several time points up to 58 weeks after infection. We found a decrease of CD91 expression during the time course of study in SIV infected animals suggesting that CD91 expression decreases in the course of infection. However, the expression of CD91 in two animals that remained uninfected after challenge with SIV also showed a decrease in CD91 expression similar to infected animals. Hence, this observation, although only for two animals, challenges the hypothesis that the CD91 expression decreases in the course of infection. We obtained five LTNP rhesus macaques as a result of some rare events in SIV vaccination studies in the primate centre. Interestingly, we observed an increased expression of CD91 on CD14 positive monocytes in LTNP when compared to the CD91 expression in disease progressive group. This could further support the observations in human LTNPs that the increased CD91 expression could be beneficial against the progression of HIV disease.

We analyzed the promoter region of CD91 gene in rhesus macaques by sequencing up to 1 kb upstream of the codon start site and looked for the presence of polymorphisms. We detected one polymorphism that lead to change of C to G allele (-703 C>G). However, we did not observe any effect of this polymorphism on CD91 expression in SIV infected rhesus macaques and the uninfected animals. Interestingly, this polymorphism occurs in the binding site of the transcription factor of nuclear factor of activated T cells (NFAT) family, namely NFATp. This family of transcription factors regulate the transcriptional of genes encoding immunomodulatory cytokines and NFATp participates in the activation of T cells (Rao et al., 1997).

7.7 Genotype distribution of LOX-1 SNPs and their effect on LOX-1 expression

LOX-1 is a member of scavenger receptor family and is increasingly seen as a vascular disease biomarker. Its role in HSP70-mediated immune regulation came into light when (Delneste et al., 2002) first showed that LOX-1 can bind to HSP70 and is involved in the HSP70-mediated antigen cross-presentation. Our interest was to analyze the polymorphisms in the LOX-1 gene and to look for their effects on LOX-1 expression and LOX-1 function. We chose three SNPs in the LOX-1 gene after HapMap database analysis of LOX-1 genomic region. Of these, two SNPs, the SNP in the exon 4 (rs11053646) and 3'UTR region (rs1050283) of this gene have been shown previously to be associated with myocardial infarction (Tatsuguchi et al., 2003); (Mango et al., 2003).

The allele frequencies of exon 4 polymorphism in our healthy volunteers (G/C of 0.93/0.07) was similar to the exon 4 SNP allele frequencies of healthy controls of an Italian population (G/C of 0.91/0.09) (Mango et al., 2003) and a Japanese population (G/C of 0.91/0.09) (Tatsuguchi et al., 2003). For the 3'UTR polymorphism (rs1050283) of LOX-1 the allele frequencies in our population (C/T of 0.5/0.5) were only slightly different from the Italian population (C/T of 0.55/0.45) (Mango et al., 2003).

Two independent studies (Mango et al., 2003; Tatsuguchi et al., 2003) reported an association between polymorphisms in the LOX-1 gene and myocardial infarction. In 102 patients with a history of myocardial infarction, a significantly higher frequency (38.2%) of the exon 4 G>C polymorphism was found compared to 102 controls (17.6%) (Tatsuguchi et al., 2003). The frequency of C allele was 0.21 in patients compared to 0.09 in controls. Another study showed that the polymorphism in the 3'UTR of the LOX1 gene, C>T, was significantly associated with myocardial infarction in a group of 150 patients (Mango et al., 2003). The frequency of T allele was 0.64 in patients compared to 0.45 in controls.

We wanted to test if these LOX-1 polymorphisms show some association to the disease state in the HIV cohort. We analyzed these polymorphisms in our HIV cohort and found no difference for allele frequencies of exon 4 polymorphism between LTNP and disease progressive groups. Though there was a small increase of T allele in disease progressive groups compared to the LTNP group (LTNP: C/T of 0.62/0.38; TIMS & RESTART: C/T of 0.55/0.45) it was not significant ($p=0.768$).

LOX-1 receptor expression is upregulated by several pro-atherogenic conditions like hypertension, dyslipidemia, and diabetes (Chen et al., 2000); (Chen et al., 2001a); (Nagase et al., 1997). LOX-1 mRNA and protein levels are also elevated by pro-inflammatory stimuli such as TGF- β (Transforming growth factor- β) (Minami et al., 2000), TNF- α (Kume et al., 1998), and angiotensin II (Li et al., 1999). Hence, it was interesting to test if any polymorphisms of LOX-1 are associated with the LOX-1 expression, as any such association would indicate genetic pre-disposition in the disease states. We investigated the effect of three SNPs (exon 4, 3'UTR and tag 45) of LOX-1 on its expression. We found no effect of these SNPs on LOX-1 expression on the cell surface of monocytes suggesting that these SNP may not regulate the expression of LOX-1.

7.8 Functional effect of LOX-1 exon 4 SNP

In vitro experiments showed that HSP70 binds in a dose dependant manner to human monocyte-derived DCs and the binding of HSP70 to DCs was completely prevented by maleylated BSA (a ligand for numerous scavenger receptors) (Delneste et al., 2002). Binding assays of scavenger receptors transfected CHO cells revealed that HSP70 specifically bound to LOX-1. Furthermore, LOX-1 was shown to be involved in HSP70-mediated antigen cross-presentation (Delneste et al., 2002). The LOX-1 receptor has two domains in the extracellular region, a neck domain and a C-type lectin like domain. Truncation of lectin domain of LOX-1 was sufficient to abrogate Ox-LDL binding activity (Chen et al., 2001b). In addition, in this study, SDM of certain lysine residues to non basic residues in lectin domain of LOX-1 also reduced its binding to Ox-LDL. The exon 4 SNP of LOX-1 leads to a non-synonymous change in amino acid from lysine to asparagine in the lectin domain of LOX-1. Therefore the question arises, whether this amino acid change in ligand binding domain of LOX-1 affects its binding to HSP70. We introduced the exon 4 SNP mutation into the LOX-1 cDNA by PCR-based SDM.

In our transient transfection experiments with LOX-1 constructs into CHO cells, we observed a low but similar expression of LOX-1 Wt and LOX-1 Mut protein on cell surface of CHO cells. So it was possible to use transient transfection approach for HSP70 binding analysis. We further tested the binding of HSP70 to these CHO cells transiently transfected with LOX-1 WT and LOX-1 Mut constructs. Binding of HSP70 was observed to the cell surface of both the LOX-1 Wt and LOX-1 Mut transfected CHO cells. Comparison of the binding of HSP70 to LOX-1 Wt and LOX-1 Mut transfected CHO cells in 10 independent transient transfection experiments showed a significant decrease in HSP70 binding to LOX-1 Mut transfected CHO cells. Hence, the presence of exon 4 SNP in LOX-1 influences its binding to HSP70. This warranted further study in a stable expression system. Our stable transfections with LOX-1 WT and LOX-1 Mut constructs in CHO cells did not generate any cell colonies expressing LOX-1. Alternatively, we generated an inducible expression system where the LOX-1 gene is turned on in the presence doxycycline. However, it was important that the surface expression of LOX-1 Wt and LOX-1 Mut from these cells is similar, in order to compare the HSP70 binding to these cells. Surprisingly, we observed that the cell surface expression of LOX-1 from all LOX-1 Mut inducible cell clones was higher than those of LOX-1 Wt cell clones. In an effort to bring the expression levels of LOX-1 to similar levels in LOX-1 WT and LOX-1 Mut clones, we varied the doxycycline concentrations but it did not have an effect on the levels of LOX-1 expression. We then decided to reduce the induction time of LOX-1 Mut clones to bring down the expression levels of LOX-1 in these clones. There was a reduced expression of LOX-1 from the LOX-1 Mut clones with shorter induction time. Hence, the induction time could be varied between the LOX-1 Wt and LOX-1 Mut clones to achieve similar levels of LOX-1 expression at the cell surface. Apart from HSP70 binding studies, these clones could be used to study the effect of exon 4 SNP in the internalization of HSP70. Furthermore, it would be also interesting to test the effect of LOX-1 exon 4 SNP on LOX-1 mediated antigen-presentation.

7.9 Possible regulation of LOX-1 expression by exon 4 SNP

We observed an increased expression of LOX-1 from LOX-1 Mut clones compared to LOX-1 Wt clones. One possibility could be the integration of LOX-1 gene could be

different between clones. It is thought that the activity of an integrated reporter gene is strong if it integrates into an accessible chromatin structure in the vicinity of an actively transcribed endogenous gene. However, this phenomenon cannot explain our observations because several clones that we analyzed for LOX-1 Mut showed higher LOX-1 expression than LOX-1 Wt clones. Recently, some studies have reported an evidence of genetic association of LOX-1 3'UTR polymorphism (rs1050283) with Alzheimer's disease (Luedeking-Zimmer et al., 2002); (Lambert et al., 2003) and myocardial infarction (Chen et al., 2003). These genetic studies were supported by some functional data suggesting reduced binding of T allele to unidentified nuclear and cytoplasmic proteins as compared to C allele determined by EMSA. Similarly, some other SNPs in LOX-1 may also influence the mRNA stability or post-translational modification of LOX-1. We performed simultaneous analysis of LOX-1 mRNA expression by real-time PCR and LOX-1 expression at the cell surface by flow cytometry of three independent LOX-1 Wt and LOX-1 Mut clones. Our results suggested a difference in cell surface expression of LOX-1 between LOX-1 Wt and LOX-1 Mut clones, but less so at the mRNA level. Therefore the difference in LOX-1 expression might indicate an effect of exon 4 SNP on the post-translational regulation of LOX-1. Post-translational modification of lysine residues such as acetylation, acylation, glycosylation, methylation and sumoylation have been implicated in protein stability, regulation of protein function and localization to membrane (Seo and Lee, 2004). Thus one of these mechanisms may be responsible for the differences in LOX-1 expression observed between the LOX-1 Wt and LOX-1 Mut clones. We did not observe any differences in LOX-1 expression on cell surface of monocytes in individuals with LOX-1 exon 4 SNP (GG vs GC genotype). It has to be noted that we had only one individual with a CC genotype in our study population. Therefore, it might be inappropriate to compare the expression observed in our transfection studies where the mutant construct has a CC genotype to the effect of CG genotype on LOX-1 expression on monocytes. Secondly, the intracellular mechanisms and machinery involved in the folding and export of protein to the cell surface could be different in epithelial cell line (HT1080) compared to the monocytes. Furthermore, in transfection studies, we induce the expression of protein which leads to rapid synthesis and transport to the cell surface which may further influence the effect of this SNP on the levels of LOX-1 expression compared to constitutively expressing monocytes.

7.10 Implications of HSP70 receptor polymorphisms for immunotherapy

Success of numerous immunotherapeutic strategies especially against cancer, has been both variable and difficult to predict. Gene polymorphisms in immunoregulatory molecules may contribute to the heterogeneity in outcome between individuals receiving the same immunotherapeutic treatment. These polymorphisms may be present in coding and noncoding regions, potentially altering protein function or abundance of regulatory molecules, and thereby influencing the efficacy of therapy or resulting in predisposition to diseases. Particular HLA polymorphisms are associated with disease susceptibility and progression in a range of predominantly inflammatory conditions (Bateman and Howell, 1999). For example, individuals developing colorectal adenocarcinoma who possess the HLA-DQB1*0301 allele (HLA class II gene) have a lower incidence of advanced stage tumors (Fossum et al., 1994). HLA-DPB1*0301 allele (HLA class II gene) confers an increase in risk for the development of Hodgkin's disease in Caucasian population (Bateman and Howell, 1999). Cytokines play a critical role both in the maturation and

differentiation of immune cells and in the activation of their functions (Jonuleit et al., 1996). Therefore the modulation of immune responses by the application of recombinant cytokines or cytokine genes has promise for application in cancer immunotherapy. A polymorphism of the IL-1 β gene has been shown to be associated with significantly shorter survival in pancreatic cancer patients (Barber et al., 2000). IL-10 promoter polymorphisms have been suggested to influence tumor development in cutaneous malignant melanoma (Howell et al., 2001). IL-10 gene polymorphisms have also been shown to be associated with the clinical course of non-Hodgkin's lymphoma progression (Kube et al., 2008)

The use of HSP vaccines in immunotherapy of cancer and infectious disease was borne out of the studies examining the relationship between cancer and immunity in mice. Mice immunized with HSPs purified from a tumor were protected from a tumor challenge if the tumor cells used for the challenge were the same as those from which the HSP was purified. In other words, immunogenicity of HSP was specific to the tumor from which it was purified and identical to the nature of immunity elicited by whole cells. Hence, HSPs derived from a different tumor or from normal tissue did not confer immunity to challenges with other tumors (Udono and Srivastava, 1994). The vaccine consists of HSP-peptide complexes isolated from a patient's tumour. After vaccination, antigenic tumour peptides are processed and presented on the surface of potent antigen-presenting cells of the immune system, such as macrophages and DCs, which results in a potent anti-tumour immune response (Parmiani et al., 2004). Recent studies in solid tumors have shown that tumor-derived HSPs, such as HSP70 and gp96, are immunogenic and potent in stimulating the generation of tumor-specific CTLs (Janetzki et al., 1998); (Rivoltini et al., 2003). In our studies we found an exon 3 polymorphism to be associated significantly with increase of CD91 expression in subgroups of HIV cohort. Even though we found this association only in the HIV disease, it could have important implications in the HSP-based immunotherapy for AIDS disease. Furthermore, we observed a decreased binding of HSP70 to LOX-1 receptor carrying exon 4 SNP. Delneste and colleagues had reported that HSP70 binds specifically to LOX-1 on cell surface of DCs (Delneste et al., 2002). DCs role as the initiators and regulators of immune response makes them a powerful tool for the therapeutic manipulation of immune reactivity to infectious disease and cancer (Banchereau et al., 2000). Though our binding studies of HSP70 to LOX-1 receptor carrying exon 4 SNP have to be further validated, these polymorphisms could contribute to the variability in outcome to HSP70-based immunotherapies.

The clinically most successful immunotherapy is currently the allogeneic hematopoietic stem cell transplantation. A major complication of this therapy is the graft-versus-host disease (GVHD). Interestingly, a role of HSP70 has been also suggested for GVHD. An increased expression of the inducible form of HSP70 in GVHD was first shown in a rat model (Goral et al., 1998). The involvement of HSP70 in GVHD alloreaactions has also been observed in an in vitro human skin explant assay (Sviland and Dickinson, 1999; Sviland et al., 1990). The skin explant assay in addition to its use in the prediction of clinical acute GVHD, has developed into a useful research tool to investigate potential mechanisms in the pathogenesis of the disease. Recently, a rat skin explant model has been established laboratory (Novota et al., 2008) and in the expression profile of genes in GVHD has been analysed. Increased expression of HSP70 (Novota et al., 2008) and LOX-1 was observed in GVHD indicating that LOX-1 could mediate some effects of HSP70 in GVHD.

7.11 Conclusion and future perspectives

The present study of CD91 expression in HIV cohort demonstrated that the expression of CD91 is significantly increased on cell surface of monocytes in LTNPs compared to the disease progressing groups, TIMS and RESTART. Of the CD91 polymorphisms analyzed, only CD91 exon 3 polymorphism was significantly associated with CD91 expression in subgroups of the HIV cohort. Our study of SIV-infected rhesus macaques showed an decrease in the expression of CD91 during the course of infection. Furthermore, the LTNP rhesus macaques showed a higher expression of CD91 on the cell surface of monocytes compared to disease progressive group. The study of LOX-1 polymorphisms demonstrated that the exon 4 SNP (rs11053646, tag 36), 3'UTR SNP (rs1050283, tag 27) and intron 2 SNP (rs3912640, tag45) of LOX-1 did not effect the expression of LOX-1 on the cell surface of monocytes. However, the exon 4 SNP that results in a change of amino acid sequence from lysine to asparagine has a functional effect. A transient transfection analysis with LOX-1 Wt and LOX-1 Mut (exon 4 SNP) constructs demonstrated a reduced binding of HSP70 to cell surface of LOX-1 Mut transfected cells compared to LOX-1 Wt transfected cells.

Recently, our laboratory developed a rat skin explant model to identify potential novel molecular markers that could be useful in predicting GVHD. In this study, increased expression of HSP70-1 and HSP70-2 genes were correlated with the degree of GVHD (Novota et al., 2008). Furthermore, when the general gene expression profile of GVHD tissue was compared to normal tissue, an increased expression of LOX-1 was observed in GVHD tissue (unpublished data). This indicates that LOX-1 along with HSP70 could be involved in the pathogenesis of GVHD. Therefore, the analysis of the LOX-1 exon 4 SNP and CD91 exon 3 SNP in GVHD could be interesting. We plan to analyze these SNPs and the expression of CD91 and LOX-1 proteins in a large collection of human GVHD samples.

8. Summary

In recent years, HSP70 and other HSPs have obtained attention for their participation in innate and adaptive immune responses. HSP70 can form stable complexes with cytoplasmic tumor antigens or the viral antigens and enter into the extracellular environment. Extracellular HSP70 has at least two major enhancing effects on APC function: (a) induction of innate immune functions through activation of the APC maturation programme and (b) induction of the adaptive immune response, leading to the transport of HSP70-bound peptide antigens into APC cells and their delivery to MHC class I molecules. Though these effects could occur through binding to one or more cell surface receptors, a major emphasis has been placed on identifying HSP70 receptors that are more important in mediating immune responses of HSP70. Although the nature of the high affinity receptors for HSP70 binding to the APC cell surface has still not been fully defined, there are several receptors that have been suggested, such as CD91, LOX-1, TLR2, TLR4, CD36, CD40, SR-A and CCR5. In our study we analyzed the expression of several HSP70 receptors on the cell surface of monocytes of healthy individuals and simultaneously measured the binding of HSP70 to monocytes. Our purpose was to determine if HSP70 binding is associated with the expression of one or several of these receptors on the cell surface of monocytes. Binding of HSP70 correlated with the expression of CD91, LOX-1, CD36 and TLR4, but not TLR2, suggesting that several receptors are involved with HSP70 binding.

An increased expression of CD91 has been described on monocytes of HIV-1-infected LTNP, HIV-1-exposed but seronegative individuals, and advanced melanoma slow progressors. We compared the expression of CD91 on cell surface of monocytes in a small cohort of LTNP and two groups of disease progressing patients (from TIMS and RESTART studies). The CD91 expression was significantly increased in LTNP compared to the disease progressing patients. We were also interested to evaluate if the expression of CD91 is altered due to HIV infection. Fortunately, we could obtain the blood samples from rhesus macaques used in SIV vaccination studies in the German Primate Center in Göttingen. The samples were obtained before infection and at several time points up to 58 weeks after infection and the CD91 expression on monocytes was measured by flow cytometry. We found a decrease in CD91 expression during the course of the disease. Interestingly, an increased expression of CD91 in LTNP animals (obtained from several studies) was observed, when compared to the disease progressive group. The expression of CD91 in LTNP animals was in a similar range to naïve animals.

We then analyzed if the polymorphisms within the CD91 gene affect the CD91 cell surface expression levels in the HIV cohort and in healthy volunteers. We analysed the effect of a CD91 promoter polymorphism and an exon 3 polymorphism on the expression of CD91. We did not find any influence of the promoter polymorphism on CD91 expression. However, we found a significant effect of the exon 3 polymorphism (T allele) on CD91 cell surface level in the patients of the TIMS group ($p=0.0242$) and a similar but only borderline effect in the LTNP group ($p=0.0403$), if a robust threshold for significance of $\alpha'=0.033$ obtained from permutated data sets was applied. We also evaluated five further SNPs in the CD91 gene determined from the HapMap database. These 5 SNP had no effect on the CD91 expression in the HIV cohort and in healthy volunteers. No effect of specific haplotypes obtained from these SNPs was observed on CD91 expression. However, it has to be noted that the sample number is too low to detect subtle differences by statistical analysis.

LOX-1 receptor expression has been found to be upregulated by several pro-atherogenic conditions like hypertension, dyslipidemia, and diabetes (Chen et al. 2000, 2001; Nagase et al. 1997). Our analysis of LOX-1 3'UTR SNP and the exon 4 SNP that leads to a change in amino acid sequence from lysine to asparagines in the binding domain of the protein, did not show any effect on LOX-1 expression on monocytes. The effect of the amino acid substitution by exon 4 polymorphism in LOX-1 ligand binding domain was tested by analyzing the binding of dye-labeled HSP70 to LOX-1. HSP70 binding to CHO cells transiently transfected with LOX-1 Mut (exon 4 SNP) was significantly reduced compared to LOX-1 Wt transfected CHO cells ($p=0.016$). The expression of LOX-1 from these two transfectants was similar, indicating that exon 4 SNP affects the binding of HSP70 to LOX-1.

In conclusion, we found an effect of CD91 exon 3 SNP on CD91 expression in subgroups of HIV cohort. We also observed that the LOX-1 exon 4 SNP reduces the binding of HSP70 to LOX-1 receptor. Thus, polymorphisms in heat shock protein receptor genes can have functional consequences and might therefore indeed affect the efficacy of HSP-based immunotherapies.

9. References

- Asea, A., Kraeft, S.K., Kurt-Jones, E.A., Stevenson, M.A., Chen, L.B., Finberg, R.W., Koo, G.C. and Calderwood, S.K. (2000) HSP70 stimulates cytokine production through a CD14-dependant pathway, demonstrating its dual role as a chaperone and cytokine. *Nat Med*, **6**, 435-442.
- Asea, A., Rehli, M., Kabingu, E., Boch, J.A., Bare, O., Auron, P.E., Stevenson, M.A. and Calderwood, S.K. (2002) Novel signal transduction pathway utilized by extracellular HSP70: role of toll-like receptor (TLR) 2 and TLR4. *J Biol Chem*, **277**, 15028-15034.
- Banchereau, J., Briere, F., Caux, C., Davoust, J., Lebecque, S., Liu, Y.J., Pulendran, B. and Palucka, K. (2000) Immunobiology of dendritic cells. *Annu Rev Immunol*, **18**, 767-811.
- Banerjee, P.P., Vinay, D.S., Mathew, A., Raje, M., Parekh, V., Prasad, D.V., Kumar, A., Mitra, D. and Mishra, G.C. (2002) Evidence that glycoprotein 96 (B2), a stress protein, functions as a Th2-specific costimulatory molecule. *J Immunol*, **169**, 3507-3518.
- Barber, M.D., Powell, J.J., Lynch, S.F., Fearon, K.C. and Ross, J.A. (2000) A polymorphism of the interleukin-1 beta gene influences survival in pancreatic cancer. *Br J Cancer*, **83**, 1443-1447.
- Basu, S., Binder, R.J., Ramalingam, T. and Srivastava, P.K. (2001) CD91 is a common receptor for heat shock proteins gp96, hsp90, hsp70, and calreticulin. *Immunity*, **14**, 303-313.
- Basu, S., Binder, R.J., Suto, R., Anderson, K.M. and Srivastava, P.K. (2000) Necrotic but not apoptotic cell death releases heat shock proteins, which deliver a partial maturation signal to dendritic cells and activate the NF-kappa B pathway. *Int Immunol*, **12**, 1539-1546.
- Bateman, A.C. and Howell, W.M. (1999) Human leukocyte antigens and cancer: is it in our genes? *J Pathol*, **188**, 231-236.
- Baum, L., Chen, L., Ng, H.K., Chan, Y.S., Mak, Y.T., Woo, J., Chiu, H.F. and Pang, C.P. (1998) Low density lipoprotein receptor related protein gene exon 3 polymorphism association with Alzheimer's disease in Chinese. *Neurosci Lett*, **247**, 33-36.
- Becker, T., Hartl, F.U. and Wieland, F. (2002) CD40, an extracellular receptor for binding and uptake of Hsp70-peptide complexes. *J Cell Biol*, **158**, 1277-1285.
- Belli, F., Testori, A., Rivoltini, L., Maio, M., Andreola, G., Sertoli, M.R., Gallino, G., Piris, A., Cattelan, A., Lazzari, I., Carrabba, M., Scita, G., Santantonio, C., Pilla, L., Tragni, G., Lombardo, C., Arienti, F., Marchiano, A., Queirolo, P., Bertolini, F., Cova, A., Lamaj, E., Ascani, L., Camerini, R., Corsi, M., Cascinelli, N., Lewis, J.J., Srivastava, P. and Parmiani, G. (2002) Vaccination of metastatic melanoma patients with autologous tumor-derived heat shock protein gp96-peptide complexes: clinical and immunologic findings. *J Clin Oncol*, **20**, 4169-4180.
- Benes, P., Jurajda, M., Zaloudik, J., Izakovicova-Holla, L. and Vacha, J. (2003) C766T low-density lipoprotein receptor-related protein 1 (LRP1) gene polymorphism and susceptibility to breast cancer. *Breast Cancer Res*, **5**, R77-81.
- Bertram, L., Parkinson, M., Mullin, K., Menon, R., Blacker, D. and Tanzi, R.E. (2004) No association between a previously reported OLR1 3' UTR polymorphism and Alzheimer's disease in a large family sample. *J Med Genet*, **41**, 286-288.

- Berwin, B., Hart, J.P., Rice, S., Gass, C., Pizzo, S.V., Post, S.R. and Nicchitta, C.V. (2003) Scavenger receptor-A mediates gp96/GRP94 and calreticulin internalization by antigen-presenting cells. *Embo J*, **22**, 6127-6136.
- Binder, R.J., Han, D.K. and Srivastava, P.K. (2000) CD91: a receptor for heat shock protein gp96. *Nat Immunol*, **1**, 151-155.
- Blachere, N.E., Li, Z., Chandawarkar, R.Y., Suto, R., Jaikaria, N.S., Basu, S., Udono, H. and Srivastava, P.K. (1997) Heat shock protein-peptide complexes, reconstituted in vitro, elicit peptide-specific cytotoxic T lymphocyte response and tumor immunity. *J Exp Med*, **186**, 1315-1322.
- Boucher, P., Gotthardt, M., Li, W.P., Anderson, R.G. and Herz, J. (2003) LRP: role in vascular wall integrity and protection from atherosclerosis. *Science*, **300**, 329-332.
- Broquet, A.H., Thomas, G., Maslah, J., Trugnan, G. and Bachelet, M. (2003) Expression of the molecular chaperone Hsp70 in detergent-resistant microdomains correlates with its membrane delivery and release. *J Biol Chem*, **278**, 21601-21606.
- Bu, G., Maksymovitch, E.A. and Schwartz, A.L. (1993) Receptor-mediated endocytosis of tissue-type plasminogen activator by low density lipoprotein receptor-related protein on human hepatoma HepG2 cells. *J Biol Chem*, **268**, 13002-13009.
- Bukau, B. and Horwich, A.L. (1998) The Hsp70 and Hsp60 chaperone machines. *Cell*, **92**, 351-366.
- Chan, T., Chen, Z., Hao, S., Xu, S., Yuan, J., Saxena, A., Qureshi, M., Zheng, C. and Xiang, J. (2007) Enhanced T-cell immunity induced by dendritic cells with phagocytosis of heat shock protein 70 gene-transfected tumor cells in early phase of apoptosis. *Cancer Gene Ther*, **14**, 409-420.
- Chen, J., Mehta, J.L., Haider, N., Zhang, X., Narula, J. and Li, D. (2004) Role of caspases in Ox-LDL-induced apoptotic cascade in human coronary artery endothelial cells. *Circ Res*, **94**, 370-376.
- Chen, M., Kakutani, M., Minami, M., Kataoka, H., Kume, N., Narumiya, S., Kita, T., Masaki, T. and Sawamura, T. (2000) Increased expression of lectin-like oxidized low density lipoprotein receptor-1 in initial atherosclerotic lesions of Watanabe heritable hyperlipidemic rabbits. *Arterioscler Thromb Vasc Biol*, **20**, 1107-1115.
- Chen, M., Nagase, M., Fujita, T., Narumiya, S., Masaki, T. and Sawamura, T. (2001a) Diabetes enhances lectin-like oxidized LDL receptor-1 (LOX-1) expression in the vascular endothelium: possible role of LOX-1 ligand and AGE. *Biochem Biophys Res Commun*, **287**, 962-968.
- Chen, M., Narumiya, S., Masaki, T. and Sawamura, T. (2001b) Conserved C-terminal residues within the lectin-like domain of LOX-1 are essential for oxidized low-density-lipoprotein binding. *Biochem J*, **355**, 289-296.
- Chen, Q., Reis, S.E., Kammerer, C., Craig, W.Y., LaPierre, S.E., Zimmer, E.L., McNamara, D.M., Pauly, D.F., Sharaf, B., Holubkov, R., Bairey Merz, C.N., Sopko, G., Bontempo, F. and Kamboh, M.I. (2003) Genetic variation in lectin-like oxidized low-density lipoprotein receptor 1 (LOX1) gene and the risk of coronary artery disease. *Circulation*, **107**, 3146-3151.
- Chen, W., Syldath, U., Bellmann, K., Burkart, V. and Kolb, H. (1999) Human 60-kDa heat-shock protein: a danger signal to the innate immune system. *J Immunol*, **162**, 3212-3219.
- Chomczynski, P. and Sacchi, N. (1987) Single-step method of RNA isolation by acid guanidinium thiocyanate-phenol-chloroform extraction. *Anal Biochem*, **162**, 156-159.
- Clayton, A., Turkes, A., Navabi, H., Mason, M.D. and Tabi, Z. (2005) Induction of heat shock proteins in B-cell exosomes. *J Cell Sci*, **118**, 3631-3638.

- Davies, E.L., Bacelar, M.M., Marshall, M.J., Johnson, E., Wardle, T.D., Andrew, S.M. and Williams, J.H. (2006) Heat shock proteins form part of a danger signal cascade in response to lipopolysaccharide and GroEL. *Clin Exp Immunol*, **145**, 183-189.
- Delneste, Y., Magistrelli, G., Gauchat, J., Haeuw, J., Aubry, J., Nakamura, K., Kawakami-Honda, N., Goetsch, L., Sawamura, T., Bonnefoy, J. and Jeannin, P. (2002) Involvement of LOX-1 in dendritic cell-mediated antigen cross-presentation. *Immunity*, **17**, 353-362.
- Duan, J., Wainwright, M.S., Comeron, J.M., Saitou, N., Sanders, A.R., Gelernter, J. and Gejman, P.V. (2003) Synonymous mutations in the human dopamine receptor D2 (DRD2) affect mRNA stability and synthesis of the receptor. *Hum Mol Genet*, **12**, 205-216.
- Elsner, L., Muppala, V., Gehrman, M., Lozano, J., Malzahn, D., Bickeboller, H., Brunner, E., Zientkowska, M., Herrmann, T., Walter, L., Alves, F., Multhoff, G. and Dressel, R. (2007) The heat shock protein HSP70 promotes mouse NK cell activity against tumors that express inducible NKG2D ligands. *J Immunol*, **179**, 5523-5533.
- Fossum, B., Breivik, J., Meling, G.I., Gedde-Dahl, T., 3rd, Hansen, T., Knutsen, I., Rognum, T.O., Thorsby, E. and Gaudernack, G. (1994) A K-ras 13Gly-->Asp mutation is recognized by HLA-DQ7 restricted T cells in a patient with colorectal cancer. Modifying effect of DQ7 on established cancers harbouring this mutation? *Int J Cancer*, **58**, 506-511.
- Friedland, J.S., Shattock, R., Remick, D.G. and Griffin, G.E. (1993) Mycobacterial 65-kD heat shock protein induces release of proinflammatory cytokines from human monocytic cells. *Clin Exp Immunol*, **91**, 58-62.
- Gallucci, S. and Matzinger, P. (2001) Danger signals: SOS to the immune system. *Curr Opin Immunol*, **13**, 114-119.
- Gao, B. and Tsan, M.F. (2003a) Endotoxin contamination in recombinant human heat shock protein 70 (Hsp70) preparation is responsible for the induction of tumor necrosis factor alpha release by murine macrophages. *J Biol Chem*, **278**, 174-179.
- Gao, B. and Tsan, M.F. (2003b) Recombinant human heat shock protein 60 does not induce the release of tumor necrosis factor alpha from murine macrophages. *J Biol Chem*, **278**, 22523-22529.
- Gehrman, M., Schmetzer, H., Eissner, G., Haferlach, T., Hiddemann, W. and Multhoff, G. (2003) Membrane-bound heat shock protein 70 (Hsp70) in acute myeloid leukemia: a tumor specific recognition structure for the cytolytic activity of autologous NK cells. *Haematologica*, **88**, 474-476.
- Gething, M.J. and Sambrook, J. (1992) Protein folding in the cell. *Nature*, **355**, 33-45.
- Goldberg, A.L., Cascio, P., Saric, T. and Rock, K.L. (2002) The importance of the proteasome and subsequent proteolytic steps in the generation of antigenic peptides. *Mol Immunol*, **39**, 147-164.
- Goral, J., Mathews, H.L. and Clancy, J., Jr. (1998) Expression of 70-kDa heat-shock protein during acute graft-versus-host disease. *Clin Immunol Immunopathol*, **86**, 252-258.
- Gromme, M. and Neefjes, J. (2002) Antigen degradation or presentation by MHC class I molecules via classical and non-classical pathways. *Mol Immunol*, **39**, 181-202.
- Gurer, C., Cimarelli, A. and Luban, J. (2002) Specific incorporation of heat shock protein 70 family members into primate lentiviral virions. *J Virol*, **76**, 4666-4670.
- Haas, I.G. (1991) BiP--a heat shock protein involved in immunoglobulin chain assembly. *Curr Top Microbiol Immunol*, **167**, 71-82.

- Habich, C., Baumgart, K., Kolb, H. and Burkart, V. (2002) The receptor for heat shock protein 60 on macrophages is saturable, specific, and distinct from receptors for other heat shock proteins. *J Immunol*, **168**, 569-576.
- Halperin, E. and Eskin, E. (2004) Haplotype reconstruction from genotype data using Imperfect Phylogeny. *Bioinformatics*, **20**, 1842-1849.
- Heath, W.R. and Carbone, F.R. (2001) Cross-presentation, dendritic cells, tolerance and immunity. *Annu Rev Immunol*, **19**, 47-64.
- Herz, J., Hamann, U., Rogne, S., Myklebost, O., Gausepohl, H. and Stanley, K.K. (1988) Surface location and high affinity for calcium of a 500-kd liver membrane protein closely related to the LDL-receptor suggest a physiological role as lipoprotein receptor. *Embo J*, **7**, 4119-4127.
- Herz, J., Kowal, R.C., Goldstein, J.L. and Brown, M.S. (1990) Proteolytic processing of the 600 kd low density lipoprotein receptor-related protein (LRP) occurs in a trans-Golgi compartment. *Embo J*, **9**, 1769-1776.
- Herz, J. and Strickland, D.K. (2001) LRP: a multifunctional scavenger and signaling receptor. *J Clin Invest*, **108**, 779-784.
- Higuchi, R., Krummel, B. and Saiki, R.K. (1988) A general method of in vitro preparation and specific mutagenesis of DNA fragments: study of protein and DNA interactions. *Nucleic Acids Res*, **16**, 7351-7367.
- Hollenbach, E., Ackermann, S., Hyman, B.T. and Rebeck, G.W. (1998) Confirmation of an association between a polymorphism in exon 3 of the low-density lipoprotein receptor-related protein gene and Alzheimer's disease. *Neurology*, **50**, 1905-1907.
- Holtzman, D.M., Pitas, R.E., Kilbridge, J., Nathan, B., Mahley, R.W., Bu, G. and Schwartz, A.L. (1995) Low density lipoprotein receptor-related protein mediates apolipoprotein E-dependent neurite outgrowth in a central nervous system-derived neuronal cell line. *Proc Natl Acad Sci U S A*, **92**, 9480-9484.
- Howell, W.M., Turner, S.J., Bateman, A.C. and Theaker, J.M. (2001) IL-10 promoter polymorphisms influence tumour development in cutaneous malignant melanoma. *Genes Immun*, **2**, 25-31.
- Janetzki, S., Blachere, N.E. and Srivastava, P.K. (1998) Generation of tumor-specific cytotoxic T lymphocytes and memory T cells by immunization with tumor-derived heat shock protein gp96. *J Immunother*, **21**, 269-276.
- Jonuleit, H., Knop, J. and Enk, A.H. (1996) Cytokines and their effects on maturation, differentiation and migration of dendritic cells. *Arch Dermatol Res*, **289**, 1-8.
- Kang, D.E., Saitoh, T., Chen, X., Xia, Y., Masliah, E., Hansen, L.A., Thomas, R.G., Thal, L.J. and Katzman, R. (1997) Genetic association of the low-density lipoprotein receptor-related protein gene (LRP), an apolipoprotein E receptor, with late-onset Alzheimer's disease. *Neurology*, **49**, 56-61.
- Kebba, A., Stebbing, J., Rowland, S., Ingram, R., Agaba, J., Patterson, S., Kaleebu, P., Imami, N. and Gotch, F. (2005) Expression of the common heat-shock protein receptor CD91 is increased on monocytes of exposed yet HIV-1-seronegative subjects. *J Leukoc Biol*, **78**, 37-42.
- Kimchi-Sarfaty, C., Oh, J.M., Kim, I.W., Sauna, Z.E., Calcagno, A.M., Ambudkar, S.V. and Gottesman, M.M. (2007) A "silent" polymorphism in the MDR1 gene changes substrate specificity. *Science*, **315**, 525-528.
- Kingo, K., Ratsep, R., Koks, S., Karelson, M., Silm, H. and Vasar, E. (2005) Influence of genetic polymorphisms on interleukin-10 mRNA expression and psoriasis susceptibility. *J Dermatol Sci*, **37**, 111-113.

- Knauer, M.F., Orlando, R.A. and Glabe, C.G. (1996) Cell surface APP751 forms complexes with protease nexin 2 ligands and is internalized via the low density lipoprotein receptor-related protein (LRP). *Brain Res*, **740**, 6-14.
- Kodama, T., Freeman, M., Rohrer, L., Zabrecky, J., Matsudaira, P. and Krieger, M. (1990) Type I macrophage scavenger receptor contains alpha-helical and collagen-like coiled coils. *Nature*, **343**, 531-535.
- Kube, D., Hua, T.D., von Bonin, F., Schoof, N., Zeynalova, S., Kloss, M., Gocht, D., Potthoff, B., Tzvetkov, M., Brockmoller, J., Loffler, M., Pfreundschuh, M. and Trumper, L. (2008) Effect of interleukin-10 gene polymorphisms on clinical outcome of patients with aggressive non-Hodgkin's lymphoma: an exploratory study. *Clin Cancer Res*, **14**, 3777-3784.
- Kume, N., Murase, T., Moriwaki, H., Aoyama, T., Sawamura, T., Masaki, T. and Kita, T. (1998) Inducible expression of lectin-like oxidized LDL receptor-1 in vascular endothelial cells. *Circ Res*, **83**, 322-327.
- Lambert, J.C., Luedeking-Zimmer, E., Merrot, S., Hayes, A., Thaker, U., Desai, P., Houzet, A., Hermant, X., Cottel, D., Pritchard, A., Iwatsubo, T., Pasquier, F., Frigard, B., Conneally, P.M., Chartier-Harlin, M.C., DeKosky, S.T., Lendon, C., Mann, D., Kamboh, M.I. and Amouyel, P. (2003) Association of 3'-UTR polymorphisms of the oxidised LDL receptor 1 (OLR1) gene with Alzheimer's disease. *J Med Genet*, **40**, 424-430.
- Lehner, T., Bergmeier, L.A., Wang, Y., Tao, L., Sing, M., Spallek, R. and van der Zee, R. (2000) Heat shock proteins generate beta-chemokines which function as innate adjuvants enhancing adaptive immunity. *Eur J Immunol*, **30**, 594-603.
- Li, D. and Mehta, J.L. (2000) Upregulation of endothelial receptor for oxidized LDL (LOX-1) by oxidized LDL and implications in apoptosis of human coronary artery endothelial cells: evidence from use of antisense LOX-1 mRNA and chemical inhibitors. *Arterioscler Thromb Vasc Biol*, **20**, 1116-1122.
- Li, D.Y., Chen, H.J., Staples, E.D., Ozaki, K., Annex, B., Singh, B.K., Vermani, R. and Mehta, J.L. (2002) Oxidized low-density lipoprotein receptor LOX-1 and apoptosis in human atherosclerotic lesions. *J Cardiovasc Pharmacol Ther*, **7**, 147-153.
- Li, D.Y., Zhang, Y.C., Philips, M.I., Sawamura, T. and Mehta, J.L. (1999) Upregulation of endothelial receptor for oxidized low-density lipoprotein (LOX-1) in cultured human coronary artery endothelial cells by angiotensin II type 1 receptor activation. *Circ Res*, **84**, 1043-1049.
- Li, Y., Wood, N., Grimsley, P., Yellowlees, D. and Donnelly, P.K. (1998) In vitro invasiveness of human breast cancer cells is promoted by low density lipoprotein receptor-related protein. *Invasion Metastasis*, **18**, 240-251.
- Lin, Z. and Floros, J. (1998) Genomic DNA extraction from small amounts of sera to be used for genotype analysis. *Biotechniques*, **24**, 937-940.
- Lin, Z. and Floros, J. (2000) Protocol for genomic DNA preparation from fresh or frozen serum for PCR amplification. *Biotechniques*, **29**, 460-462, 464, 466.
- Lindquist, S. (1986) The heat-shock response. *Annu Rev Biochem*, **55**, 1151-1191.
- Lindquist, S. and Craig, E.A. (1988) The heat-shock proteins. *Annu Rev Genet*, **22**, 631-677.
- Liu, Y., Jones, M., Hingtgen, C.M., Bu, G., Larabee, N., Tanzi, R.E., Moir, R.D., Nath, A. and He, J.J. (2000) Uptake of HIV-1 tat protein mediated by low-density lipoprotein receptor-related protein disrupts the neuronal metabolic balance of the receptor ligands. *Nat Med*, **6**, 1380-1387.

- Livak, K.J. and Schmittgen, T.D. (2001) Analysis of relative gene expression data using real-time quantitative PCR and the 2(-Delta Delta C(T)) Method. *Methods*, **25**, 402-408.
- Luedeking-Zimmer, E., DeKosky, S.T., Chen, Q., Barmada, M.M. and Kamboh, M.I. (2002) Investigation of oxidized LDL-receptor 1 (OLR1) as the candidate gene for Alzheimer's disease on chromosome 12. *Hum Genet*, **111**, 443-451.
- MacKenzie, A., Wilson, H.L., Kiss-Toth, E., Dower, S.K., North, R.A. and Surprenant, A. (2001) Rapid secretion of interleukin-1beta by microvesicle shedding. *Immunity*, **15**, 825-835.
- Mambula, S.S. and Calderwood, S.K. (2006a) Heat induced release of Hsp70 from prostate carcinoma cells involves both active secretion and passive release from necrotic cells. *Int J Hyperthermia*, **22**, 575-585.
- Mambula, S.S. and Calderwood, S.K. (2006b) Heat shock protein 70 is secreted from tumor cells by a nonclassical pathway involving lysosomal endosomes. *J Immunol*, **177**, 7849-7857.
- Mango, R., Biocca, S., del Vecchio, F., Clementi, F., Sangiuolo, F., Amati, F., Filareto, A., Grelli, S., Spitalieri, P., Filesi, I., Favalli, C., Lauro, R., Mehta, J.L., Romeo, F. and Novelli, G. (2005) In vivo and in vitro studies support that a new splicing isoform of OLR1 gene is protective against acute myocardial infarction. *Circ Res*, **97**, 152-158.
- Mango, R., Clementi, F., Borgiani, P., Forleo, G.B., Federici, M., Contino, G., Giardina, E., Garza, L., Fahdi, I.E., Lauro, R., Mehta, J.L., Novelli, G. and Romeo, F. (2003) Association of single nucleotide polymorphisms in the oxidised LDL receptor 1 (OLR1) gene in patients with acute myocardial infarction. *J Med Genet*, **40**, 933-936.
- Martin, C.A., Carsons, S.E., Kowalewski, R., Bernstein, D., Valentino, M. and Santiago-Schwarz, F. (2003) Aberrant extracellular and dendritic cell (DC) surface expression of heat shock protein (hsp)70 in the rheumatoid joint: possible mechanisms of hsp/DC-mediated cross-priming. *J Immunol*, **171**, 5736-5742.
- Matsunaga, S., Xie, Q., Kumano, M., Niimi, S., Sekizawa, K., Sakakibara, Y., Komba, S. and Machida, S. (2007) Lectin-like oxidized low-density lipoprotein receptor (LOX-1) functions as an oligomer and oligomerization is dependent on receptor density. *Exp Cell Res*, **313**, 1203-1214.
- May, P., Rohlmann, A., Bock, H.H., Zurhove, K., Marth, J.D., Schomburg, E.D., Noebels, J.L., Beffert, U., Sweatt, J.D., Weeber, E.J. and Herz, J. (2004) Neuronal LRP1 functionally associates with postsynaptic proteins and is required for normal motor function in mice. *Mol Cell Biol*, **24**, 8872-8883.
- McIlroy, S.P., Dynan, K.B., Vahidassr, D.J., Lawson, J.T., Patterson, C.C. and Passmore, P. (2001) Common polymorphisms in LRP and A2M do not affect genetic risk for Alzheimer disease in Northern Ireland. *Am J Med Genet*, **105**, 502-506.
- Mehta, J.L., Chen, J., Hermonat, P.L., Romeo, F. and Novelli, G. (2006) Lectin-like, oxidized low-density lipoprotein receptor-1 (LOX-1): a critical player in the development of atherosclerosis and related disorders. *Cardiovasc Res*, **69**, 36-45.
- Minami, M., Kume, N., Kataoka, H., Morimoto, M., Hayashida, K., Sawamura, T., Masaki, T. and Kita, T. (2000) Transforming growth factor-beta(1) increases the expression of lectin-like oxidized low-density lipoprotein receptor-1. *Biochem Biophys Res Commun*, **272**, 357-361.
- Murase, T., Kume, N., Korenaga, R., Ando, J., Sawamura, T., Masaki, T. and Kita, T. (1998) Fluid shear stress transcriptionally induces lectin-like oxidized LDL receptor-1 in vascular endothelial cells. *Circ Res*, **83**, 328-333.

- Nackley, A.G., Shabalina, S.A., Tchivileva, I.E., Satterfield, K., Korchynskyi, O., Makarov, S.S., Maixner, W. and Diatchenko, L. (2006) Human catechol-O-methyltransferase haplotypes modulate protein expression by altering mRNA secondary structure. *Science*, **314**, 1930-1933.
- Nagase, M., Hirose, S., Sawamura, T., Masaki, T. and Fujita, T. (1997) Enhanced expression of endothelial oxidized low-density lipoprotein receptor (LOX-1) in hypertensive rats. *Biochem Biophys Res Commun*, **237**, 496-498.
- Nakamura, T., Hinagata, J., Tanaka, T., Imanishi, T., Wada, Y., Kodama, T. and Doi, T. (2002) HSP90, HSP70, and GAPDH directly interact with the cytoplasmic domain of macrophage scavenger receptors. *Biochem Biophys Res Commun*, **290**, 858-864.
- Nassar, T., Akkawi, S., Shina, A., Haj-Yehia, A., Bdeir, K., Tarshis, M., Heyman, S.N. and Higazi, A.A. (2004) In vitro and in vivo effects of tPA and PAI-1 on blood vessel tone. *Blood*, **103**, 897-902.
- Neefjes, J.J., Momburg, F. and Hammerling, G.J. (1993) Selective and ATP-dependent translocation of peptides by the MHC-encoded transporter. *Science*, **261**, 769-771.
- Noessner, E., Gastpar, R., Milani, V., Brandl, A., Hutzler, P.J., Kuppner, M.C., Roos, M., Kremmer, E., Asea, A., Calderwood, S.K. and Issels, R.D. (2002) Tumor-derived heat shock protein 70 peptide complexes are cross-presented by human dendritic cells. *J Immunol*, **169**, 5424-5432.
- Novota, P., Sviland, L., Zinocker, S., Stocki, P., Balavarca, Y., Bickeboller, H., Rolstad, B., Wang, X.N., Dickinson, A.M. and Dressel, R. (2008) Correlation of Hsp70-1 and Hsp70-2 gene expression with the degree of graft-versus-host reaction in a rat skin explant model. *Transplantation*, **85**, 1809-1816.
- Osterloh, A., Kalinke, U., Weiss, S., Fleischer, B. and Breloer, M. (2007) Synergistic and differential modulation of immune responses by Hsp60 and lipopolysaccharide. *J Biol Chem*, **282**, 4669-4680.
- Panjwani, N.N., Popova, L. and Srivastava, P.K. (2002) Heat shock proteins gp96 and hsp70 activate the release of nitric oxide by APCs. *J Immunol*, **168**, 2997-3003.
- Parmiani, G., Testori, A., Maio, M., Castelli, C., Rivoltini, L., Pilla, L., Belli, F., Mazzaferro, V., Coppa, J., Patuzzo, R., Sertoli, M.R., Hoos, A., Srivastava, P.K. and Santinami, M. (2004) Heat shock proteins and their use as anticancer vaccines. *Clin Cancer Res*, **10**, 8142-8146.
- Parsell, D.A. and Lindquist, S. (1993) The function of heat-shock proteins in stress tolerance: degradation and reactivation of damaged proteins. *Annu Rev Genet*, **27**, 437-496.
- Peetermans, W.E., Raats, C.J., van Furth, R. and Langermans, J.A. (1995) Mycobacterial 65-kilodalton heat shock protein induces tumor necrosis factor alpha and interleukin 6, reactive nitrogen intermediates, and toxoplasmastatic activity in murine peritoneal macrophages. *Infect Immun*, **63**, 3454-3458.
- Rao, A., Luo, C. and Hogan, P.G. (1997) Transcription factors of the NFAT family: regulation and function. *Annu Rev Immunol*, **15**, 707-747.
- Rivoltini, L., Castelli, C., Carrabba, M., Mazzaferro, V., Pilla, L., Huber, V., Coppa, J., Gallino, G., Scheibenbogen, C., Squarcina, P., Cova, A., Camerini, R., Lewis, J.J., Srivastava, P.K. and Parmiani, G. (2003) Human tumor-derived heat shock protein 96 mediates in vitro activation and in vivo expansion of melanoma- and colon carcinoma-specific T cells. *J Immunol*, **171**, 3467-3474.
- Robinson, M.B., Tidwell, J.L., Gould, T., Taylor, A.R., Newbern, J.M., Graves, J., Tytell, M. and Milligan, C.E. (2005) Extracellular heat shock protein 70: a critical component for motoneuron survival. *J Neurosci*, **25**, 9735-9745.

- Rock, K.L., York, I.A., Saric, T. and Goldberg, A.L. (2002) Protein degradation and the generation of MHC class I-presented peptides. *Adv Immunol*, **80**, 1-70.
- Rutherford, S.L. and Lindquist, S. (1998) Hsp90 as a capacitor for morphological evolution. *Nature*, **396**, 336-342.
- Sandford, A.J. and Pare, P.D. (1997) Direct PCR of small genomic DNA fragments from serum. *Biotechniques*, **23**, 890-892.
- Schulz, S., Schagdarsurengin, U., Greiser, P., Birkenmeier, G., Muller-Werdan, U., Hagemann, M., Riemann, D., Werdan, K. and Glaser, C. (2002) The LDL receptor-related protein (LRP1/A2MR) and coronary atherosclerosis--novel genomic variants and functional consequences. *Hum Mutat*, **20**, 404.
- Schumacher, T.N., Kantesaria, D.V., Heemels, M.T., Ashton-Rickardt, P.G., Shepherd, J.C., Fruh, K., Yang, Y., Peterson, P.A., Tonegawa, S. and Ploegh, H.L. (1994) Peptide length and sequence specificity of the mouse TAP1/TAP2 translocator. *J Exp Med*, **179**, 533-540.
- Seo, J. and Lee, K.J. (2004) Post-translational modifications and their biological functions: proteomic analysis and systematic approaches. *J Biochem Mol Biol*, **37**, 35-44.
- Shaley, A., Blair, P.J., Hoffmann, S.C., Hirshberg, B., Peculis, B.A. and Harlan, D.M. (2002) A proinsulin gene splice variant with increased translation efficiency is expressed in human pancreatic islets. *Endocrinology*, **143**, 2541-2547.
- Shepherd, J.C., Schumacher, T.N., Ashton-Rickardt, P.G., Imaeda, S., Ploegh, H.L., Janeway, C.A., Jr. and Tonegawa, S. (1993) TAP1-dependent peptide translocation in vitro is ATP dependent and peptide selective. *Cell*, **74**, 577-584.
- Srivastava, P. (2002) Roles of heat-shock proteins in innate and adaptive immunity. *Nat Rev Immunol*, **2**, 185-194.
- Srivastava, P.K. (2006) Therapeutic cancer vaccines. *Curr Opin Immunol*, **18**, 201-205.
- Srivastava, P.K. and Amato, R.J. (2001) Heat shock proteins: the 'Swiss Army Knife' vaccines against cancers and infectious agents. *Vaccine*, **19**, 2590-2597.
- Srivastava, P.K., Menoret, A., Basu, S., Binder, R.J. and McQuade, K.L. (1998) Heat shock proteins come of age: primitive functions acquire new roles in an adaptive world. *Immunity*, **8**, 657-665.
- Srivastava, P.K., Udono, H., Blachere, N.E. and Li, Z. (1994) Heat shock proteins transfer peptides during antigen processing and CTL priming. *Immunogenetics*, **39**, 93-98.
- Stebbing, J., Bower, M., Gazzard, B., Wildfire, A., Pandha, H., Dagleish, A. and Spicer, J. (2004) The common heat shock protein receptor CD91 is up-regulated on monocytes of advanced melanoma slow progressors. *Clin Exp Immunol*, **138**, 312-316.
- Stebbing, J., Gazzard, B., Kim, L., Portsmouth, S., Wildfire, A., Teo, I., Nelson, M., Bower, M., Gotch, F., Shaunak, S., Srivastava, P. and Patterson, S. (2003) The heat-shock protein receptor CD91 is up-regulated in monocytes of HIV-1-infected "true" long-term nonprogressors. *Blood*, **101**, 4000-4004.
- Stephens, M. and Donnelly, P. (2003) A comparison of bayesian methods for haplotype reconstruction from population genotype data. *Am J Hum Genet*, **73**, 1162-1169.
- Stephens, M., Smith, N.J. and Donnelly, P. (2001) A new statistical method for haplotype reconstruction from population data. *Am J Hum Genet*, **68**, 978-989.
- Su, H.P., Nakada-Tsukui, K., Tosello-Tramont, A.C., Li, Y., Bu, G., Henson, P.M. and Ravichandran, K.S. (2002) Interaction of CED-6/GULP, an adapter protein involved in engulfment of apoptotic cells with CED-1 and CD91/low density lipoprotein receptor-related protein (LRP). *J Biol Chem*, **277**, 11772-11779.

- Sviland, L. and Dickinson, A.M. (1999) A human skin explant model for predicting graft-versus-host disease following bone marrow transplantation. *J Clin Pathol*, **52**, 910-913.
- Sviland, L., Dickinson, A.M., Carey, P.J., Pearson, A.D. and Proctor, S.J. (1990) An in vitro predictive test for clinical graft-versus-host disease in allogeneic bone marrow transplant recipients. *Bone Marrow Transplant*, **5**, 105-109.
- Tamura, Y., Peng, P., Liu, K., Daou, M. and Srivastava, P.K. (1997) Immunotherapy of tumors with autologous tumor-derived heat shock protein preparations. *Science*, **278**, 117-120.
- Tatsuguchi, M., Furutani, M., Hinagata, J., Tanaka, T., Furutani, Y., Imamura, S., Kawana, M., Masaki, T., Kasanuki, H., Sawamura, T. and Matsuoka, R. (2003) Oxidized LDL receptor gene (OLR1) is associated with the risk of myocardial infarction. *Biochem Biophys Res Commun*, **303**, 247-250.
- Todryk, S., Melcher, A.A., Hardwick, N., Linardakis, E., Bateman, A., Colombo, M.P., Stoppacciaro, A. and Vile, R.G. (1999) Heat shock protein 70 induced during tumor cell killing induces Th1 cytokines and targets immature dendritic cell precursors to enhance antigen uptake. *J Immunol*, **163**, 1398-1408.
- Toepoel, M., Joosten, P.H., Knobbe, C.B., Afink, G.B., Zotz, R.B., Steegers-Theunissen, R.P., Reifemberger, G. and van Zoelen, E.J. (2008) Haplotype-specific expression of the human PDGFRA gene correlates with the risk of glioblastomas. *Int J Cancer*, **123**, 322-329.
- Udono, H. and Srivastava, P.K. (1993) Heat shock protein 70-associated peptides elicit specific cancer immunity. *J Exp Med*, **178**, 1391-1396.
- Udono, H. and Srivastava, P.K. (1994) Comparison of tumor-specific immunogenicities of stress-induced proteins gp96, hsp90, and hsp70. *J Immunol*, **152**, 5398-5403.
- Vabulas, R.M., Ahmad-Nejad, P., Ghose, S., Kirschning, C.J., Issels, R.D. and Wagner, H. (2002) HSP70 as endogenous stimulus of the Toll/interleukin-1 receptor signal pathway. *J Biol Chem*, **277**, 15107-15112.
- Waldron, E., Jaeger, S. and Pietrzik, C.U. (2006) Functional role of the low-density lipoprotein receptor-related protein in Alzheimer's disease. *Neurodegener Dis*, **3**, 233-238.
- Wallin, R.P., Lundqvist, A., More, S.H., von Bonin, A., Kiessling, R. and Ljunggren, H.G. (2002) Heat-shock proteins as activators of the innate immune system. *Trends Immunol*, **23**, 130-135.
- Wang, Y., Kelly, C.G., Karttunen, J.T., Whittall, T., Lehner, P.J., Duncan, L., MacAry, P., Younson, J.S., Singh, M., Oehlmann, W., Cheng, G., Bergmeier, L. and Lehner, T. (2001) CD40 is a cellular receptor mediating mycobacterial heat shock protein 70 stimulation of CC-chemokines. *Immunity*, **15**, 971-983.
- Whittall, T., Wang, Y., Younson, J., Kelly, C., Bergmeier, L., Peters, B., Singh, M. and Lehner, T. (2006) Interaction between the CCR5 chemokine receptors and microbial HSP70. *Eur J Immunol*, **36**, 2304-2314.
- Woolfson, A., Stebbing, J., Tom, B.D., Stoner, K.J., Gilks, W.R., Kreil, D.P., Mulligan, S.P., Belov, L., Chrisp, J.S., Errington, W., Wildfire, A., Erber, W.N., Bower, M., Gazzard, B., Christopherson, R.I. and Scott, M.A. (2005) Conservation of unique cell-surface CD antigen mosaics in HIV-1-infected individuals. *Blood*, **106**, 1003-1007.
- Xie, Q., Matsunaga, S., Niimi, S., Ogawa, S., Tokuyasu, K., Sakakibara, Y. and Machida, S. (2004) Human lectin-like oxidized low-density lipoprotein receptor-1 functions as a dimer in living cells. *DNA Cell Biol*, **23**, 111-117.

- Yewdell, J.W. and Bennink, J.R. (1999) Mechanisms of viral interference with MHC class I antigen processing and presentation. *Annu Rev Cell Dev Biol*, **15**, 579-606.
- Zhang, L., Yu, W., He, T., Yu, J., Caffrey, R.E., Dalmasso, E.A., Fu, S., Pham, T., Mei, J., Ho, J.J., Zhang, W., Lopez, P. and Ho, D.D. (2002) Contribution of human alpha-defensin 1, 2, and 3 to the anti-HIV-1 activity of CD8 antiviral factor. *Science*, **298**, 995-1000.
- Zitzler, S., Hellwig, A., Hartl, F.U., Wieland, F. and Diestelkötter-Bachert, P. (2008) Distinct binding sites for the ATPase and substrate-binding domain of human Hsp70 on the cell surface of antigen presenting cells. *Mol Immunol*, **45**, 3974-3983.

10. Acknowledgement

It is my great pleasure to thank the many people who made this thesis possible.

I would like to thank my Ph.D supervisor, PD Dr. Ralf Dressel. He provided encouragement, sound advice, and good teaching.

I am grateful to PD Dr. Sigrid Hoyer-Fender for her stimulating discussions and moral support during my Ph.D study. I thank Prof. Dr. Friedrich-Wilhelm Schürmann for agreeing to be the co-referent for my thesis.

I would like to acknowledge the financial and structural support of my thesis work by the research training group GRK 1034 financed by the Deutsche Forschungsgemeinschaft.

I would like to thank my colleague within the GRK 1034 Ms. Jingky Lozano and her supervisor Prof. Dr. Heike Bickeböller, Department of Genetic Epidemiology, for their statistical analyses of my data.

I would like to extend my special thanks to PD.Dr.Lutz Walter and all the colleagues in his laboratory who extended their helping hands and provided a friendly environment during the entire period of my Ph.D study.

I also thank Dr. Christiane Stahl-Hennig and the colleagues in her laboratory for making the work on SIV-infected primate samples possible.

I am indebted to my student colleagues and many friends for providing a stimulating and fun environment in which to learn and grow. I am especially grateful to Sara Demirogulu for being a nice and helpful colleague. My heartfelt thanks to some great friends, Krishna Pantakani, Santosh Lakshmi Gande, Sridhar Sreeramulu, Kifayatullah, Ajaya Kunwar, Sudhakar, Sridhar Bopanna, Karthikeyan and Raju who have extended their help and moral support during my Ph.D work.

My very special thanks to Leslie Elsner for creating a friendly environment and extending her support and helping hand at all times in the lab. I also thank Peter Novota for being a nice friend and colleague in the lab.

Lastly, and most importantly, I thank my wife Cheng I-Fen, my kids Vivin Muppala and Nitin Muppala and my parents Chengal Raju Muppala and Bharathi Muppala for their love and support. To them I dedicate my thesis.

Publications

Elsner L, Flügge PF, Lozano J, **Muppala V**, Eiz-Vesper B, Demiroglu SY, Malzahn D, Herrmann T, Brunner E, Bickeböller H, Multhoff G, Walter L, Dressel R. The stress-inducible endogenous danger signals HSP70 and MICA synergistically activate the cytotoxic effector functions of human NK cells, submitted.

Elsner L, **Muppala V**, Gehrman M, Lozano J, Malzahn D, Bickeböller H, Brunner E, Zientkowska M, Herrmann T, Walter L, Alves F, Multhoff G, Dressel R (2007) The heat shock protein HSP70 promotes mouse NK cell activity against tumors that express inducible NKG2D ligands. *J Immunol* 179: 5523-5533.

Averdam A, Seelke S, Grützner I, Rosner C, Roos C, Westphal N, Stahl-Hennig C, **Muppala V**, Schrod A, Sauermann U, Dressel R, Walter L (2007) Genotyping and segregation analyses indicate the presence of only two functional MIC genes in rhesus macaques. *Immunogenetics* 59: 247-251.

Lee YH, Magnuson MA, **Muppala V**, Chen SS (2003) Liver-specific reactivation of the inactivated Hnf-1alpha gene: elimination of liver dysfunction to establish a mouse MODY3 model. *Mol Cell Biol* 23: 923-932.*

Chen SS, Chen JF, Johnson PF, **Muppala V**, Lee YH (2000) C/EBPbeta, when expressed from the C/ebpalpha gene locus, can functionally replace C/EBPalpha in liver but not in adipose tissue. *Mol Cell Biol* 20: 7292-7299.*

Muppala V, Lin CS, Lee YH (2000) The role of HNF-1alpha in controlling hepatic catalase activity. *Mol Pharmacol* 57: 93-100.*

Saleem Q, Ganesh S, **Vijaykumar M**, Reddy YC, Brahmachari SK, Jain S (2000) Association analysis of 5HT transporter gene in bipolar disorder in the Indian population. *Am J Med Genet* 96: 170-172.*

Saleem Q, **Vijayakumar M**, Mutsuddi M, Chowdhary N, Jain S, Brahmachari SK (1998) Variation at the MJD locus in the major psychoses. *Am J Med Genet* 81: 440-442.*

* previous publications which are not related to this Ph.D thesis.

Curriculum Vitae

【 Personal Information 】

✦ NAME : Muppala. Vijayakumar ✦ GENDER : Male
✦ DOB : 10/05/1973

✦ TEL(Off) : 49-551-395854
✦ Mobile : 49-176-21503499
✦ E-mail : muppalavk@hotmail.com

【 Educational Background 】

University	Period	Course	Class
University of Pondicherry	1993 ~ 1996	Medical Biochemistry M.Sc	I
University of Madras	1990 ~ 1993	Biochemistry B.Sc	I

SCHOLARSHIPS / PRIZES

1. Awarded Merit Scholarship in B.Sc by Tamilnadu Government, India
2. Awarded Merit Scholarship in M.Sc by Birla Smarak Kosh, India.

【 Research Experience 】

1. Ph.D Thesis (2005 - 2008)
Department of Cellular and Molecular Immunology, University of Göttingen, Germany.
2. Junior research fellow (2002-2005)
Division of Molecular and Genomic Medicine, National Health Research Institute, Taiwan. Joined a group working on “Cancer Genomics and Biology”
3. Junior research fellow (1998-2002)
Institute of molecular biology, Academia Sinica, Taiwan. Joined a group working on “Obesity and Diabetes Research : Mouse Models and Therapy Development”.
4. Research Assistant (1996-1998)
Indian Institute of Science, Bangalore, India. Joined a group working on “Genetic Basis of Neuropsychiatric Disorders”.